AWARD NUMBER: W81XWH-20-C-0077

TITLE: Correlation of Laboratory-Based Hearing Protection Evaluation Methods with Human Performance

PRINCIPAL INVESTIGATOR: Theodore Argo, Ph.D.

CONTRACTING ORGANIZATION: Applied Research Associates, Inc.

REPORT DATE: August 2022

TYPE OF REPORT: Annual

PREPARED FOR: U.S. Army Medical Research and Development Command

Fort Detrick, Maryland 21702-5012

REPORT DOCUMENTATION PAGE

Form Approved
OMB No. 0704-0188

1. REPORT DATE	2. REPORT TYPE	3. DATES COVERED
August 2022	Annual	28JUL2021 – 27JUL2022

4. TITLE AND SUBTITLE

Correlation of Laboratory-Based Hearing Protection Evaluation Methods with Human Performance

5a. CONTRACT NUMBER
W81XWH-20-C-0077

5b. GRANT NUMBER

5c. PROGRAM ELEMENT NUMBER

6. AUTHOR(S)
Theodore Argo, Ph.D.; Greg Rule, P.E.; Alexandria Podolski; Jennifer Jerding; Nathanial T. Greene, Ph.D.; Carol Sammeth, Ph.D.; Andrew Brown, Ph.D.; David Audet, Au.D.; Aoi Hunsaker
E-Mail: targo@ara.com

5d. PROJECT NUMBER

5e. TASK NUMBER

5f. WORK UNIT NUMBER

7. PERFORMING ORGANIZATION NAME(S) AND ADDRESS(ES)

Applied Research Associates, Inc.
7921 Shaffer Parkway
Littleton, CO 8127

University of Washington
Dept. of Speech and Hearing Sciences
1417 NE 42nd St.
Seattle, WA 98105

Univ. of Colorado School of Medicine
Department of Otolaryngology
Research Complex 1-N Rm 7104
12800 E 19th Ave.
Aurora, CO 80045

8. PERFORMING ORGANIZATION REPORT NUMBER

9. SPONSORING / MONITORING AGENCY NAME(S) AND ADDRESS(ES)

U.S. Army Medical Research and Development Command
Fort Detrick, Maryland 21702-5012

10. SPONSOR/MONITOR'S ACRONYM(S)

11. SPONSOR/MONITOR'S REPORT NUMBER(S)

12. DISTRIBUTION / AVAILABILITY STATEMENT
Approved for Public Release; Distribution Unlimited

13. SUPPLEMENTARY NOTES

14. ABSTRACT
Military personnel require hearing protection for a wide variety of environments and the current method of selecting appropriate hearing protection devices (HPDs) is based largely on guesswork. Only the Noise Reduction Rating (NRR) is used as a standard HPD specification; other important characteristics of advanced HPDs are not evaluated or reported in a standardized manner. The primary objective of this effort is to verify electromechanical test methods for evaluation of advanced HPDs to reduce stakeholders' long-term dependence on time-consuming and expensive human subject testing. A second objective of this effort is to develop a software tool using these verified HPD performance metrics to enable mission planners and Warfighters to select HPDs appropriate to support specific mission profiles, thereby optimizing Warfighter performance. In Year 1 of this program the human subject evaluation protocols and associated instrumentation were developed and approved. Electromechanical test apparatus were refined in preparation for evaluation of a broad set of HPDs. Development of the software tool was initiated to support determination of a transition path. In Year 2, electromechanical and human subject measurements were performed on an array of HPDs and compared before inclusion within the software tool database.

15. SUBJECT TERMS
Hearing Protection, Electromechanical Testing, Acoustics, Audiology, Hearing Conservation

16. SECURITY CLASSIFICATION OF:			17. LIMITATION OF ABSTRACT	18. NUMBER OF PAGES	19a. NAME OF RESPONSIBLE PERSON
a. REPORT	b. ABSTRACT	c. THIS PAGE			USAMRDC
Unclassified	Unclassified	Unclassified	Unclassified	83	19b. TELEPHONE NUMBER *(include area code)*

Correlation of Electromechanical Hearing Protection Test Methods with Human Performance

Year 2 Annual Report

27 August 2022

Prepared for:
Joint Warfighter Medical Research Program
Congressionally Directed Medical Research Programs
Fort Detrick, MD 21702

Submitted by:
Ted Argo, Ph.D.
Principal Investigator

Prepared by:

Applied Research Associates, Inc.

Ted Argo, Ph.D.
Greg Rule, P.E.
Alexandria Podolski
Jennifer Jerding

University of Colorado School of Medicine

Nate Greene, Ph.D.
Carol Sammeth, Ph.D.

University of Washington

Andrew Brown, Ph.D.
David Audet, Au.D.
Aoi Hunsaker

Award Number W81XWH-20-C-0077

Table of Contents

List of Figures

List of Tables

1. Introduction

Military personnel require hearing protection for a wide variety of environments, and the current method of selecting appropriate hearing protection devices (HPDs) is based largely on guesswork. The only standard HPD rating currently available is the Noise Reduction Rating [NRR; Occupational Safety and Health Administration (OSHA) 1910.95]); other important characteristics of advanced HPDs are neither evaluated nor reported in a standardized manner. HPD characteristics may be evaluated using human subjects or electromechanical test methods. While human subject testing is the gold standard for final HPD evaluation (Berger 2005), the use of human subjects is a time-consuming and expensive process due to the regulatory and scientific protocols necessary to obtain reliable results. Human subject testing is particularly impractical for the purposes of HPD research and development, compounded by now prevalent rapid prototyping capabilities (Attaran 2017) and the need for quick evaluation. Human subject testing is also impractical for operational hearing protection qualification, due to the potentially large number of device variations and performance characteristics that may be important to the Warfighter. Therefore, electromechanical test methods are necessary to guide and constrain the need for high amounts of human subject testing. To address this challenge, ARA will deliver (1) a verified suite of quantitative, sensor-based tests to quickly, inexpensively, and comprehensively evaluate candidate HPDs for military use, and (2) a software tool to be used by operational planners to identify the optimal HPD solution based on mission requirements.

In the first year of this program, Team ARA completed protocol design and experiment development. A suite of electromechanical tests developed under previous funding were updated to improve the valid range. For each of these tests, we also developed a human subject protocol to compare human subject performance on auditory tasks with the calculated output of the electromechanical test. We developed and acquired the equipment necessary to support each test and began recruitment of human subjects for pilot data collection. We initiated development of the HPD optimization software tool and began discussions with various Department of Defense (DoD) organizations regarding transition planning.

In the second year of this program, Team ARA completed the human subject pilot tests, updated the human test protocols and began enrolling participants in the full study. A total of 77 human subjects were enrolled across study sites, leading to approximately 50 complete datasets, with active testing still underway on approximately 15 subjects and frequent new enrollments ongoing. We also reviewed existing acoustic testing standards to establish a baseline for writing the new electromechanical test method in accordance with ANSI requirements. Negotiations continued with the DoD, and specifically the Defense Logistics Agency (DLA) to establish a transition pathway for the standards and the optimization tool. Additional design work on the design tool was completed to include demonstrations with the Hearing Center of Excellence (HCE) and the Medical Research and Development Command (MRDC). Details of these efforts are described in the following sections.

2. Key Words

Hearing Protection, Electromechanical Testing, Acoustics, Audiology, Hearing Conservation

3. Accomplishments

3.1. What were the major goals and objectives of the project?

The primary objective of this effort is to verify electromechanical test methods for evaluation of advanced HPDs to reduce stakeholders' long-term dependence on time-consuming and expensive human subject testing. A second objective of this effort is to develop a software tool using these verified HPD performance metrics to enable mission planners and Warfighters to select HPDs appropriate to support specific mission profiles, thereby optimizing Warfighter safety and effectiveness.

The overarching goal of the proposed effort is to verify that a battery of previously developed electromechanical test methods for evaluation of HPD performance is predictive of human auditory performance. Thus, parallel electromechanical and human subject data sets will be measured. Concurrent with these efforts, verified HPD test data will be compiled to create an advanced HPD selection software tool for mission planners and Warfighters. Collectively, these advances will increase the efficiency and effectiveness of advanced HPD development and deployment, enhancing Warfighter protection and mission effectiveness.

Specific Aim 1: Human auditory performance during HPD use will be evaluated for comparison to parallel electromechanical test methods. Live human subjects will be evaluated for performance on speech perception in noise (hSQ), sound source localization (hSL), sound level-dependent attenuation across frequency (hLD), and audibility at low sound levels (hSN). Cadaveric human subjects will be evaluated for high-level impulse noise transmission to the inner ear (hIN). Outcomes are absolute performance measures for hearing protection devices needed for verification of the analogous relative measures produced by the electromechanical test methods.

Specific Aim 2: Results of the absolute measurements of human performance will be compared to the relative metrics produced by the electromechanical methods for signal quality (eSQ), sound localization (eSL), level-dependent frequency response (eLD), self-noise (eSN), and impulse noise attenuation (eIN). These methods will be modified and refined to implement source signals (durations, levels, spacing), analysis methods, and interpretation guidelines that best reflect the range of observed human performance and enable differentiation of HPDs. The results of the human subject and electromechanical test methods will be used to support development of relevant military and civilian HPD evaluation standards.

Specific Aim 3: Both human and electromechanical tests will be applied to a range of hearing protection devices to ensure the relationships developed in Specific Aims 1 and 2 hold across device types. Electromechanical metrics (verified by human performance) will then be used to generate an expandable database of advanced HPD performance ratings. This database will be incorporated into a tool through which end-users and acquisitions personnel may select optimal hearing protection devices for specific mission profiles and military occupational specialties.

3.2. What was accomplished under these goals?

3.2.1. Specific Aim 1, Major Task 1: Submission of Human Use Protocols and Preparation of Facilities

3.2.1.1. Subtask 1. Develop Human Use Protocols

This subtask is complete, as summarized in the prior annual report.

3.2.1.2. Subtask 2: Develop Human Cadaver Use Protocols

This subtask is complete, as summarized in the prior annual report.

3.2.1.3. Subtask 3: Prepare Human Test Facilities

All human test facilities are complete, as summarized in the first annual report. However, some testing requires in-ear sound measurement. While acoustic test fixtures usefully capture typical acoustic impacts of in-ear devices such as HPDs – a foundational premise of the present effort – variation across the morphology and resultant acoustics of real human subjects' ears is expected to introduce a degree of individual variability in HPD impact. While such variability could be conveyed by an error term in our electromechanical metric, we considered that individual measurement of HPD impacts with in-ear microphones could allow us to quantify individual acoustic variability *directly* to evaluate its impact on corresponding localization behavior.

Thus, an in-ear microphone system was developed to measure acoustic signals in the ear canals of individual test subjects, both with and without HPDs in place. Very small MEMS (micro-electromechanical system) microphones were selected (CUI CMM-2718AT-42308-TR) and a preamplifier circuit was designed to amplify the microphone signal to ensure the output can be recorded with standard recording equipment; the resultant sensitivity of the system is roughly 630 mV/Pa. The microphones are placed at the end of a long, thin flex circuit that can be inserted in a subject's ear canal alongside earplugs or worn under earmuffs. In the case of a roll-down foam earplug, such as the EAR Classic, the flex circuit may be inserted through the middle of the earplug. A picture of a fully assembled in-ear microphone prototype is shown in Figure 1.

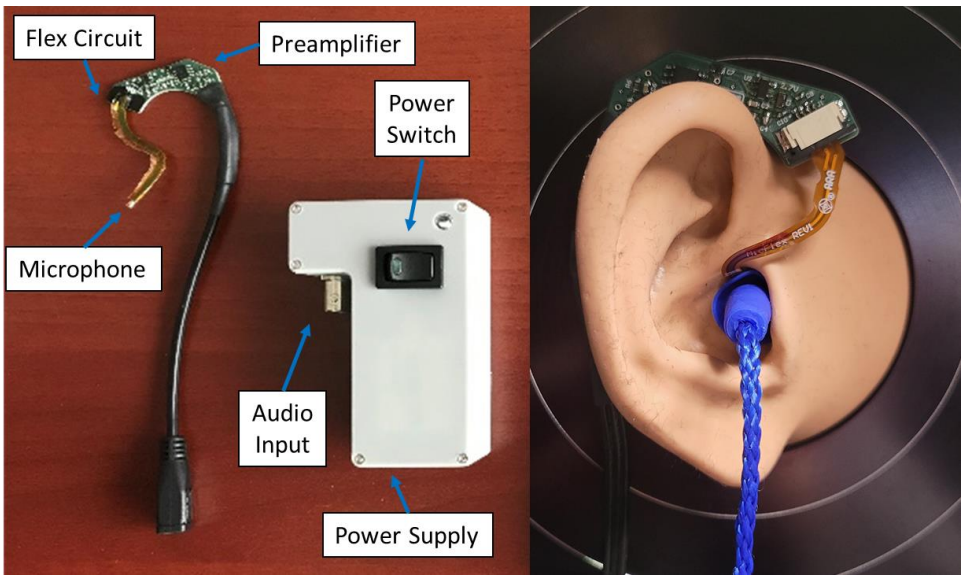

Figure 1. In-ear microphone prototype. Left: flex circuit/preamplifier and power supply. The microphone itself is positioned at the end of the flex circuit, appearing as a gold-colored dot. Right: The microphone inserted into the ear of a test fixture with an Elvex Quattro HPD.

Prototypes were tested by comparing the insertion loss measured in a GRAS 45CA test fixture. Ten tests were conducted with no flex circuit penetrating the seal of an HPD and measuring the signal using the internal microphones and ten tests were conducted with the flex circuit

penetrating the seal of an HPD and measuring the signal using the internal microphones. For the tests where the seal was penetrated by the flex circuit, the pressure in the ear canal was also measured by the MEMS microphone.

Typical examples of the results of this testing are shown in Figure 2 for the Comtac V and the TEP 200 HPDs. In both cases, the solid lines represent the mean of the measurements, and the semitransparent bands represent the standard deviation. In both cases there is very good agreement between the measurements indicating that the in-ear prototype does not strongly affect the insertion loss. When reduced to octave band or one-third octave band averages, the results converge further. One notable feature in the Comtac V measurement is the gain in insertion loss when the preamplifier is in place. In this case, the seal of the HPD is slightly broken at low frequencies due to the cable running from the preamplifier to the power module, leading to the change in insertion loss.

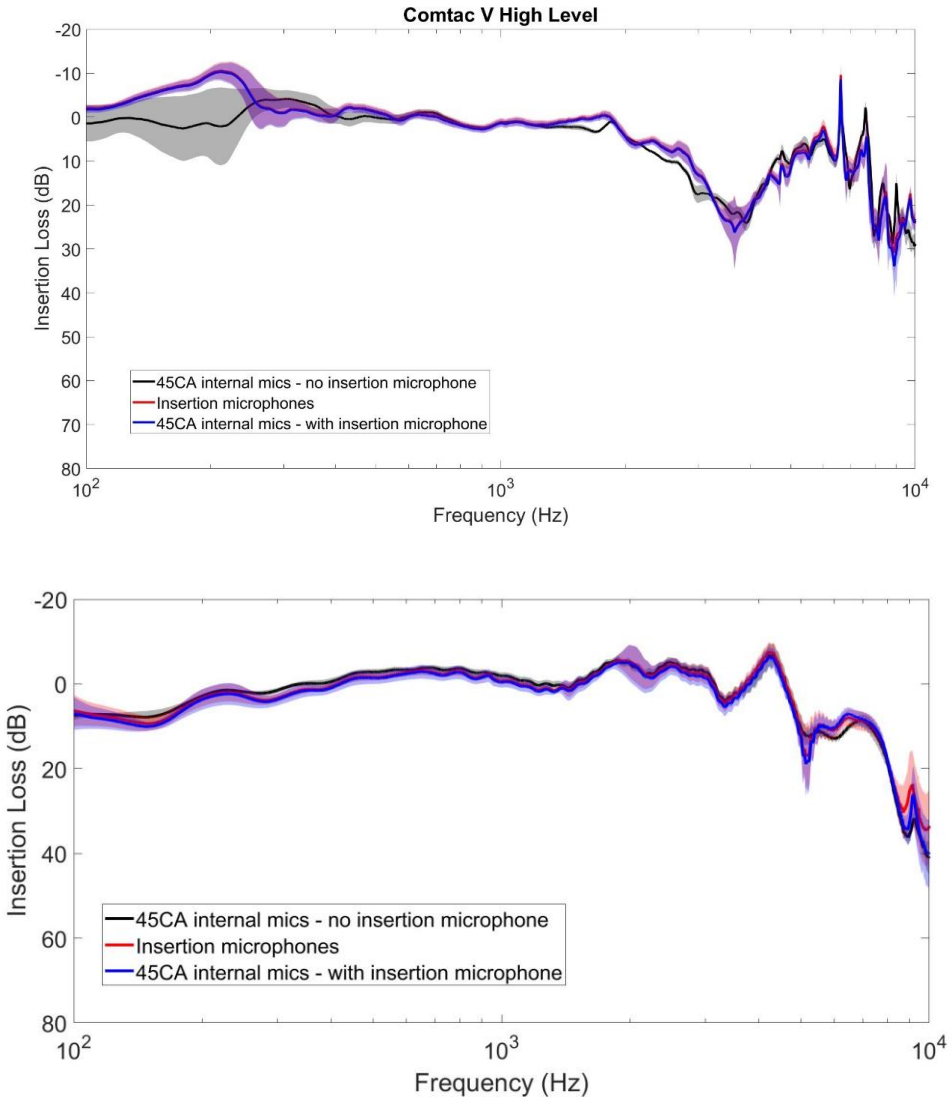

Figure 2. Signals measured by the prototype in-ear microphone system. Top – Comtac V over-ear muffs. Bottom – TEP200 electronic insert HPDs.

An example set of test results was obtained in a human subject, giving the amplitude spectrum of recorded sound, both with open ears and while using two HPDs (EAR Classic and Comtac V), as shown in Figure 3. These measurements show that the Comtac V restores normal hearing levels up to about 3 kHz before demonstrating a high attenuation notch consistent with test fixture testing (See Figure 2). The EAR Classic demonstrates high broadband attenuation, increasing with frequency. Completion of similar measurements in additional subjects will provide insight on how acoustic distortions experienced by actual subjects deviate (or do not deviate) from acoustic test-fixture-based measurements.

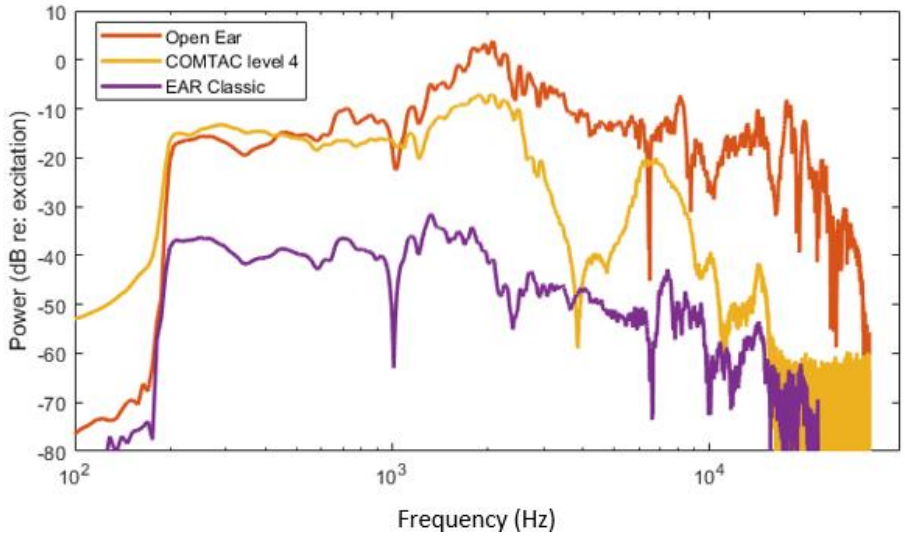

Figure 3. Test results with the in-ear microphone prototype for open ears, the Comtac V at volume level 4, and the EAR Classic.

A second revision of the in-ear microphone for collecting in-ear subject Head Related Transfer Function (HRTF) measurements was then completed. The second revision has a thinner and more flexible flex circuit with a MEMS microphone on the tip for insertion into the ear canal as well as a second microphone on the circuit board that fits over the ear for measuring the sound before it enters the ear canal. Pictures of a prototype are shown in Figure 4.

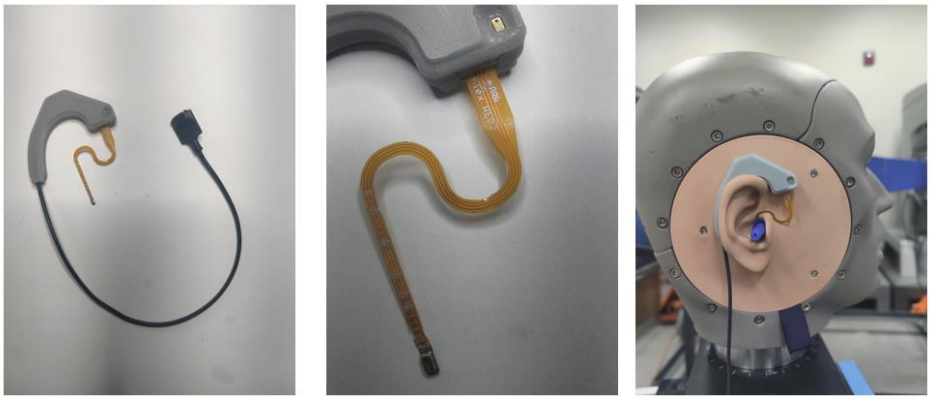

Figure 4. (Left) Completed prototype in-ear microphone assembly with flex circuit and preamp. (Center) Close-up on the in-ear flex circuit. (Right) The in-ear microphone assembly mounted on the 45CB test fixture and inserted alongside an HPD.

Initial prototypes (first revision) had issues with the stiff flex circuit breaking the seal of the HPDs and general comfort in the ears of subjects. The new, thinner flex circuit was designed to have less effect on the seal of HPDs against the ear canal by allowing it to conform more to the curved surface. The seal was tested by inserting the flex microphone and over-ear preamp assembly into the GRAS 45CB test fixture and measuring the insertion loss with various HPDs used alongside the flex microphone. Measurements were made by playing 10 seconds of white noise through Sennheiser HD600 headphones placed over the ears of the 45CB and recording the response through the built-in test fixture microphones. The in-ear microphones were not used in these tests and the devices were powered off as we were only interested in testing the seal of the HPDs. Results are shown in Figure 5.

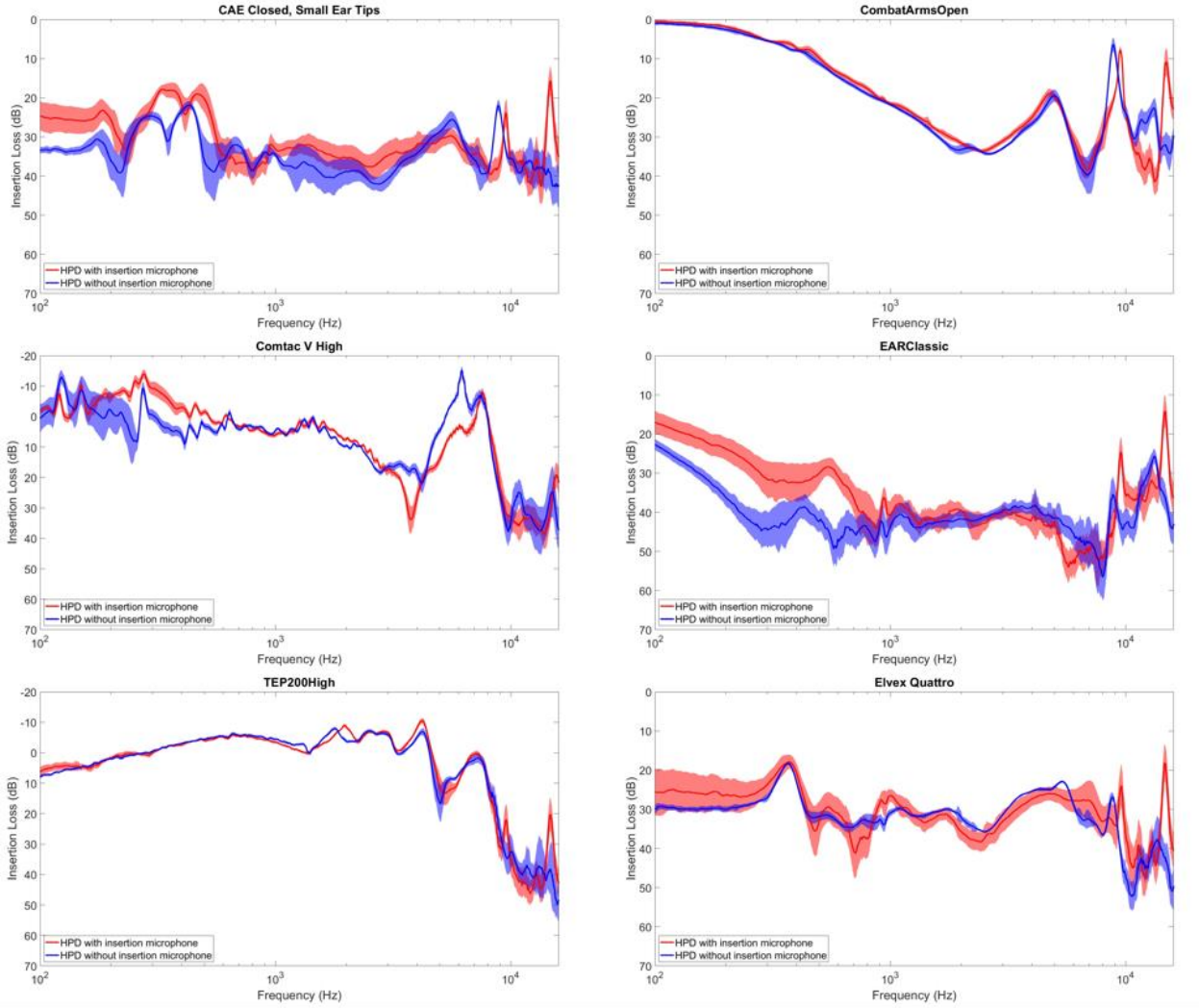

Figure 5. Insertion loss measurements for various HPDs with (red) and without (blue) the in-ear microphone, averaged over 5 trials. Line represents the mean insertion loss with 1 standard deviation shown as a lighter cloud around each measurement.

Preliminary measurements were similarly made in one of the investigators' ears in the CU anechoic chamber to assess the function of the microphone system in a real ear, and to verify the acoustic stimuli and recording system was operating appropriately. Preliminary results (not

shown) clearly revealed the expected features of an HRTF (i.e., a fixed ear canal resonance and high frequency spectral notches that vary systematically with sound source location) in the open ear condition, and substantial attenuation during HPD use. Results of this testing revealed the need for a plastic cover, tacky silicon pad to hold the microphone in place, and strain relief on the cable which were also implemented.

Milestone 1: Local IRB approval

Completed, as summarized in the prior annual report.

Milestone 2: HRPO approval

Completed, as summarized in the prior annual report.

3.2.2. Specific Aim 1, Major Task 2: Test Method Verification in Human Subjects

All four tests to be conducted in human subjects were developed (including software and hardware), brought online, and piloted at both University of Washington (UW) and University of Colorado (CU) testing sites by the end of the previous year. During year 2, we ran additional pilot subjects at both sites and developed new analysis tools to further refine parameter selections, identify potential pitfalls, and adjust protocols as indicated to improve the value and usability of obtained measurements. In service of efficiently concluding the pilot phase, the UW team has focused on the development of analysis tools and software and the subsequent evaluation and refinement of protocol details, while the CU team has focused on data acquisition and the cadaver testing outlined in a subsequent section. In the following, we summarize test-specific developments and insights gained.

3.2.2.1. Subtask 1: Obtain pilot psychoacoustic measures of hearing protective device (HPD) effects and Subtask 2: Analyze pilot psychoacoustic measures of HPD effects

Data from pilot testing at both sites have been collected and effectively leveraged to identify minor adjustments in testing protocols and to develop appropriate software analysis tools.

3.2.2.1.1. Sound Localization (hSL)

Human sound localization (hSL) testing is the most substantial component of the human subject test battery in terms of facilities preparation, hardware and software development, and testing time per subject. The specific hearing protection devices (HPDs) under test, which were selected in consultation with stakeholders, span a range of form factors, active (electronic)/passive functionality, and associated attenuation characteristics. Pilot hSL testing was effectively completed during the first quarter of Year 2. Updates on hSL behavioral measurements, which are proceeding at scale presently, are confined to Section 3.2.2.2 below. In service of correlative behavioral-electromechanical analysis efforts, the project team identified an innovative approach for individualized acoustic measurements that is expected to augment our ability to identify acoustic correlates of sound localization behavior during HPD use. Here, we summarize this development.

All HPDs tested to date (by our group and others) are known to disrupt the spatial acoustic information – specifically the “spectral shape” of transmitted sound – listeners depend on to accurately locate sound sources. Key developments of the present effort include (1) testing of

localization performance in both azimuth and elevation and (2) quantification of error patterns with respect to observed spectral shape cue transformations across HPDs.

Figure 6 provides a graphical illustration of the loudspeaker array (Figure 6A) and a scatterplot of two-dimensional (polar) angular error for a subject seated at the center of the array. The subject was instructed to orient toward illuminated LEDs on each of 24 loudspeakers, thereby demonstrating the accuracy of our head position tracking system (developed last year and described in the previous annual report). During the present reporting period, testing has continued with all hearing protectors at both sites, supporting evaluation of response patterns, and consideration of specific testing protocol elements. Figure 7 represents typical pilot sound localization performance data for three subjects as outlined in previous reports.

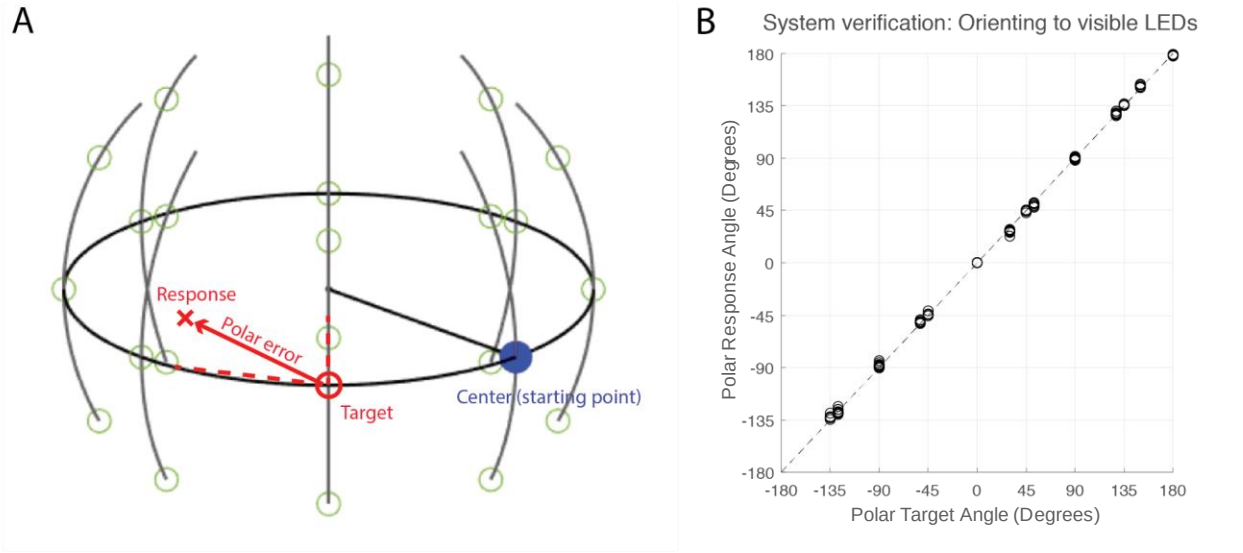

Figure 6. (A) Graphical illustration of the loudspeaker array used in localization testing (Washington site illustrated). The subject begins each trial facing the loudspeaker at 0º azimuth, 0º elevation (illustrated with blue circle). Response error is calculated in terms of two-dimensional polar error, i.e. the "diagonal" angular distance between the response and target locations. (B) Orientation responses, in terms of polar angle, to visual targets, demonstrating the accuracy of our new head position tracking system.

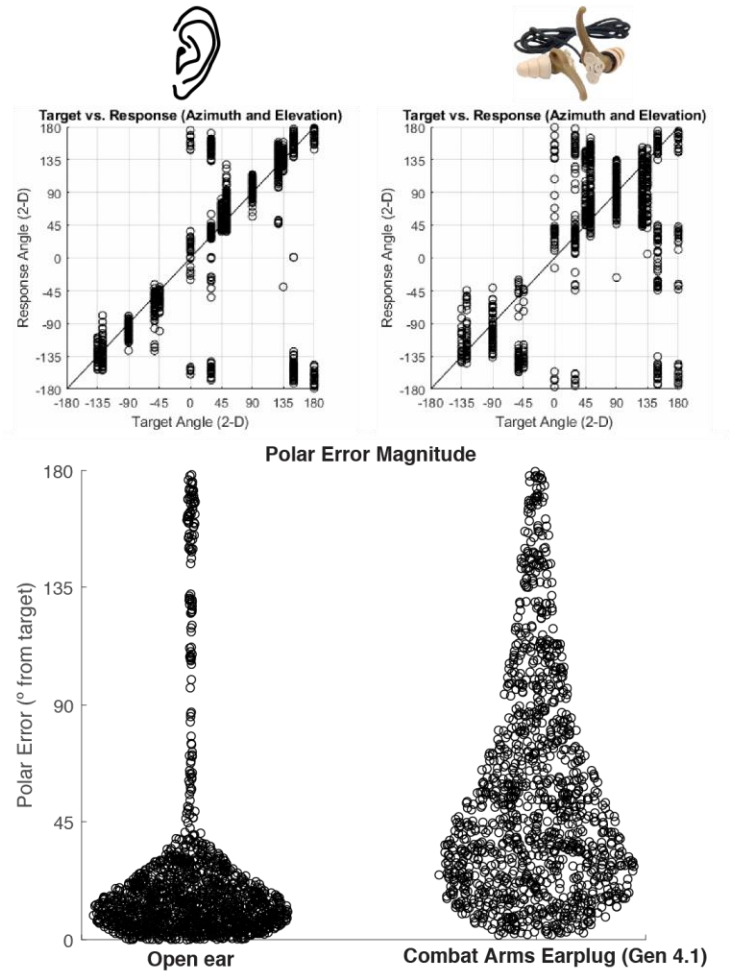

Figure 7. Upper panels: Scatterplot of polar target angle versus polar response angle for open ear (left) and for a passive HPD (Combat Arms Gen. 4.1). Data are pooled across 3 subjects tested at the UW site. Lower panel: Polar error (calculated as in Figure 6A using the data in upper panels of the present figure) is shown for open ear and Combat Arms performance. This representation is known as a 'swarm chart'' in which the horizontal spread of points in each column reflects the density of the underlying distribution. The upward expansion of the swarm in the Combat Arms condition reflects the poor performance observed, with many polar errors in excess of 90 degrees.

3.2.2.1.2. Speech in Noise (hSQ)

Development and initial testing of the speech-in-noise (hSQ) was described in the previous annual report. Pilot testing of the hSQ test was completed in Year 2 with testing proceeding at scale. hSQ testing consists of testing with the Modified Rhyme Test (MRT), pseudo-randomly distributing available words across test conditions such that each condition (open ear, and each of the four HPDs at each siter) are tested with 60 words. To compare MRT results with a commonly used clinical test, testing is additionally conducted using the QuickSIN test battery. Two QuickSIN word lists are presented for each HPD condition (also totaling 60 target words), counterbalanced across subjects to prevent order effects.

Completion and analysis of pilot MRT and QuickSIN testing revealed two issues.

1. MRT target words are presented in a background of omnidirectional pink noise. Signal-to-noise ratios from 0 (equal target and noise amplitudes) to +6 (word 6 dB more intense than background) were presented. Subjective reports and empirical analysis (see Figure 8) suggested that these signal-to-noise ratios did not make the task difficult enough, leading to ceiling effects (performance near ceiling at +6 dB in particular). As a result of this analysis, the issue has been resolved by reducing the range of signal-to-noise ratios by 3 dB (now -3 dB to +3 dB).
2. QuickSIN testing is normally conducted in an audiometric booth with signals presented over earphones; subjects provide a verbal response, repeating back six target sentences in series as the level of background noise (multitalker babble) steadily increases. To adapt this test for use with HPDs, signals are presented over loudspeakers inside anechoic chambers at each site. However, loudspeaker playback of background babble during non-target 'gaps' between target sentences was found to mask subject verbal responses. To resolve the issue, background babble during the QuickSIN stimulus presentation has consequently been attenuated during the non-target periods to improve audibility of the subject's responses and facilitate scoring.

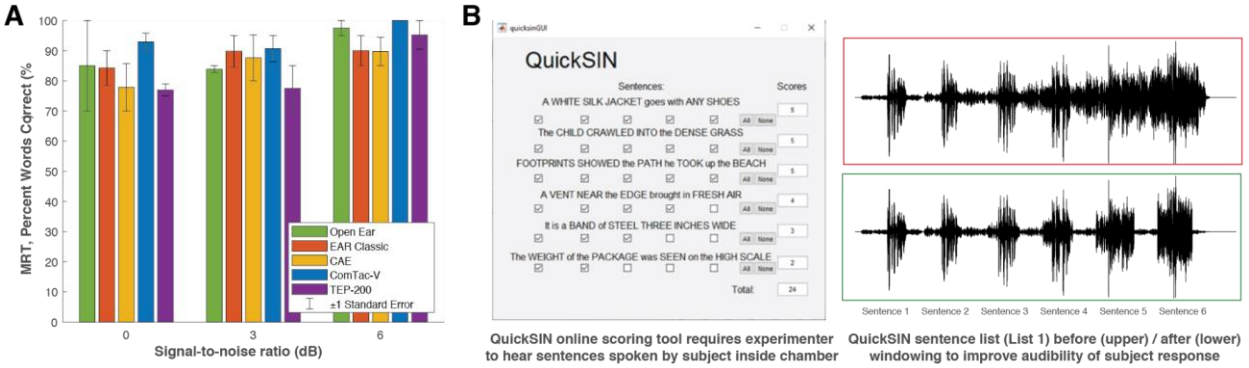

QuickSIN online scoring tool requires experimenter to hear sentences spoken by subject inside chamber

QuickSIN sentence list (List 1) before (upper) / after (lower) windowing to improve audibility of subject response

Figure 8. (A) Preliminary data evidence limited variation across signal-to-noise ratio, particularly at +6dB. To capture a broader range of performance and improve separation across devices, the amended protocol uses -3, 0, and +3 dB SNR. (B) QuickSIN scoring (left) requires the experimenter to hear and understand words repeated back by the subject. During loudspeaker playback, steadily increasing background noise (multi-talker babble) level can mask the subject's verbal response. Increasing babble level during the response windows between sentences is not important to the task, thus we have developed list-specific attenuation windows for all Lists (1-12) in the QuickSIN battery, and applied windowing to improve the audibility of subject responses. The audibility issue has thus been resolved and testing with the improved procedure is underway.

3.2.2.1.3. Level Dependence (hLD) and Self-Noise (hSN) testing

Development and initial testing of the human level-dependence (hLD) and self-noise (hSN) tests were described, and preliminary data provided, in the previous annual report. Both tests leverage more traditional audiometric test equipment and protocols (as compared to testing in the anechoic chambers), so initially required less development effort in terms of both software and hardware. They are completed in a sound booth setting and take significantly less time than hSQ and hLD testing. Both hLD and hSN tests can be completed across open ear and

active HPD conditions within a single session and the 'testing matrix' (sequencing of testing appointments per subject) has been programmed accordingly. Custom software to run the tests was successfully developed, verified, and piloted during the prior year, as summarized in the Year 1 annual report.

However, one issue was identified during pilot testing: How should a controlled stimulus playback be provided for conditions using earmuff-style HPDs (e.g., Comtac V). We attempted to address this issue via development of new earphones customized for use for with earmuff-style protectors (Figure 9), described below.

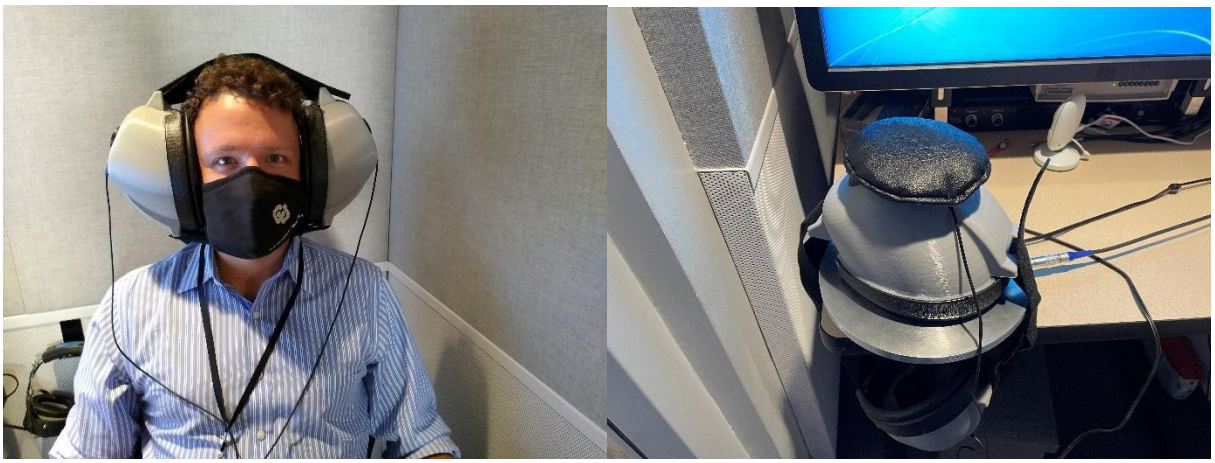

Figure 9. Left: Custom extra-large-volume earphones on the custom flat plate adapter during calibration. Right: Demonstration of use of the earphones; adjustable straps are used to position and secure the earphones over earmuff-style HPDs.

Both hSN and hLD testing was to be conducted using a set of large-volume circumaural headphones placed over the HPDs under test. Testing with earplug-style hearing protectors is conducted using commercially available earphones (Michael and Associates) developed for use with a proprietary HPD fit-testing system. These earphones, however, are not sufficiently large to fit over earmuff-style HPDs such as the Comtac V (chosen in the current study per request from stakeholders). We addressed this issue by designing and 3-D printing new, extra-large volume earphones with a form factor sufficient to fit over earmuff-style protectors. Earphones were calibrated using a Larson-Davis sound level meter, using a custom flat-plate adapter for a standard ear simulator. The commercial (Michael & Associates) and custom-built extra-large earphones use the same drivers (Tungtech) and were correspondingly found to produce similar output suitable for testing.

Initially, in a small cohort of pilot subjects, the new phones were found to be sufficient for the hSN task: They could be positioned over the Comtac V earmuffs with the assistance of the experimenter to achieve a good seal and allow for calibrated presentation of test stimuli. However, the hLD task, by its design, requires open, then unilateral, then bilateral fitting of the HPD under test. While the Comtac Vs can be worn unilaterally by folding one earcup away from the pinna, we found headband/circumaural earphone positioning in this arrangement to be too challenging for reproducible/reliable placement across subjects, even with experimenter assistance. Additionally, in attempting to apply the new phones for testing in additional subjects in the hSN task, the variability of placement success increased; particularly for subjects with smaller heads, it was often not possible to achieve a good seal. Therefore, for both the hLD and hSN tasks, we

moved to replace the Comtac V with another active device requested by stakeholders, the Invisio X5. Testing in hSN and hLD progressed rapidly thereafter, leading to the accumulation of data sufficient to more fully evaluate both tasks. Testing at scale continues at both the CU and UW sites in the hSN task; additional challenges and solutions for hLD are described below.

3.2.2.2. Subtask 3: Obtain psychoacoustic measures of HPD effects

Full-scale testing across sites follows a pre-programmed testing matrix (Table 1) in which the ordering of testing across tasks and hearing protectors is appropriately counterbalanced to ensure even accumulation of data and account for anticipated subject attrition, with testing blocked such that subjects will complete all testing within a minimal number of sessions, while maximizing the likelihood that complete data for a given task will be obtained in the event of attrition. This protocol also reduces variability of hearing protector placement across trials within each task, minimizing that potential source of variability.

Table 1. Final testing matrix for full-scale testing. The ordering of tasks, HPD types, and test materials is counter-balanced to ensure even accumulation of data across the testing period, and to anticipate impacts of subject attrition. Additional subjects can be added to the schedule using the same schedule if required. Matrix is shown for UW site; a parallel matrix is established for the CU site.

SUBJECT ID	HPD ORDER	QSIN ORDER	Enrollment Appointment	paid	SESSION 1	X(notes)	paid	SESSION 2	X(notes)	paid	SESSION 3	X(notes)	paid	SESSION 4	X(notes)	paid	SESSION 5	X(notes)	paid	SESSION 6	X(notes)	paid	SESSION 7	X(notes)	paid	(SESSION 8)	X(notes)	paid	OTHER NOTES?
W01	Order1	Qorder1	Enrolled date: MMDDYY		hSQ			hSL			hSL			hSL			hSL			hSL			hSL			hSN/hLD			
W02	Order1	Qorder2	Enrolled date: MMDDYY		hSL			hSL			hSL			hSL			hSL			hSL			hSN/hLD			hSQ			
W03	Order1	Qorder3	Enrolled date: MMDDYY		hSN/hLD			hSQ			hSL			hSL			hSL			hSL			hSL			hSL			
W04	Order1	Qorder4	Enrolled date: MMDDYY		hSQ			hSN/hLD			hSL			hSL			hSL			hSL			hSL			hSL			
W05	Order1	Qorder5	Enrolled date: MMDDYY		hSL			hSL			hSL			hSL			hSL			hSL			hSQ			hSN/hLD			
W06	Order1	Qorder6	Enrolled date: MMDDYY		hSN/hLD			hSL			hSL			hSL			hSL			hSL			hSL			hSQ			
W07	Order2	Qorder1	Enrolled date: MMDDYY		hSQ			hSL			hSL			hSL			hSL			hSL			hSN/hLD						
W08	Order2	Qorder2	Enrolled date: MMDDYY		hSL			hSL			hSL			hSL			hSL			hSN/hLD			hSQ						
W9	Order2	Qorder3	Enrolled date: MMDDYY		hSN/hLD			hSQ			hSL			hSL			hSL			hSL			hSL						
W10	Order2	Qorder4	Enrolled date: MMDDYY		hSQ			hSN/hLD			hSL			hSL			hSL			hSL			hSL						
W11	Order2	Qorder5	Enrolled date: MMDDYY		hSL			hSL			hSL			hSL			hSL			hSQ			hSN/hLD						
W12	Order2	Qorder6	Enrolled date: MMDDYY		hSN/hLD			hSL			hSL			hSL			hSL			hSL			hSQ						
W13	Order3	Qorder1	Enrolled date: MMDDYY		hSQ			hSL			hSL			hSL			hSL			hSL			hSL			hSN/hLD			
W14	Order3	Qorder2	Enrolled date: MMDDYY		hSL			hSL			hSL			hSL			hSL			hSL			hSN/hLD			hSQ			
W15	Order3	Qorder3	Enrolled date: MMDDYY		hSN/hLD			hSQ			hSL			hSL			hSL			hSL			hSL			hSL			
W16	Order3	Qorder4	Enrolled date: MMDDYY		hSQ			hSN/hLD			hSL			hSL			hSL			hSL			hSL			hSL			
W17	Order3	Qorder5	Enrolled date: MMDDYY		hSL			hSL			hSL			hSL			hSL			hSL			hSQ			hSN/hLD			
W18	Order3	Qorder6	Enrolled date: MMDDYY		hSN/hLD			hSL			hSL			hSL			hSL			hSL			hSL			hSQ			
W19	Order4	Qorder1	Enrolled date: MMDDYY		hSQ			hSL			hSL			hSL			hSL			hSL			hSL			hSN/hLD			
W20	Order4	Qorder2	Enrolled date: MMDDYY		hSL			hSL			hSL			hSL			hSL			hSL			hSN/hLD			hSQ			
W21	Order4	Qorder3	Enrolled date: MMDDYY		hSN/hLD			hSQ			hSL			hSL			hSL			hSL			hSL			hSL			
W22	Order4	Qorder4	Enrolled date: MMDDYY		hSQ			hSN/hLD			hSL			hSL			hSL			hSL			hSL			hSL			
W23	Order4	Qorder5	Enrolled date: MMDDYY		hSL			hSL			hSL			hSL			hSL			hSL			hSQ			hSN/hLD			
W24	Order4	Qorder6	Enrolled date: MMDDYY		hSN/hLD			hSL			hSL			hSL			hSL			hSL			hSL			hSQ			
W25	Order5	Qorder1	Enrolled date: MMDDYY		hSQ			hSL			hSL			hSL			hSL			hSL			hSN/hLD						
W26	Order5	Qorder2	Enrolled date: MMDDYY		hSL			hSL			hSL			hSL			hSL			hSN/hLD			hSQ						
W27	Order5	Qorder3	Enrolled date: MMDDYY		hSN/hLD			hSQ			hSL			hSL			hSL			hSL			hSL						
W28	Order5	Qorder4	Enrolled date: MMDDYY		hSQ			hSN/hLD			hSL			hSL			hSL			hSL			hSL						
W29	Order5	Qorder5	Enrolled date: MMDDYY		hSL			hSL			hSL			hSL			hSL			hSL			hSQ			hSN/hLD			
W30	Order5	Qorder6	Enrolled date: MMDDYY		hSN/hLD			hSL			hSL			hSL			hSL			hSL			hSQ						
W31	Order6	Qorder1	Enrolled date: MMDDYY		hSQ			hSL			hSL			hSL			hSL			hSL			hSL			hSN/hLD			
W32	Order6	Qorder2	Enrolled date: MMDDYY		hSL			hSL			hSL			hSL			hSL			hSL			hSN/hLD			hSQ			
W33	Order6	Qorder3	Enrolled date: MMDDYY		hSN/hLD			hSQ			hSL			hSL			hSL			hSL			hSL			hSL			
W34	Order6	Qorder4	Enrolled date: MMDDYY		hSQ			hSN/hLD			hSL			hSL			hSL			hSL			hSL			hSL			
W35	Order6	Qorder5	Enrolled date: MMDDYY		hSL			hSL			hSL			hSL			hSL			hSL			hSQ			hSN/hLD			
W36	Order6	Qorder6	Enrolled date: MMDDYY		hSN/hLD			hSL			hSL			hSL			hSL			hSL			hSL			hSQ			
W37	Order1	Qorder1	Enrolled date: MMDDYY		hSQ			hSL			hSL			hSL			hSL			hSL			hSL			hSN/hLD			
W38	Order1	Qorder2	Enrolled date: MMDDYY		hSL			hSL			hSL			hSL			hSL			hSL			hSN/hLD			hSQ			
W39	Order1	Qorder3	Enrolled date: MMDDYY		hSN/hLD			hSQ			hSL			hSL			hSL			hSL			hSL			hSL			
W40	Order1	Qorder4	Enrolled date: MMDDYY		hSQ			hSN/hLD			hSL			hSL			hSL			hSL			hSL			hSL			
W41	Order1	Qorder5	Enrolled date: MMDDYY		hSL			hSL			hSL			hSL			hSL			hSL			hSQ			hSN/hLD			
W42	Order1	Qorder6	Enrolled date: MMDDYY		hSN/hLD			hSL			hSL			hSL			hSL			hSL			hSL			hSQ			
W43	Order2	Qorder1	Enrolled date: MMDDYY		hSQ			hSL			hSL			hSL			hSL			hSL			hSN/hLD						
W44	Order2	Qorder2	Enrolled date: MMDDYY		hSL			hSL			hSL			hSL			hSL			hSN/hLD			hSQ						
W45	Order2	Qorder3	Enrolled date: MMDDYY		hSN/hLD			hSQ			hSL			hSL			hSL			hSL			hSL						
W46	Order2	Qorder4	Enrolled date: MMDDYY		hSQ			hSN/hLD			hSL			hSL			hSL			hSL			hSL						
W47	Order2	Qorder5	Enrolled date: MMDDYY		hSL			hSL			hSL			hSL			hSL			hSQ			hSN/hLD						
W48	Order2	Qorder6	Enrolled date: MMDDYY		hSN/hLD			hSL			hSL			hSL			hSL			hSL			hSQ						
W49	Order3	Qorder1	Enrolled date: MMDDYY		hSQ			hSL			hSL			hSL			hSL			hSL			hSL			hSN/hLD			
W50	Order3	Qorder2	Enrolled date: MMDDYY		hSL			hSL			hSL			hSL			hSL			hSL			hSN/hLD			hSQ			
W51	Order3	Qorder3	Enrolled date: MMDDYY		hSN/hLD			hSQ			hSL			hSL			hSL			hSL			hSL			hSL			
W52	Order3	Qorder4	Enrolled date: MMDDYY		hSQ			hSN/hLD			hSL			hSL			hSL			hSL			hSL			hSL			
W53	Order3	Qorder5	Enrolled date: MMDDYY		hSL			hSL			hSL			hSL			hSL			hSL			hSQ			hSN/hLD			
W54	Order3	Qorder6	Enrolled date: MMDDYY		hSN/hLD			hSL			hSL			hSL			hSL			hSL			hSL			hSQ			
W55	Order4	Qorder1	Enrolled date: MMDDYY		hSQ			hSL			hSL			hSL			hSL			hSL			hSL			hSN/hLD			
W56	Order4	Qorder2	Enrolled date: MMDDYY		hSL			hSL			hSL			hSL			hSL			hSL			hSN/hLD			hSQ			
W57	Order4	Qorder3	Enrolled date: MMDDYY		hSN/hLD			hSQ			hSL			hSL			hSL			hSL			hSL			hSL			
W58	Order4	Qorder4	Enrolled date: MMDDYY		hSQ			hSN/hLD			hSL			hSL			hSL			hSL			hSL			hSL			
W59	Order4	Qorder5	Enrolled date: MMDDYY		hSL			hSL			hSL			hSL			hSL			hSL			hSQ			hSN/hLD			
W60	Order4	Qorder6	Enrolled date: MMDDYY		hSN/hLD			hSL			hSL			hSL			hSL			hSL			hSL			hSQ			

3.2.2.2.1. Enrollment Update

Study enrollment is actively underway at both Washington and Colorado study sites. Both sites have recruited subjects through a combination of recruitment flyers, word-of-mouth, and email contacts. At the Washington site, 50 subjects have been enrolled in the study, with 9 additional subjects tested but failing to qualify. At the Colorado site, 27 subjects have been enrolled in the study, with 2 additional subjects tested but failing to qualify. The number of complete datasets per device per task varies across sites. At UW, hSQ testing has been completed in 33 subjects, hSL testing has been completed in open ear and at least one device condition in 29 subjects, and hSN

testing has been completed in 27 subjects. At CU, hSQ testing has been completed in 21 subjects, hSL testing has been completed in open ear and at least one device condition in 20 subjects, and hSN testing has been completed in 17 subjects.

For both UW and CU study sites, the goal is to continue to enroll at minimum 15 subjects per quarter (roughly 1 per week) for the duration of Year 3 until the target number of 60 complete datasets per device per task is reached at both sites.

Enrollment status is summarized in Table 2.

Table 2. Human subject enrollment status. *The number of "completed" subjects is based on the task at each site for which the fewest complete datasets exist, i.e. other tasks have accumulated a greater number of complete datasets on one or more devices.

Site	Screened	Scheduled	Completed
University of Colorado	29	27	17*
University of Washington	59	50	27*

3.2.2.2.2. Testing Results

3.2.2.2.2.1. Sound Localization (hSL)

Subjects are actively completing localization (hSL) in the order specified in the testing matrix in Full-scale testing across sites follows a pre-programmed testing matrix (Table 1) in which the ordering of testing across tasks and hearing protectors is appropriately counterbalanced to ensure even accumulation of data and account for anticipated subject attrition, with testing blocked such that subjects will complete all testing within a minimal number of sessions, while maximizing the likelihood that complete data for a given task will be obtained in the event of attrition. This protocol also reduces variability of hearing protector placement across trials within each task, minimizing that potential source of variability.

Table 1. Summary hSL results from UW and CU sites are illustrated below. Two styles of plot are shown. First, raw response data are given as scatterplots for each condition, in which perfect performance (no error) would fall along the y=x unity line (dashed black), and datapoints falling further from the unity line indicate larger error magnitudes. Because plots contain thousands of datapoints, the horizontal positions of points within each cluster (clusters corresponding to discrete target angles) are randomly jittered based on the densities of the distribution of points. Second, a summary of combined error magnitude (both azimuth and elevation components) is shown as a grid. Note that, throughout, data are in the same format for UW and CU sites, but the set of elevations under test differs at the two sites (-30, 0, +30 at UW, 0, +30, +60 at CU).

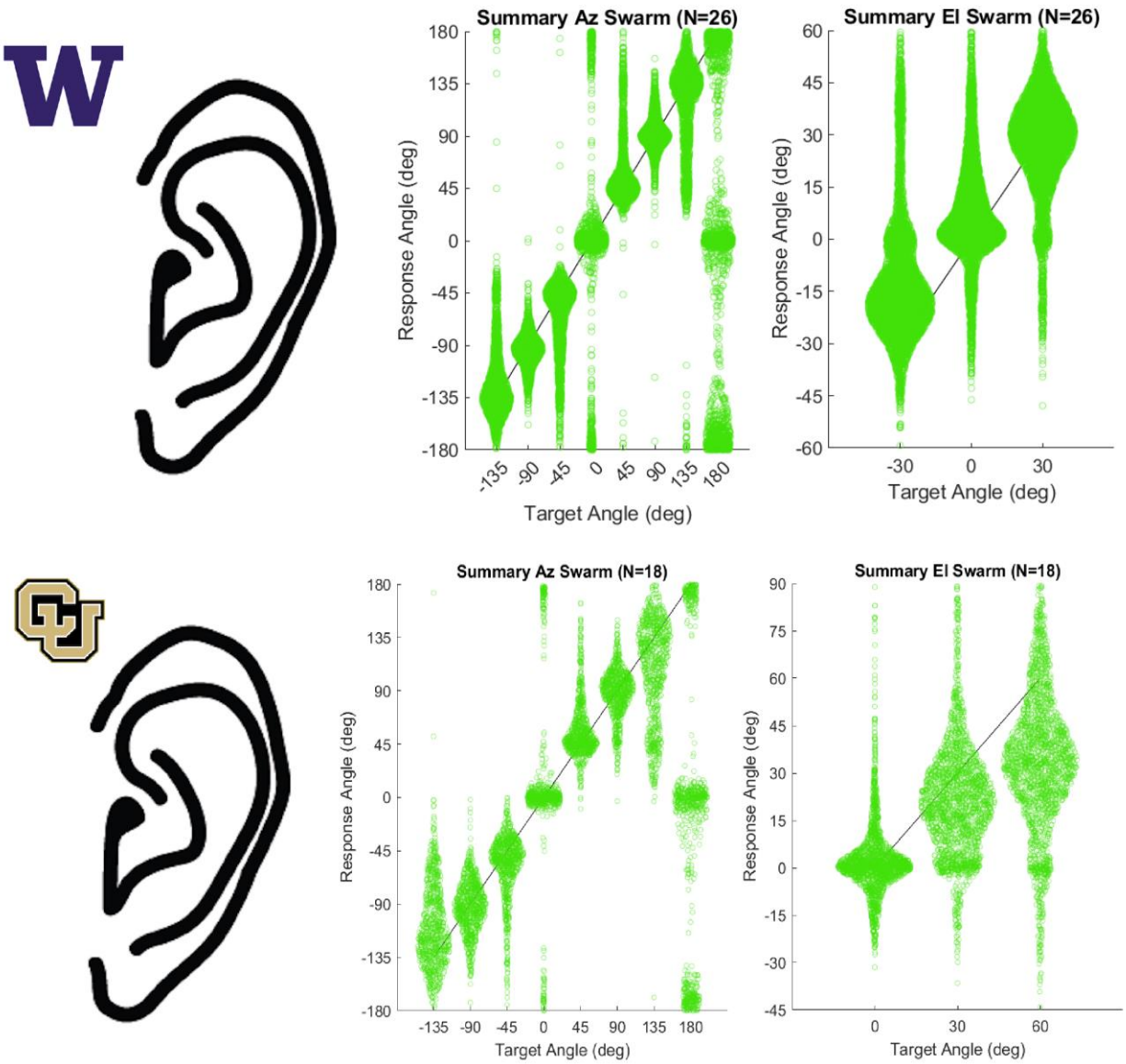

Figure 10. Performance is shown for subjects at both UW (upper) and CU (lower) sites in the open ear condition. Plots show response angle (y) versus target angle (x). The left plots show all responses pooled across subjects (number of subjects given in panel title) in terms of azimuth; the right plots show the same in terms of elevation. Within each panel, perfect performance is indicated by the dashed black unity line (y=x). Points falling further from this line evidence larger error components. Because thousands of points are shown, horizontal positions are randomly jittered by a magnitude determined by the density of the underlying distribution. In general, open ear performance clusters around the unity line, although secondary clusters, most especially a cluster near 0° given a source at 180° (the classic front-back confusion) are evident at both sites. At the CU site, responses for the most eccentric elevation (+60°) tended to undershoot the target (+60°), a phenomenon described previously (e.g., Makous, J. C., & Middlebrooks, J. C. (1990). Two-dimensional sound localization by human listeners. Journal of the Acoustical Society of America, 87(5), 2188–2200.)

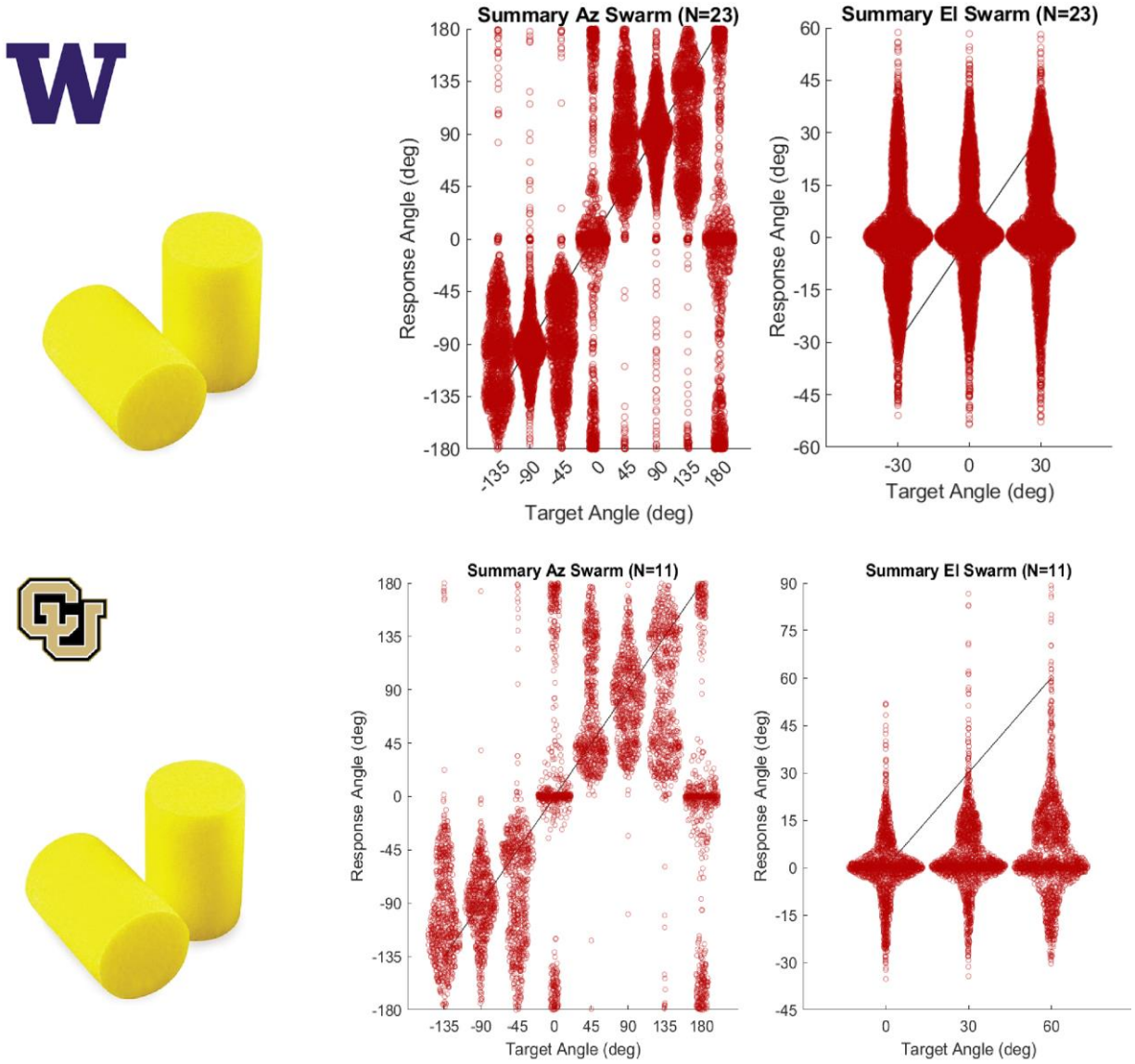

Figure 11. Performance is shown for subjects at both UW (upper) and CU (lower) sites in the EAR Classic condition. Format as in Figure 10. Azimuthal responses show a dramatic increase in large errors (vertical spread), particularly front/back errors, compared to the open ear condition. Elevation errors also show increased spread, but a prominent mode at the horizon is evident in all cases, indicating that subjects perceive a majority of targets near the horizon regardless of the target elevation.

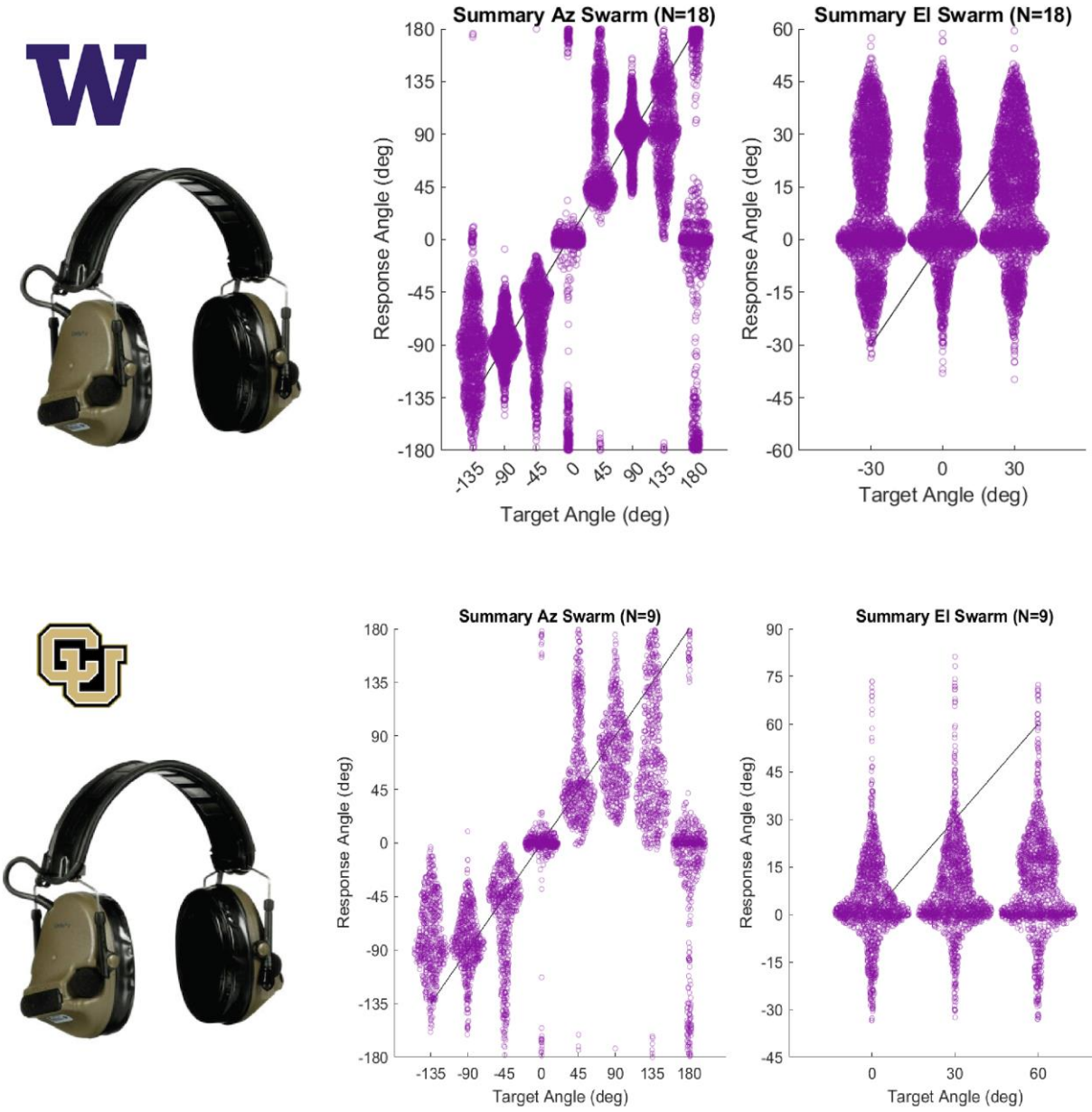

Figure 12. Performance is shown for subjects at both UW (upper) and CU (lower) sites in the Peltor Com-Tac V condition. Azimuth responses feature a decreased density of rear-hemifield responses, showing that subjects tend to perceive rear hemifield targets in the frontal hemifield. Elevation responses again appear to have collapsed towards 0° elevation for all elevation targets, although a secondary 'swell' in the elevation swarm chart is evident, attributable to a subset of subjects who tend to perceive all targets 15-30 degrees above the horizon.

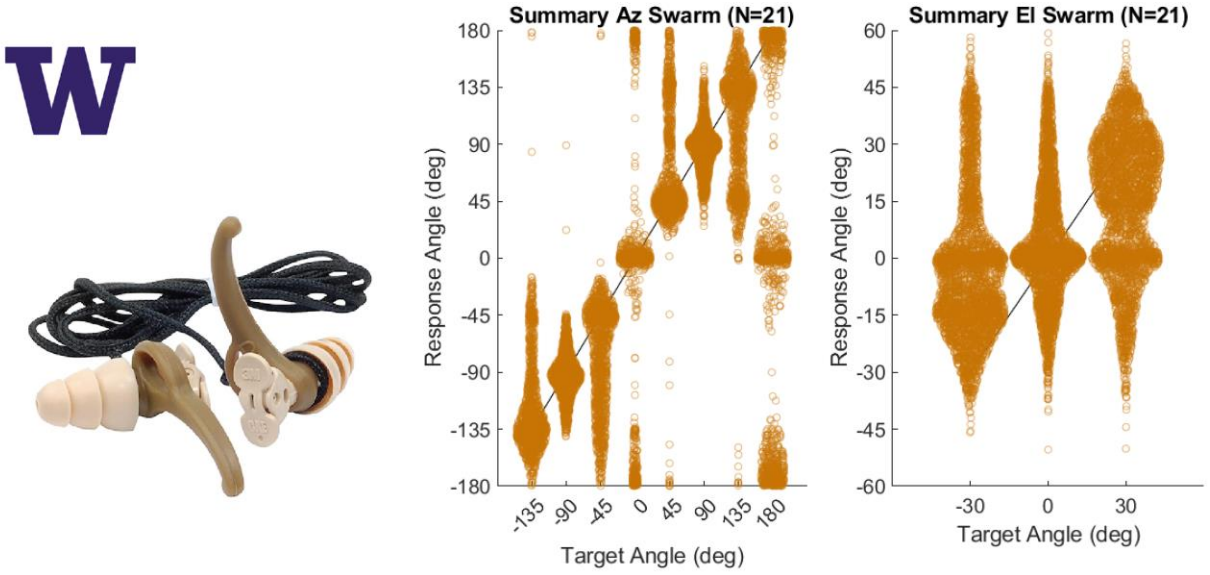

Figure 13. Performance is shown for subjects at the UW site using the CAE Gen. 4.1 HPDs in open mode. Azimuthal responses show greater localization error (except at 0° azimuth) and front/back errors than the open ear condition. Interestingly, while many elevation responses cluster around the horizon, leading to a mode near 0 degrees elevation for all three source elevations (-30, 0, +30), several subjects demonstrated systematic variation of elevation responses, such that the dominant mode of each swarm is in the direction of the veridical elevation. CAEs are tested at UW only.

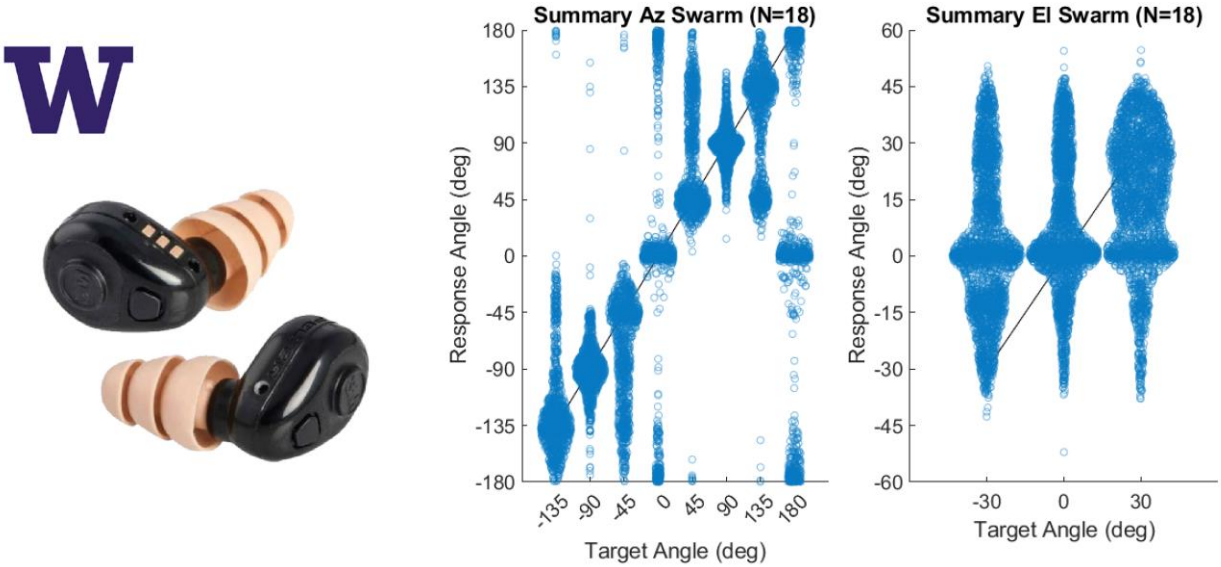

Figure 14. Performance is shown for subjects at the UW site using the TEP-200 active earplug in gain setting #2. Azimuth and elevation responses are both severely disrupted, with a high degree of spread for both, although the distribution of elevation responses at target +30° includes a mode in the vicinity of the target elevation. TEP-200s are tested at UW only.

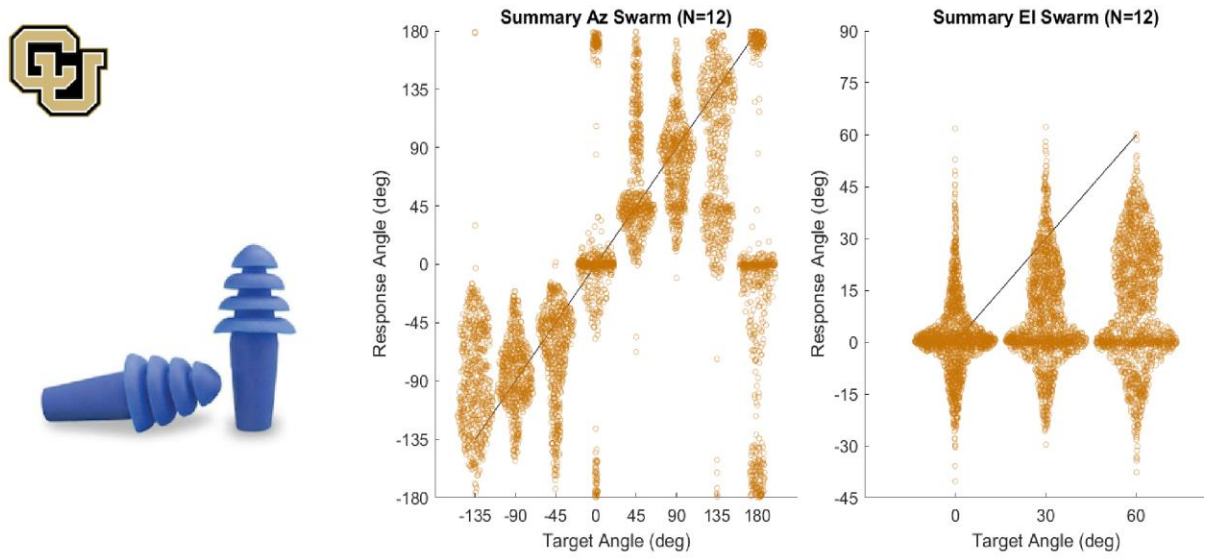

Figure 15. Performance is shown for subjects at the CU site using the Elvex Quattro. Azimuth and elevation responses are both degraded relative to open ear, but, interestingly, demonstrate less spread than those for the other high-attenuation passive device in the present study, the EAR Classic. The dominant mode of elevation responses, however, remains at 0º (i.e., on the horizon, regardless of the target elevation). The Elvex Quattro is only tested at the CU study site.

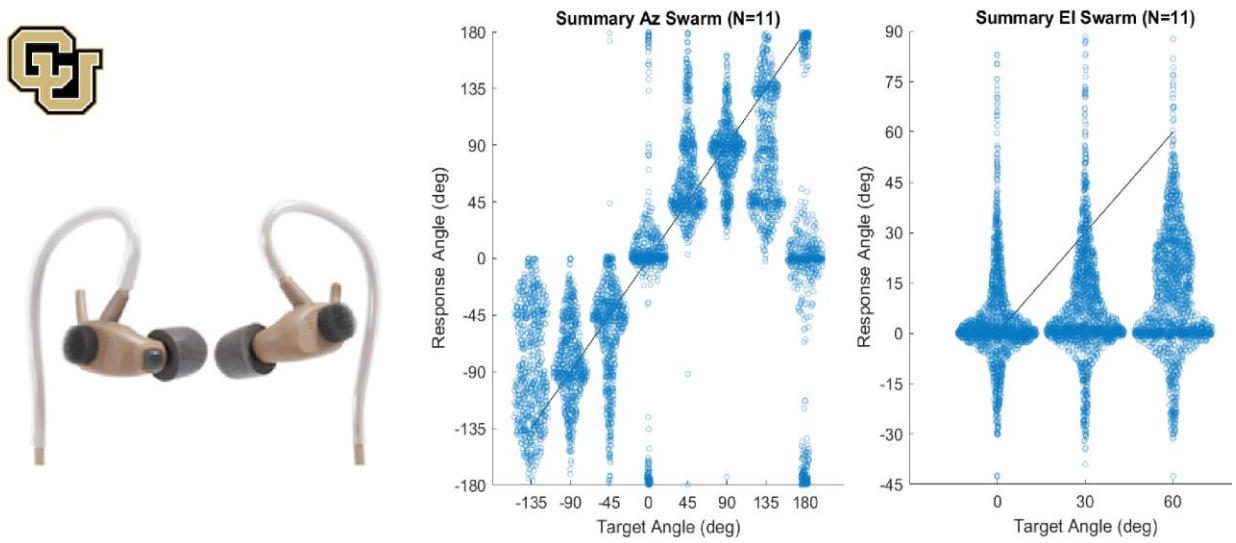

Figure 16. Performance is shown for subjects at the CU site using the Invisio X5 active earplug in gain setting #2. Azimuthal responses again show a significant increase in spread relative to the open ear condition, and also an apparent decrease in rear hemifield responses (i.e., more sources perceived in front). Elevation responses are also again degraded, with significant spread and a prominent mode near the horizon. The Invisio X5 is only tested in the hSL task at the CU site.

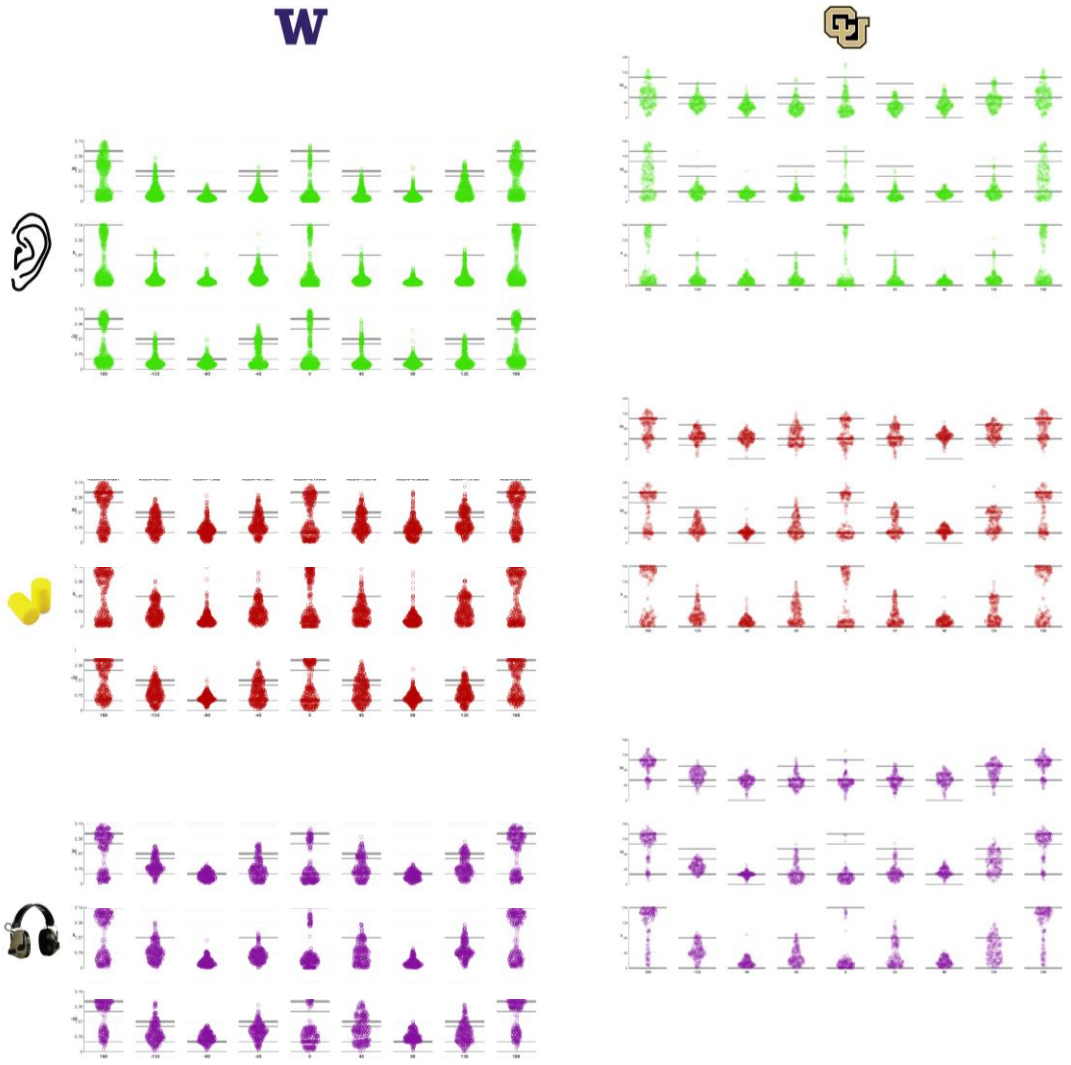

Figure 17 (electronic version may be zoomed to increase detail). Localization errors, expressed as total error magnitude in radians for the full 'grid' of speaker locations at each site for the three hSL conditions tested at both (open, EAR, Com-Tac). Within each of the 6 panels, columns are target azimuths and rows are unique target elevations. From left to right, target azimuths are -180, -135, -90, -45, 0, 45, 90, 135, and 180 (180º data are duplicated/plotted twice to enable visualization of error trends in either direction). Rows are elevations; for the UW site (left), -30, 0, +30; for the CU site (right), 0, +30, +60 (bottom to top). CU and UW plots are horizontally staggered to enable side-by side comparison of the 16 overlapping speaker locations at each site. Points within each sub panel describe the distribution of errors for the given location. Perfect performance (0 error) would lead to a density of points at the bottom of each sub-panel. The largest possible error is 180º/pi radians (response in diametric opposition to target), most commonly observed in HPD conditions for sources at 0º elevation and 0º or 180º azimuth (i.e., classic front-back confusions). Gray lines within each panel demarcate expected values of errors given a hemifield reversal in azimuth and collapse-to-zero error in elevation (thick line), a hemifield reversal only (elevation accurate) (medium line), or collapse-to-zero error in elevation only (hemifield/azimuth) accurate (thin line). The distribution of errors across sites is broadly similar; cross-site comparison will be formalized in Year 3.

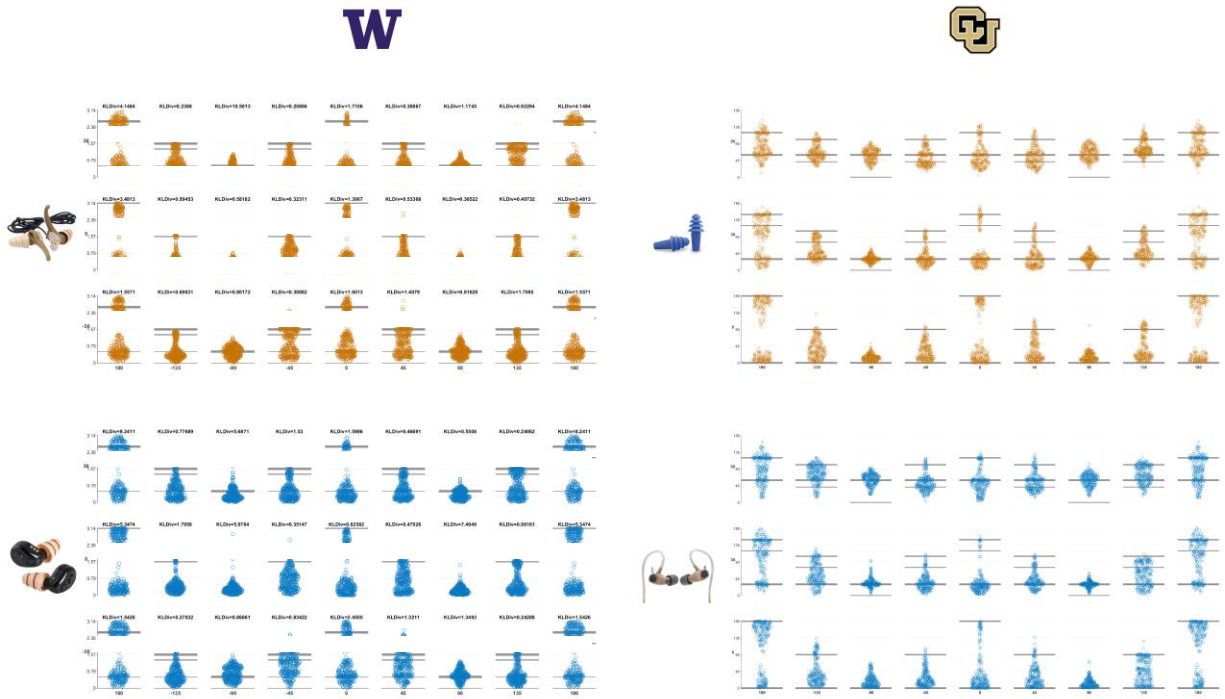

Figure 18 (electronic version may be zoomed to increase detail). Localization errors, expressed as total error magnitude in radians for the full 'grid' of speaker locations for the UW site in the CAE Gen 4.1 open mode (upper left) and TEP-200 active earplug (lower left) conditions, and for the CU site in the Elvex Quattro (upper right) and Invisio X5 active earplug (lower right) conditions. Format as in Figure 17. Distributions suggest notably different patterns (distributions and modes) of errors across devices, consistent with cross-device differences in scatterplots of Figures 13-16.

3.2.2.2.2.2. Sound Quality (hSQ)

Human Sound Quality testing has progressed at both UW and CU study sites. hSQ consists of two separate speech-in-noise tasks: (1) the QuickSIN, which presents a target sentence co-located in a background of multi-talker babble and requires subjects to verbally repeat back the sentences to the experimenter, and (2) the Modified Rhyme Test (MRT), which presents target words in a background of omnidirectional pink noise and requires subjects to identify the target word using a keypad given a closed set of 6 similar (rhyming) words, which are displayed on a monitor inside the testing arena. Performance is quantified, across Open Ear and HPD conditions, according to the percent of target words correctly identified as a function of signal-to-noise ratio. Lower signal-to-noise ratios make the task more difficult, resulting in lower percent-correct (or number-of-words-correct) scores. Exemplar data from the UW study site are shown in Figure 19 (QuickSIN data) and Figure 20 (MRT data).

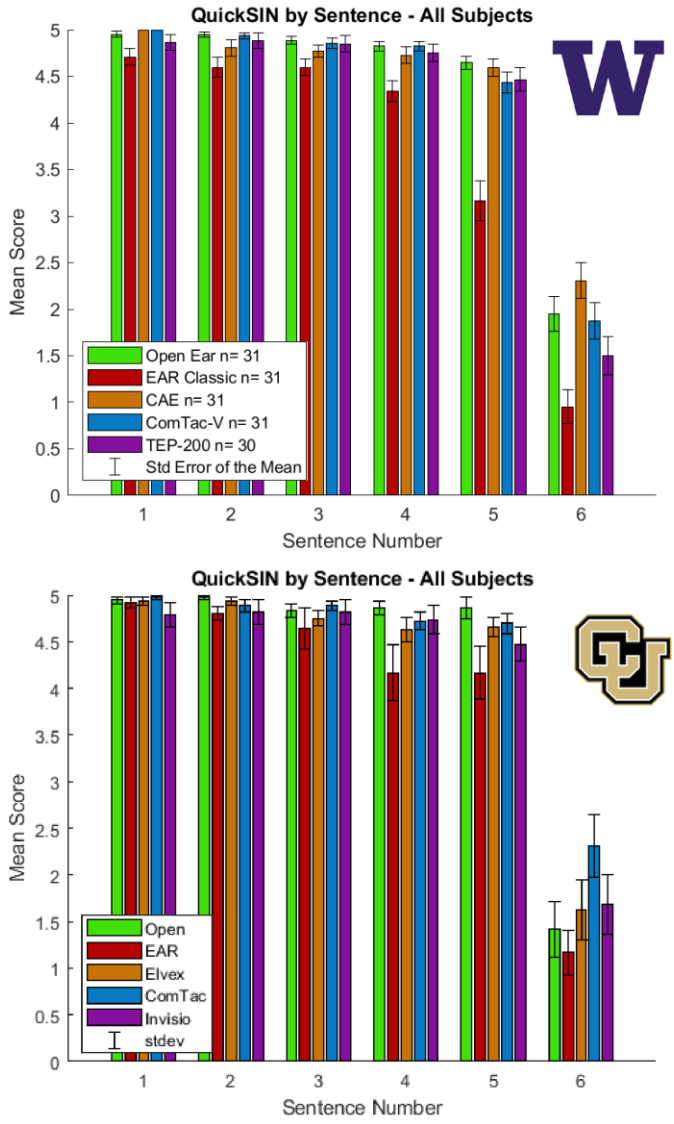

Figure 19. Summary QuickSIN data from the UW study site (upper panel) and the CU study site (lower panel). Major groupings are sentence numbers in the QuickSIN sequence. In this sequence, each sentence becomes progressively more difficult to hear as the level of background noise (multi-talker babble) increases (i.e., as the SNR decreases in 5-dB decrements from +25 dB in Sentence One to 0 dB in Sentence Six. Bars show mean words correct (out of 5; equivalent percent correct can be obtained by multiplying these values by 20). Error bars given the standard error of the mean (N at UW indicated in the inset legend; N at CU = 19). Patterns are broadly similar across sites; for most sentence numbers (SNRs), best performance is observed in the Open condition, though active HPDs (ComTac, TEP-200 (UW), or Invisio (CU) produce similarly good performance in many cases. The EAR Classic (high attenuation passive device) produces the worst performance in all cases at both sites. At the lowest SNR (0 dB), performance approaches the floor, with 1-2 words (of 5) correct on average, and increased variability. In this case, at UW, the best absolute mean score is with the CAE (not tested at CU), while the second best is with the ComTac. At CU (at 0 dB), best performance is with the ComTac.

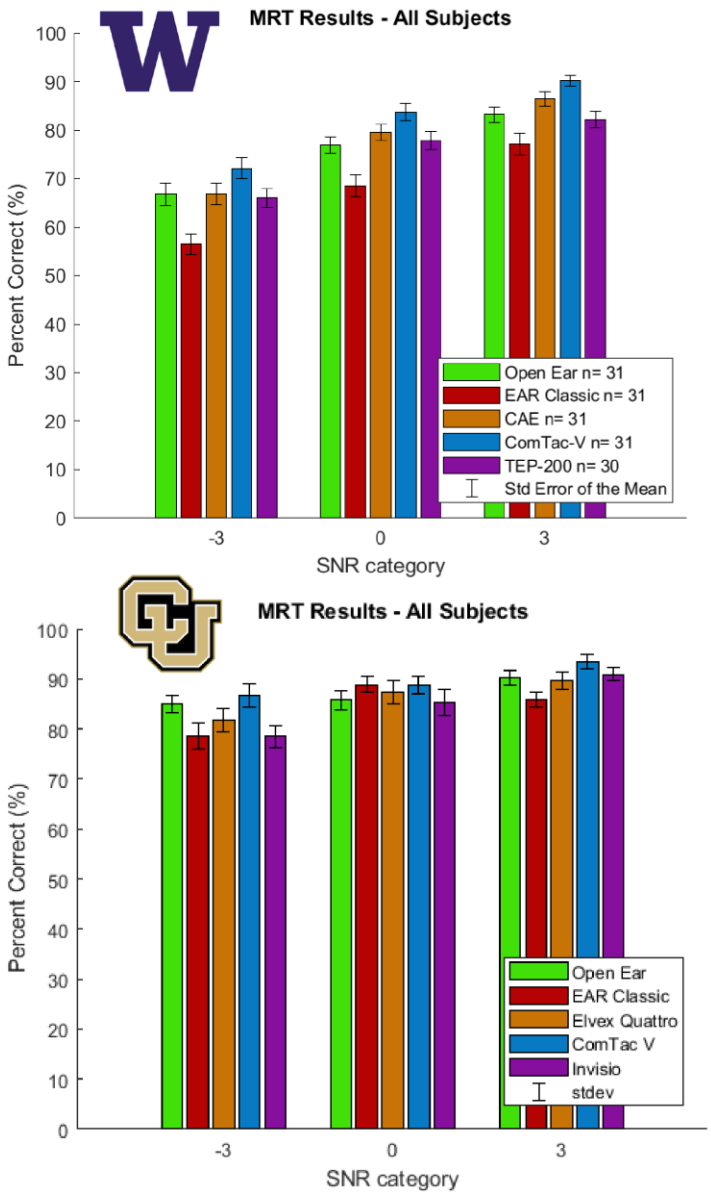

Figure 20. Summary MRT data from the UW study site (upper panel) and the CU study site (lower panel). Major groupings are the signal-to-noise ratios (-3, 0, +3) defined by variation in the level of presented pink noise. Error bars give standard error of the mean (N at UW indicated in the inset legend; N at CU = 19). The pattern of performance is broadly similar across sites. Performance improves with increasing SNR, but is generally worst for the EAR Classic and best for the ComTac V. Notably, in this task, the target is presented from 0 degrees (directly in front of the subject) while pink noise is presented from ±45, ±90, ±135, and 180 degrees. Therefore, a device with a strong forward-directional characteristic (e.g., such as the forward-directional microphones of the ComTac) should be expected to outperform comparatively omnidirectional open ears. To capture this influence, a portion of future testing will present the target word from an off-midline location. Some performance differences across sites (somewhat higher overall scores at CU; no apparent cross-device differences at CU at 0 dB SNR only) will be monitored as the number of complete datasets across sites becomes more similar.

3.2.2.2.2.3. Self-Noise (hSN)

The human subjects self-noise test leverages a real-ear-attenuation-at-threshold (REAT) under headphones paradigm to measure the effective change in auditory sensitivity produced by active HPDs. Specifically, while active HPDs are designed to 'pass' low-level sounds, hum from active electronics may serve to mask sounds near threshold. In practice, REAT in the hSN task is calculated by computing the difference between open-ear thresholds and active-HPD-affected thresholds. Positive values indicate that thresholds were higher for the given HPD than for open ear. Both Washington and Colorado study sites are testing the TEP-200 and Invisio X5 active HPDs. Data from Washington is shown in Figure 21. Data from Colorado is shown in Figure 22.

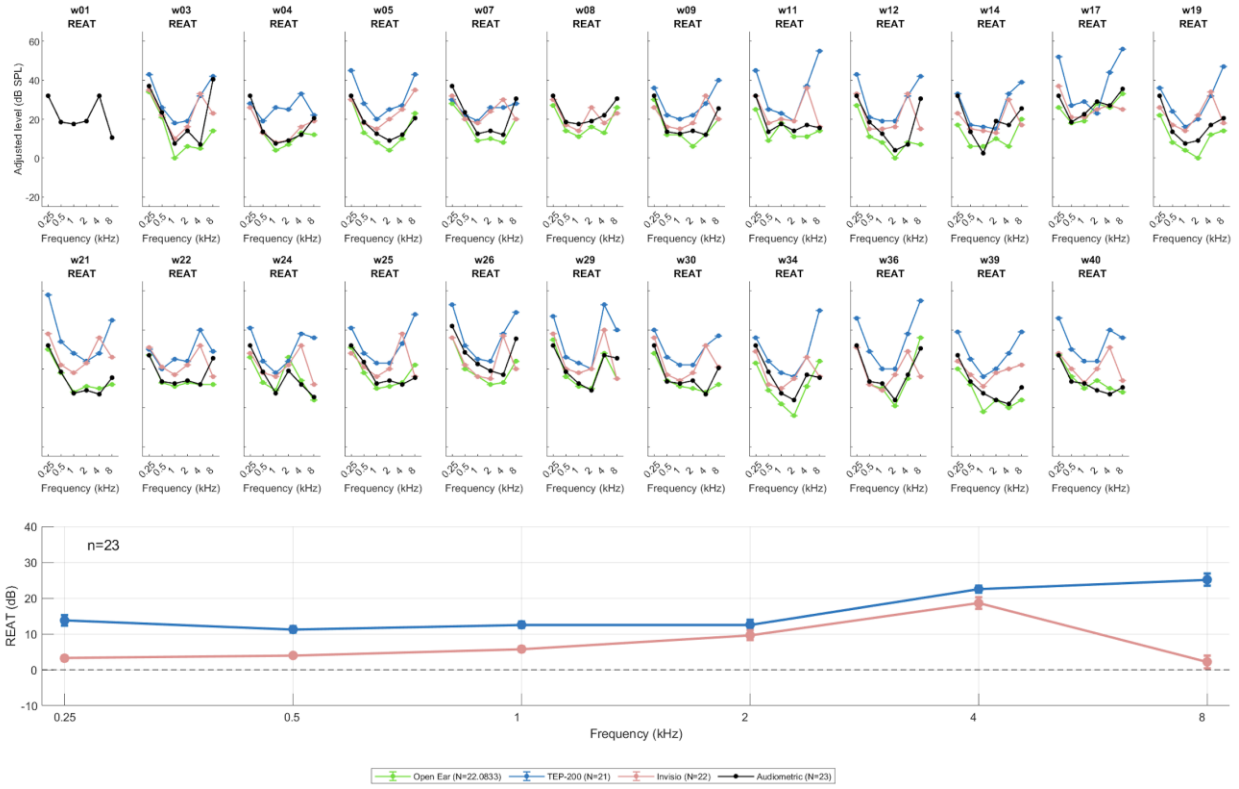

Figure 21. Exemplar hSN data from the UW study site. Small upper panels show data for individual subjects across 3 conditions: Open ear (green), TEP-200 (blue), and Invisio X5 (red). The TEP-200 was tested in Gain setting 2 of 4. The Invisio X5 was tested in gain setting 2 of 3. For comparison purposes, the open-ear audiogram measured by an audiologist at the intake appointment is plotted in black, generally following and often intersecting the self-determined open-ear threshold. Blue and red curves fall above green curves in most but not all cases. Subsets of data are missing for a few subjects. Lower panel: Mean computed REAT values for TEP-200 and Invisio X5 (effectively, the distance from red or blue to green curves) across subjects. Error bars plot the standard error of the mean (across N subjects as indicated). Performance patterns are compared to expected gain and self-noise characteristics of these devices/settings.

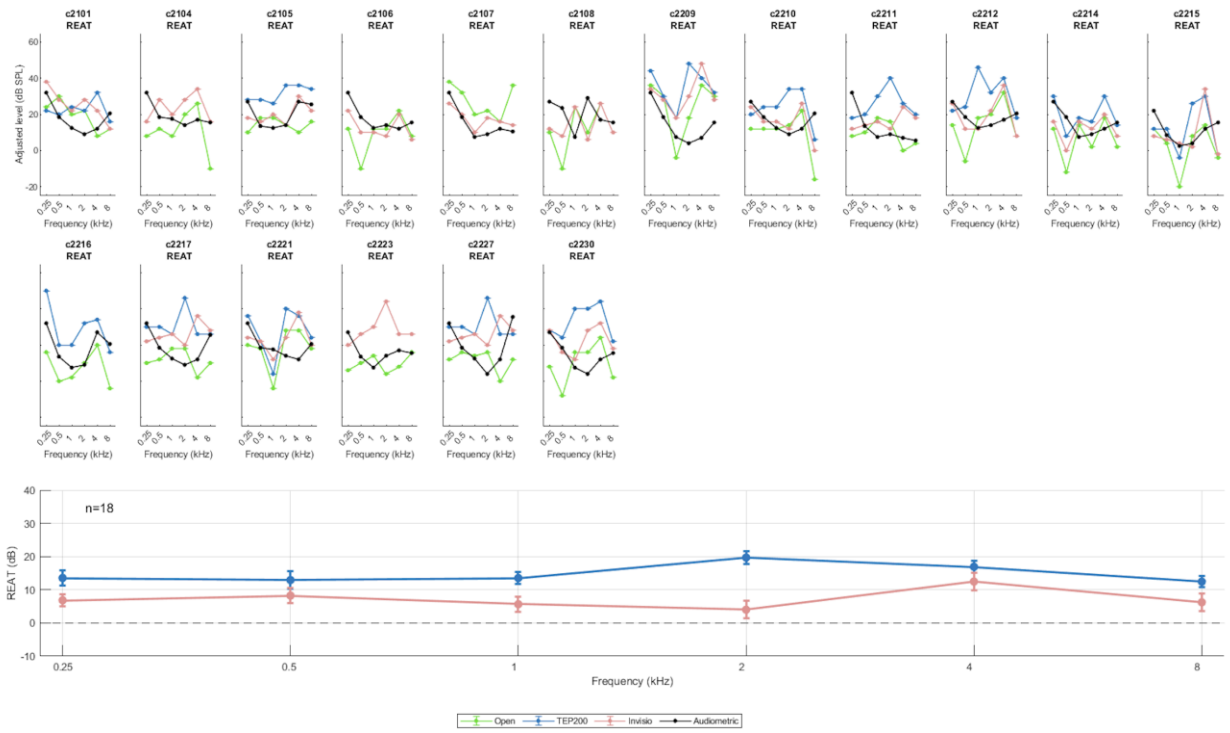

Figure 22: Exemplar hSN data from the CU study site. Format as in Figure 21. Upper panels display data for 18 individual subjects. Subsets of data are missing for a few subjects. Blue and red curves (HPD conditions) again generally fall above green curves (open condition) evidencing threshold elevation during active HPD use. However, the agreement between green curves and black curves (audiometric intake data) is not as clear, and there are several points of significant divergence. The origin of these discrepancies is under investigation, and may relate to calibrations at the CU site. Note that since REAT is a relative measure, calibrations (affecting absolute values in dB SPL) would not be expected to impact REAT calculations. Lower panel: Mean computed REAT values for TEP-200 and Invisio X5 (effectively, the distance from red or blue to green curves) across subjects. Error bars plot the standard error of the mean. As at the UW site, REAT values are higher for the TEP-200 than for the Invisio X5. Pending confirmation and resolution of SPL absolute values, CU data will be compared with UW data and entered into the electromechanical comparison workflow.

3.2.2.2.2.4. Level-Dependence (hLD)

The human subject level-dependence task (hLD) was designed to capture the nonlinear attenuation characteristics of active HPDs by leveraging an alternating-binaural-loudness-balancing (ABLB) paradigm, in which subjects are required to perceptually match the sound level between the ears (to produce an 'intracranially centered' auditory image). The task is performed in a three-step sequence: (1) match the ears with both open, (2) match the ears with an HPD in one ear (to the extent that HPD provides attenuation, upward level adjustment of that ear will be required), (3) match the ears with HPDs in both ears (following step 2, additional upward adjustment should be required in the second ear to re-balance the effective level since both ears are now impacted by attenuation). Step 2 provides a "between-ear" estimate of attenuation, while Step 3 provides a "within-ear" estimate of attenuation. To the extent that the attenuation provided by a given device is level-dependent, higher presentation levels should elicit greater attenuation,

as indexed by more adjustment required in the HPD-impacted ear(s). Both UW and CU study sites proceeded testing TEP-200 and Invisio X5 HPDs, with UW accumulating data for 21 subjects and CU accumulating data for 8 subjects.

Interim analysis of hLD data led to the identification of two fundamental issues. The first issue is that engaging the limiting behavior of the devices requires the intentional presentation of high-intensity signals. While OSHA standards specify exposure time limits as a function of level up to 115 dBA, subjects may find excessive presentation levels in a research setting uncomfortable, raising ethical concerns. Thus, our maximum presentation level was limited to 90 dB SPL – a level above, but only approximately 5 dB above, the expected limiting level of the devices under test. Thus, appropriate task performance would be expected to reveal nonlinearity in attenuation on the order of 5 dB. However, a second issue that emerged was performance variability, ostensibly due to the complexity of the task, requiring multiple steps of headphone removal and HPD placement – which is also technically difficult because of the necessity to align active HPDs inside the headphone earcups in a reproducible fashion without causing discomfort or triggering device feedback. The foregoing issues are evidenced in summary data shown for the UW site in Figure 23 (N=21 subjects); similar observations (data not shown) were made at the CU site in a smaller number of subjects (N=8).

Higher-intensity presentation levels (≫100 dB SPL) would be expected to more fully reveal level-dependent attenuation, perhaps allowing (with sufficient statistical power) identification of level-dependence in attenuation. However, variability in device placement and/or device performance could potentiate injurious sound exposures to subjects, making the use of such higher levels, in our view, unethical. This pitfall was foreseen as a possibility in the original proposal, with the alternate solution as follows: A modified version of hLD testing will be transitioned to cadaveric specimens, for which it will be possible to empirically measure transmission/attenuation of arbitrary sound levels (well exceeding those possible with human subjects). These measurements will proceed in tandem with hIN measurements (below) in Year 3.

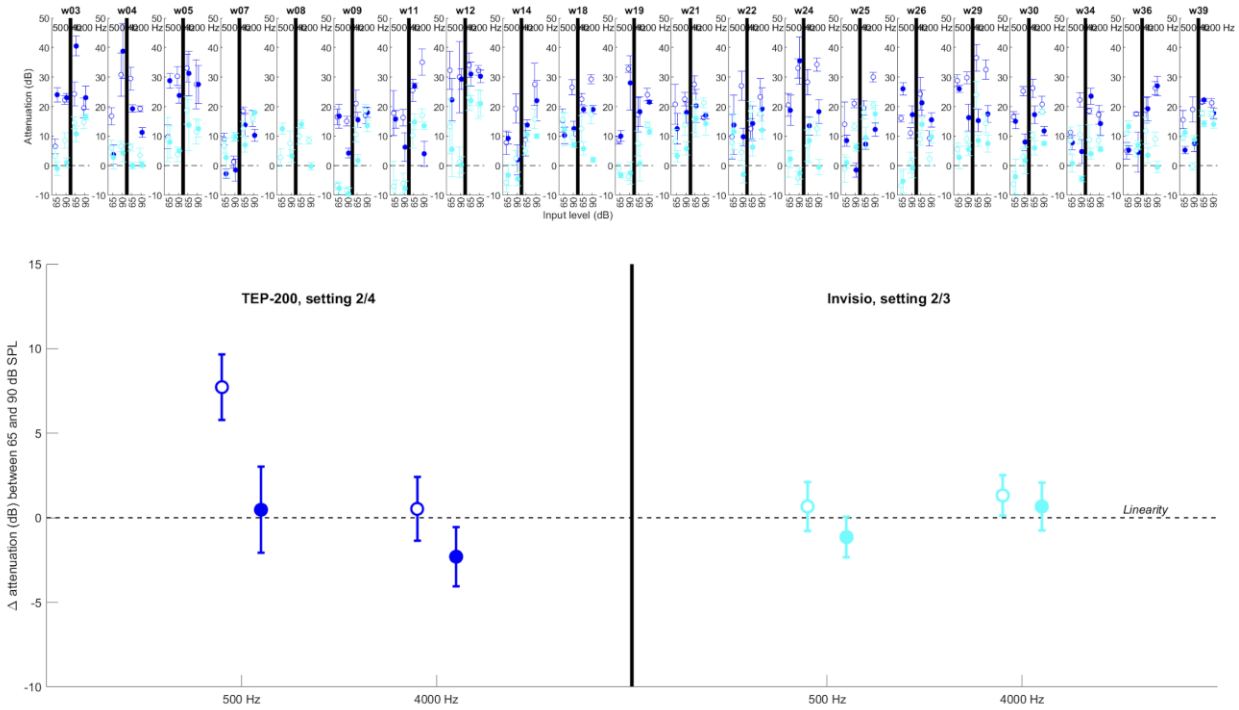

Figure 23. Exemplar hLD data from the UW study site. Top row: Panels show data for 21 individual subjects tested with TEP-200 (dark blue) and Invisio X5 (light blue) HPDs. Within each panel, data show attenuation estimates for tones of 500 Hz (left of black vertical bar) or 4000 Hz (right of black vertical bar) at 65 or 90 dB SPL (as labeled). Given level-dependent performance, a 90-dB SPL signal is expected to produce greater attenuation (so values should fall higher above abscissa). In each case, open circles indicate the 'between ear' estimate obtained from 'Step 2' of the ABLB procedure, while closed circles indicate the 'within ear' estimate obtained from 'Step 3' (see text). Bottom row: Data from the top row are averaged across subjects (error bars indicate standard error of the mean) and replotted to explicitly show the change in attenuation for a 90 dB SPL source versus a 65 dB SPL source across conditions. Values above the dashed line (0 change, i.e. linear performance) indicate greater attenuation for a 90 dB SPL source. 6 out of 8 mean values (across devices, adjustment step, and frequency) fall above the dashed line (linearity), but the majority only slightly so, and in 7 out of 8 cases error bars approach or intersect the line of linearity. Data thus evidence little or no level-dependence at the levels tested, leading the team to shift to use of cadaveric specimens for completion of hLD testing in Year 3 (see text).

3.2.2.3. Subtask 4: Analyze pilot human cadaver measures of HPD attenuation to impulse noise exposures

Preliminary data collected in cadaveric human specimens with four HPDs during exposure to acoustic shock waves was collected under Contract W81XWH-15-2-0002 by members of the project team. Complete analysis of this data has not been previously published, but has direct bearing on the current program, thus further analysis was undertaken to estimate results planned during this program. A manuscript reporting on those preliminary results, specifically spectral insertion loss calculated from high level impulse noise exposures, has been submitted for peer review. Briefly, the signal-to-noise ratio is small for many frequency components, even at high

peak pressure levels. We concluded that multiple measurements, averaged together, provide improved signal-to-noise, and have modified our test matrix for this program accordingly.

3.2.2.3.1. Data collection

During the prior project (no new data collection was conducted for this effort), data collection was conducted under four blast loading conditions; peak pressures presented were 1, 4, 8, and 12 psi. The highest-pressure exposures resulted in tympanic membrane rupture and additional anatomical damage, thus were generally excluded from further analysis. The lower pressure exposures tended to produce low signal strengths during frequency domain analysis, thus initial efforts were aimed at developing methods to increase the signal-to-noise ratio across a broad frequency band. See Greene et al. 2018 for a detailed description of data collection and analysis methods for unoccluded ear noise measurements. Prior assessment of the HPD conditions presented below, using a band-filtering approach has similarly been presented previously. (Walilko et al. 2017)

Free-field pressure sensor *Ear canal pressure sensor*

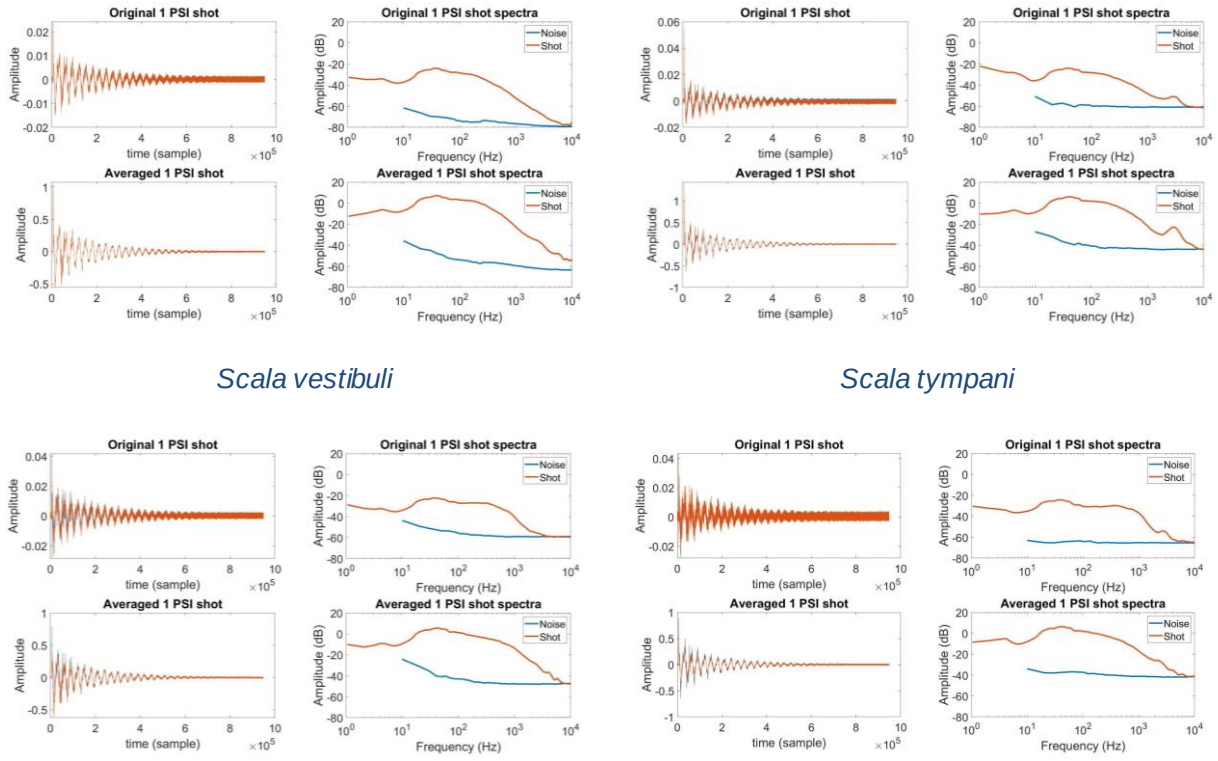

Scala vestibuli *Scala tympani*

Figure 24. Example shock wave exposure measurements from a single specimen, for the free-field, ear canal, scala vestibuli, and scala tympani pressure sensors. Each set of panels shows pressure measurements in the time domain for an individual noise exposure (upper left), for the average across all several exposures at this level (lower left), as well as the magnitude of the signal and an estimate of the background noise (estimated from the period immediately preceding the noise exposure) in the frequency domain for the individual and averaged noise exposures.

3.2.2.3.2. Noise reduction and signal to noise ratio improvements

While responses were typically only recorded once at each exposure level, for each HPD condition, the 1 PSI low-level exposures were repeated multiple times throughout the experiment day to verify measurements were consistent throughout the day and damage was not occurring. We took advantage of these repeated measurements by averaging these noise exposures (after adjusting the amplitude and latency of the pressure measurements based on the incident exposure measured in the free-field sensor). Results from single exposures, as well as from the average of multiple exposures, in both the time and frequency domain, are shown for a single specimen shown in Figure 24 below. Data analysis is focused on developing a frequency-specific insertion loss metric, therefore analysis is primarily conducted in the frequency domain.

The SNR improvement derived from averaging multiple low-level exposures was calculated, and is shown in Figure 25 below for the ear canal, and each of the intracochlear pressures, revealing significant improvement in signal strength in each signal measured.

Ear Canal

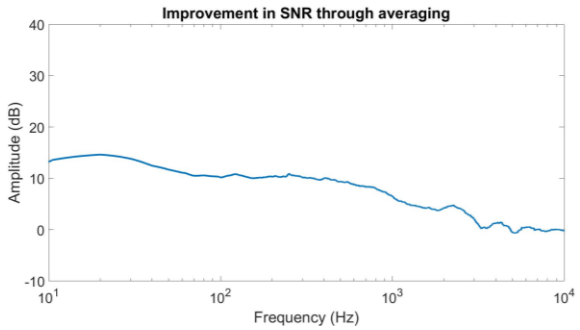

Scala Vestibuli

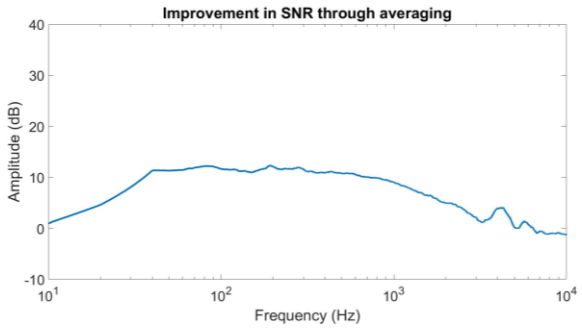

Scala Tympani

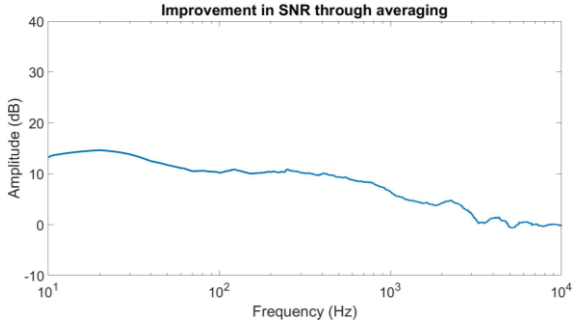

Figure 25. Signal-to-noise ratio improvement in the ear canal, scala vestibuli, and scala tympani pressure sensors due to averaging individual shock wave exposures

3.2.2.3.3. Insertion loss

The goal of the program is to calculate insertion loss from HPD insertion, considering secondary transmission pathways to the inner ear via, e.g., bone conduction. Traditional insertion loss (i.e., sound levels in the ear canal) was calculated in the frequency domain for each of the four HPDs tested. Responses are shown in Figure 26 for signals with a SNR greater than 3 dB, resulting in substantial gaps in data due to low signal strength (averaging as discussed above was not possible due to lack of repeat measurements).

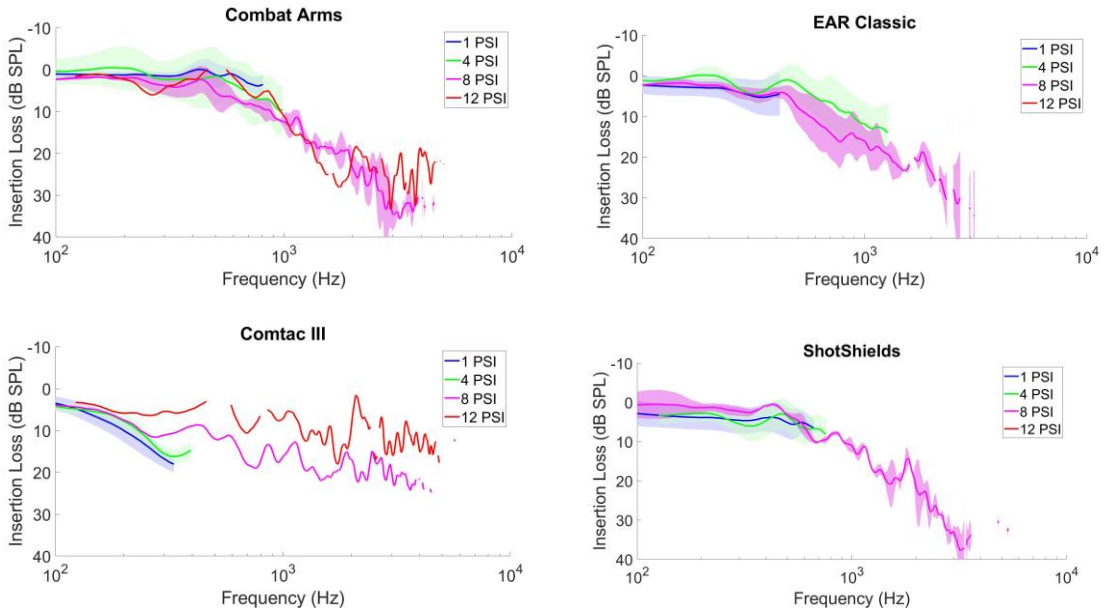

Figure 26. Insertion loss calculated from ear canal pressure sensors

Insertion loss was then calculated from the differential intracochlear pressure (the complex difference in pressure between the scala vestibuli and scala tympani: $P_{diff} = P_{sv} - P_{st}$), which is a direct measure of the driving force to the basilar membrane from acoustical exposure and is highly correlated with auditory nerve activity in animal studies (Dancer and Franke 1980). Results for each of the four HPDs are shown in Figure 27 below, in the same format as the traditional insertion loss measures shown above.

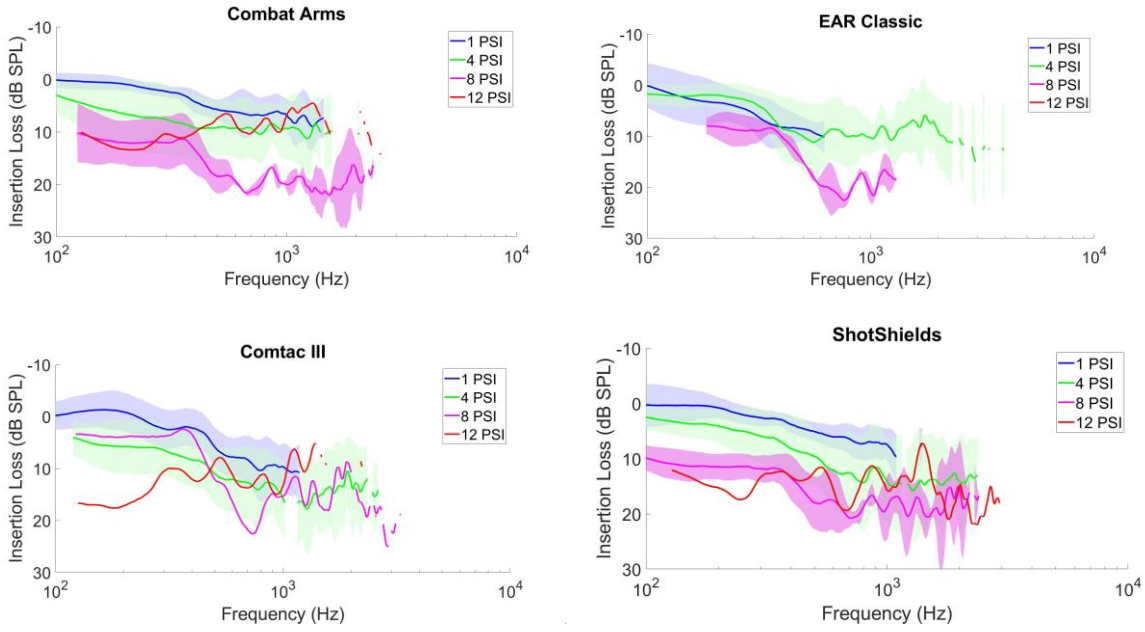

Figure 27. Insertion loss calculated from drive to the basilar membrane, calculated as the difference in pressure between the pressure sensors in the scala vestibuli and scala tympani.

Insertion loss increases with frequency in both traditional and intracochlear pressure calculations, however notable differences, particularly at low frequencies, are visible. Insertion loss from intracochlear pressure produced substantially higher insertion losses at lower frequencies, particularly in the two nonlinear HPDs (Combat Arms and ShotShields). Higher frequencies showed somewhat lower insertion losses. These differences are variable, however, and could be a result of damage or other variability in the measurements collected. Results from this prior data collection therefore serve primarily to develop the analysis methods, and data collection in this project will therefore prioritize specimen condition, data validity, and exposure repetitions.

3.2.2.4. Subtask 5: Obtain human cadaver measures of HPD attenuation to impulse noise exposures

The impulse noise (hIN) metric will consist of measures of insertion loss to impulse noise exposures measured in post-mortem human specimens (PMHS). We completed preliminary testing in two specimens to develop test methods, verify equipment function, and begin collecting pilot data. Briefly, fiber-optic pressure probes will be inserted into the cochlea of PMHS, then exposed to shock waves generated by the ANSI compliant shock tube at CU. Figure 28 shows the setup during preliminary testing. The 4” diameter shock tube was set up in a double-walled sound attenuating chamber without the expansion cone. A cadaveric specimen was outfitted with pressure sensors, oriented upside-down in front of the driven section of the shock tube. A probe tube microphone sampled sound pressure level adjacent to the ear canal of the left ear. A mirrored polycarbonate sheet protected the back wall of the sound booth and redirected the reflected shock wave away from the specimen.

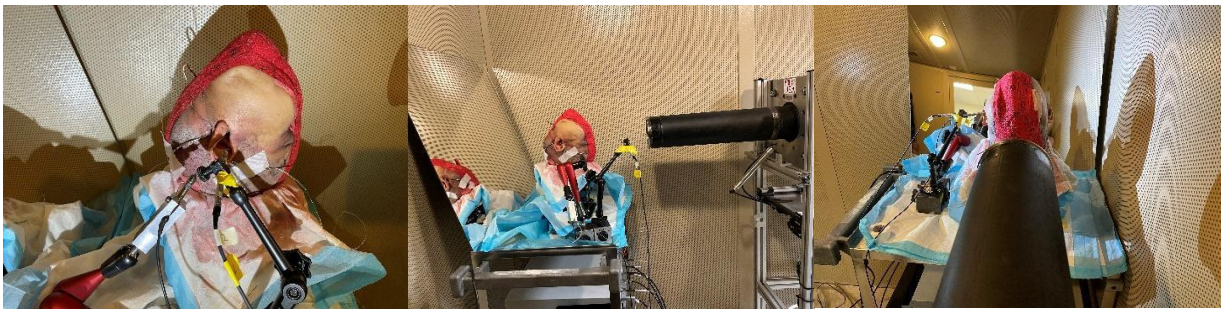

Figure 28. Equipment and specimen setup for PMHS shock wave exposures. The equipment and specimen were mounted on a mobile cart and elevated to center the specimen in front of the shock tube outlet. Pressure sensors were inserted into the cochlea and held in place using stainless steel guide tubes but were damaged during testing regardless. Greater efforts to protect the entire length of the sensor cabling will be undertaken in subsequent testing.

Results of shock tube exposures were highly variable in the first specimen, which appears to be a result of damage to the pressure probes and loss of the seal between the probes and the PMHSs cochlear wall. Future measurements will include increased efforts to protect and secure pressure probes, comparable to the effort expended on prior measurements discussed in the previous section.

A second human cadaveric specimen was prepared with intracochlear pressure sensors and exposed to impulse noise from the ANSI S12.42-2010 compliant shock tube at CU, with and without hearing protection. The method for inserting and protecting the intracochlear pressure sensors was revised from the first measurement, and measurement reliability and reproducibility

was significantly improved. Preliminary analysis of this data, as guided by the analysis of the pilot cadaver data analysis described in the previous section, is shown below, and additional development of both measurement techniques and analysis is ongoing.

Development of new analysis tools was required due to differences in the data collection hardware and software between the previous and current studies. Data are initially loaded in Matlab, then the timing of the impulse arrival is registered using a correlation-based technique on the response from a free-field microphone located adjacent to the ear. Responses from 5 measurements are then averaged together in the time domain.

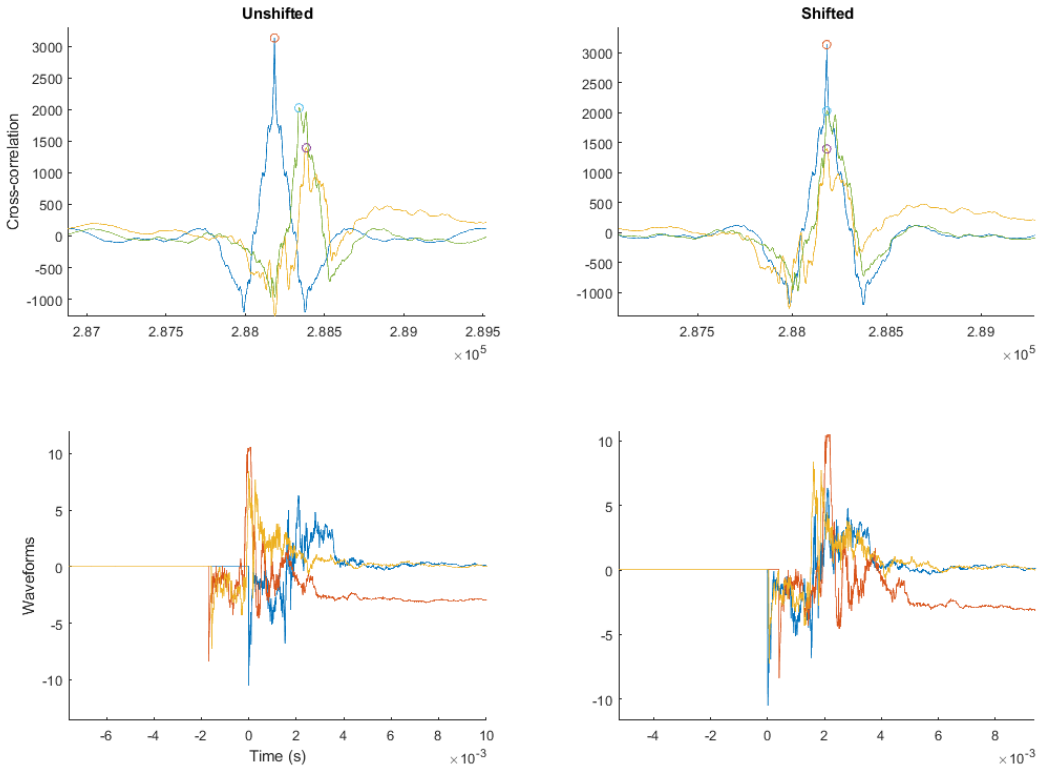

Figure 29. Multiple impulse noise exposures were synchronized using a cross-correlation based technique. Top-left: the cross correlation of each recording and the first recording were calculated. The index (o) of the maxima of that cross correlation function was identified. Bottom-left: Impulse noise exposures are first synchronized to the maximum value in the time domain recording, but variability across recordings and poorly defined onset times result in poorly synchronized waveforms. Top-right: the maxima index was subtracted from each time vector in order to synchronize waveforms, as indicated in the cross correlations. Bottom-right: similarly, impulse noise pressure recordings are better synchronized once time shifted by the index of the maxima.

After synchronizing repeated impulse noise measurements for each condition, they were averaged together. Impulses are shown as a function of HPD condition and recording location in Figure 30. Responses are shown for a free-field microphone located next to the test ear, a probe tube microphone in the (unoccluded) external auditory canal (EAC), fiber optic pressure probes

in the scala vestibuli (P_{sv}) and scala tympani (P_{st}), as well as the differential intracochlear pressure (P_{diff}), calculated as the difference (in the time domain) between the scala vesitibuli and scala tympani ($P_{diff} = P_{sv} - P_{st}$). The average peak pressures were generally reduced in all HPD conditions and all physiological recording locations (P_{sv}, P_{st}, and P_{diff}).

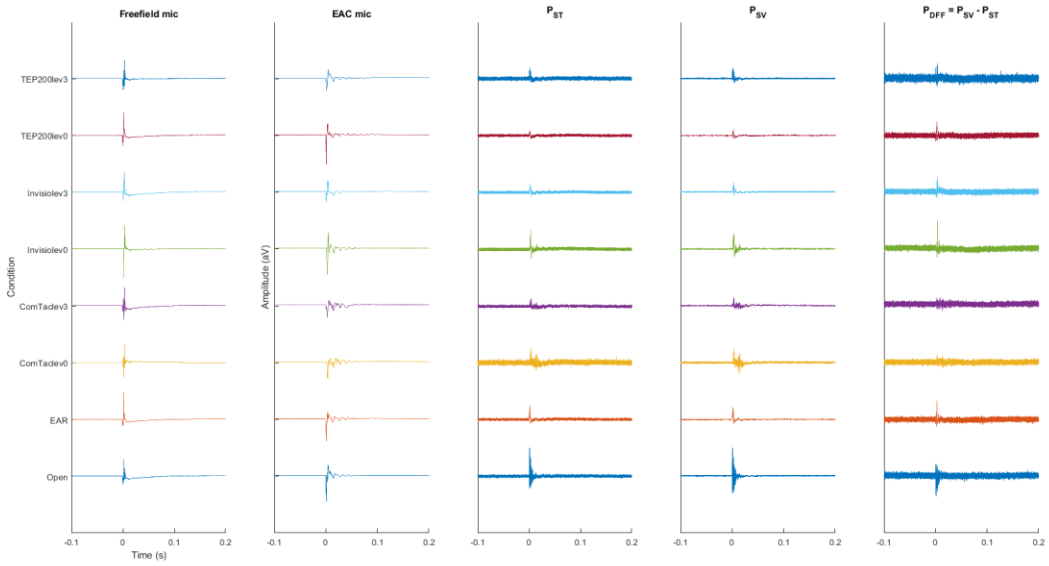

Figure 30. Average impulse exposures recorded from a free-field microphone located next to the ear, a probe tube microphone in the un-occluded ear, fiber optic pressure probes in the cochlea, in the scala vestibuli (P_{SV}) and scala tympani (P_{ST}), and the difference between the two intracochlear pressures (P_{Diff}). Impulses are shown for each HPD condition (shown by the y-offset), and are normalized to the maximimum recorded for each measurement.

Insertion loss will only be calculated for frequency bands with signal to noise ratios greater than 3 dB. Noise from filling the shock tube is present immediately prior to the impulse arrival, thus noise is estimated from a 1 second period, 2 seconds prior to the arrival of the shock wave. Signal strength is similarly calculated from the 1 second immediately following the impulse arrival. Magnitude spectra, and the impulse spectral insertion loss, are calculated from a 1 second long period beginning at the arrival of the transient, and are shown in Figure 31. The estimated background noise for each sensor is shown in the top row as dotted lines, the signal present during the 1 second analysis period is shown as solid lines (colors match signal and noise). Signal strength is substantially larger than noise in frequencies between 10 and 1000 Hz.

Insertion loss is calculated as the difference between each HPD condition and the open ear condition. Results are only shown for frequency bands revealing greater than 3 dB signal to noise ratio. Insertion loss (bottom row) is calculated for each measurement. The free-field and EAC microphones are unaffected by HPD insertion, and accordingly, do not show any change in HPD condition. On the other hand, P_{sv} (and to a lesser extent P_{st} and P_{diff} conditions) shows substantial decreases in signal magnitude across HPD conditions, indicating increasing insertion loss. Substantial noise is visible in all measurements and all HPD conditions, limiting the frequency bands in which signal is present.

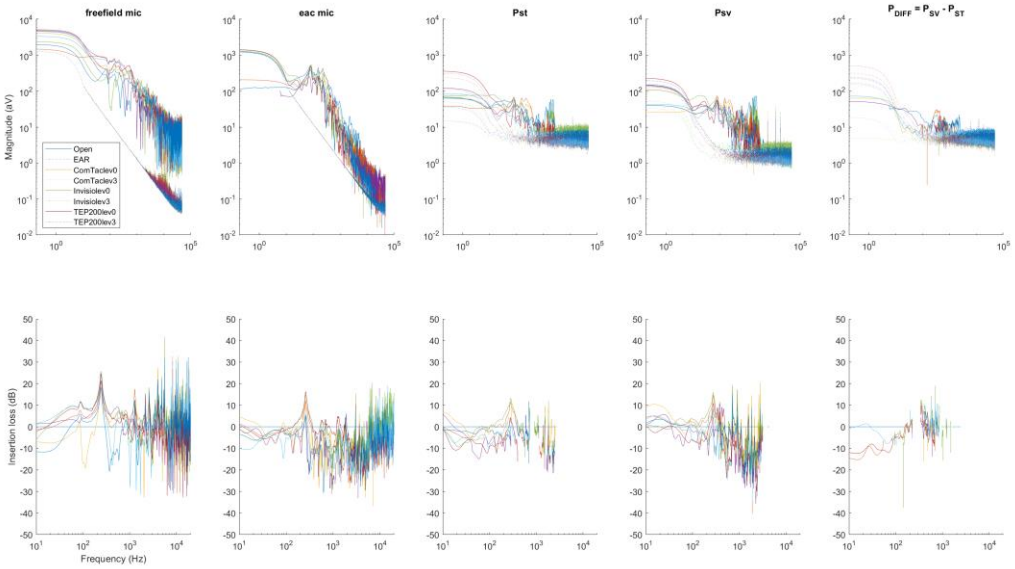

Figure 31. Average impulse exposures recorded from a free-field microphone located next to the ear, a probe tube microphone in the un-occluded ear, fiber optic pressure probes in the cochlea, in the scala vestibuli (P_{SV}) and scala tympani (P_{ST}), and the difference between the two intracochlear pressures (P_{Diff}). Impulses are shown for each HPD condition (shown by the y-offset), and are normalized to the maximimum recorded for each measurement.

Preliminary results from specimen 2 reveal comparable signal to noise issues as in our previous study, and future measurements will require more repetitions, as well as further attention devoted to improving signal strength and reducing background noise. These initial measurements were treated as pilot studies, future experiments will include microphone and intracochlear pressure measurements in both ears, in addition to the free-field sound pressure measurement. Calculations will be conducted in a similar manner as above, and insertion loss calculated from the EAC will be compared to those from intracochlear pressures (particularly P_{diff}), to allow estimation of the bone conducted component of the sound transmission into the inner ear.

Additional measurements will involve measurements of steady state tones and noise at several levels from 94 dB SPL (1 Pa, the approximate noise floor of the intracochlear pressure sensors), and the maximum output of our loudspeaker system, in order to estimate the nonlinear attenuation of the electronic earplugs. This final measurement is intended to replace the ABLB human measurements described above, as we may safely present sounds at higher levels to cadavers than to human participants.

3.2.2.5. Subtask 6: Conduct ongoing quality assurance review of psychoacoustic, cadaver, and associated data

Ongoing through the project period of performance.

3.2.3. Specific Aim 2, Major Task 1: Verification of Electromechanical Test Methods

Four categories of electromechanical tests are performed on HPDs: Signal Quality and Localization (eSQ/eSL), Level-Dependent Frequency Response (eLD), electronic Self-Noise

(eSN), and Impulse Noise (eIN). Table 3 shows the expanded list of HPDs that have been evaluated. In this table, an X indicates that usable data has been collected for a device. The number of test iterations varies for each test, with eSQ/eSL and eLD tests having 5 iterations, eSN having a single iteration, and eIN tests having 10 iterations with each shocktube. An unmodified X indicates that all necessary iterations have been completed. An X modified with a + or * indicate that an additional 5 or 1 additional iterations respectively are needed to complete the set.

Table 3. HPD electromechanical test status matrix

HPD	eSQ/eSL	eLD	eSN	eIN (SD/ANSI)
3M1100	X	X		X
Alpine	X	X		X
Combat Arms 4.1 (Closed Mode)	X	X		X*
Combat Arms 4.1 (Open Mode)	X	X		X
3M Peltor ComTac V (High Volume)	X	X	X	X*
3M Peltor ComTac V (Low Volume)	X	X	X	X*
EAR Classic	X	X		X
Elvex Quattro	X	X		X*
Etymotic	X	X		X
Sense Defense FiRes	X	X		X
Honeywell Fusion	X	X		X
Honeywell LaserLite	X	X		X
Howard Leight Air Soft	X	X		X
Invisio V50/X5 (High Volume)	X	X	X	
Invisio V50/X5 (Low Volume)	X	X	X	
Sense Defense Whisperhawk	X	X		X
Shooters	X	X		X
Surefire EP7	X	X		X
3M Peltor TEP-200 (High Volume)	X	X	X	X
3M Peltor TEP-200 (Low Volume)	X	X	X	X
Vibes	X	X		X
Westone TRU WM16	X	X		X
Westone TRU WR20	X	X		X
Westone TRU WM25	X	X		X

3.2.3.1. Signal Quality (eSQ) and Localization (eSL)

The virtual hemispheric array (VHA) used in the eSQ/eSL test (shown in Figure 32) has been re-calibrated and initial test validation has been completed. A GRAS 45CB headform manikin, compliant with ANSI S12.42, is used for testing and rotates to allow for data collection at a user-specified set of azimuth values. On the right is a loudspeaker connected to a curved track that can be raised to a specified set of elevation values. The GRAS 45CB test fixture is ordinarily fitted with 40BP high-pressure microphones for use in high-pressure shock wave testing; however, for the eSQ and eSL tests, where the test signals are of much lower amplitude, the ear simulators in the 45CB are switched to use 40AP high-sensitivity microphones rather than the 40BPs. This switch lowers the system's noise floor and will allow for much more sensitive eSQ and eSL measurements, especially for high insertion loss devices such as the EAR Classic.

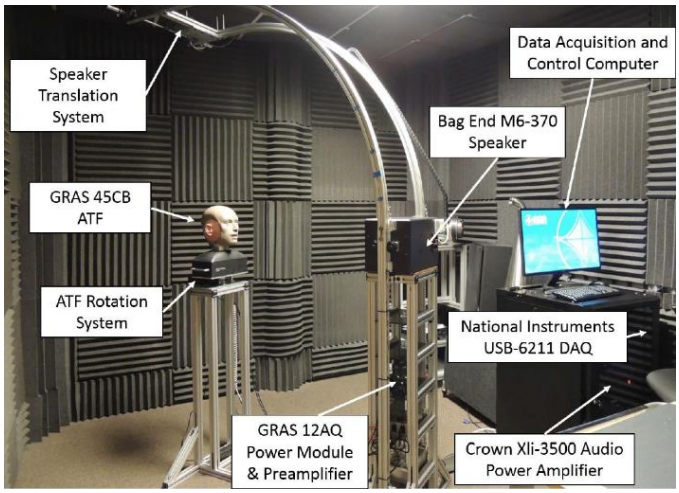

Figure 32. eSL and eSQ test apparatus.

The eSQ and eSL tests are based on the calculation of an SQ (Signal Quality) metric that is designed to compare signal fidelity between unoccluded and occluded ears in a test fixture at a variety of azimuth and elevation points. The eSQ metric, by itself, is an indicator of signal fidelity only at 0 degrees azimuth and 0 degrees elevation, while eSL is a metric combining eSQ values for many different directions. In Year 2, alternative methods for calculating eSQ and eSL metrics that are more robust to certain types of distortion were explored.

The originally proposed method of calculating eSQ (referred to in this report as eSQ_{org}) calculates the cross-correlation of the occluded and unoccluded signals, squares the result and normalizes by dividing the result by the autocorrelation of both the occluded and unoccluded signals. Assuming that the unoccluded signal is $x(t)$, the occluded signal is $y(t)$, the autocorrelation function of $x(t)$ is R_{xx}, the autocorrelation function of $y(t)$ is R_{yy}, and the cross-correlation function is R_{xy}, the equation becomes:

$$eSQ_{org} = \frac{\max(R_{xy})^2}{\max(R_{xx})\max(R_{yy})}$$

Concerns arose that this method of calculating an eSQ metric is too sensitive to phase changes between the unoccluded and occluded signals. As an experiment, a wideband chirp was filtered through an all-pass digital filter that slightly altered the phase of the signal while leaving the magnitude response unchanged (time domain signal, as well as magnitude and phase of the original chirp and all-pass filtered chirp are shown in Figure 33). The calculated eSQ_{org} value for these two signals is only 0.48, which is lower than would be expected for a transfer function with no changes to the magnitude response.

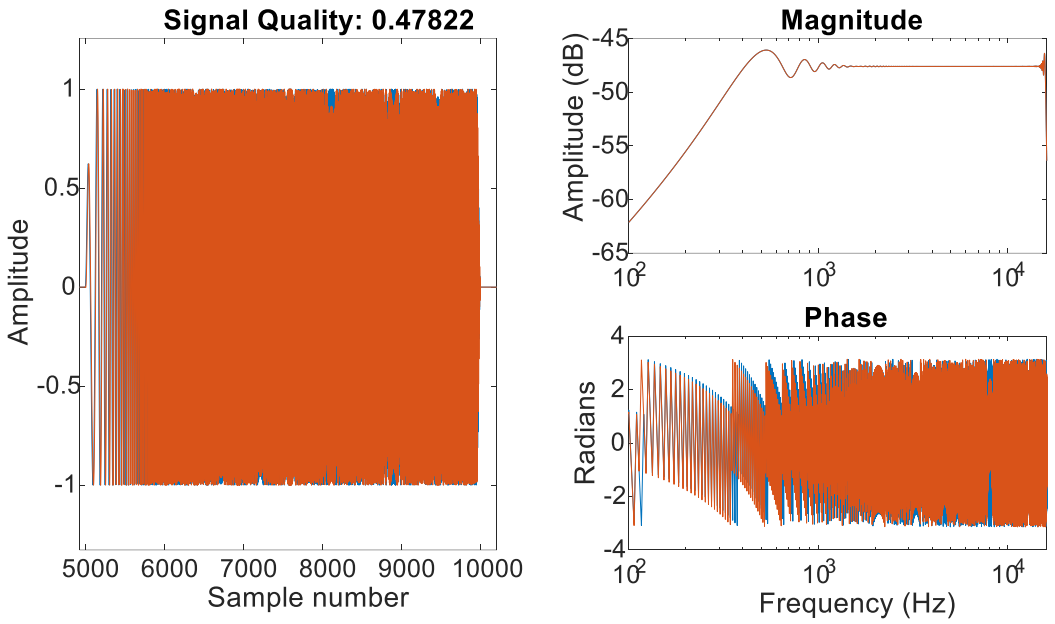

Figure 33. (Left) Time-domain signals: orange is the original chirp and blue is the same chirp after all-pass filtering. (Upper right) comparison of the FFT magnitudes of the two chirps, illustrating that no change has occurred. (Bottom right) Comparison of the FFT phase of the two chirps, illustrating a slight phase distortion that causes a low eSQ value.

Alternative methods for calculating an eSQ metric are being considered. These methods must meet the following requirements to be useful and concise for the end user:

- A linear scaling of the signal must result in an eSQ value of 1.
- Reported values must be scalable to a range of 0 (poor fidelity) to 1 (high fidelity).

One potential method that was identified is based on the *Directional Transfer Function Similarity Index* developed by Van Wanrooij and Van Opstral.[1] In this method, the 512-point magnitude DFT $F_{ij}(f)$ is measured and calculated for each set of angle i and elevation j pairs, for both unoccluded and occluded cases ($F_{Uij}(f)$ and $F_{Oij}(f)$, respectively). For each case, the Directional Transfer Function (DTF) is calculated as the DFT divided by the average spectral response for that case:

$$DTF_{Uij}(f) = \frac{|F_{Uij}(f)|}{\sum_i \sum_j |F_{Uij}(f)|} \text{ and } DTF_{Oij}(f) = \frac{|F_{Oij}(f)|}{\sum_i \sum_j |F_{Oij}(f)|}$$

The eSQ_{SI} (for similarity index) value at any angle and elevation pair (i,j) is then calculated as the correlation coefficient $C(i,j)$ between $DTF_{Uij}(f)$ and $DTF_{Oij}(f)$, treating both DFTs as 512-point vectors. $C(i,j)$ essentially determines the cosine of the angle between the vectors, which has a range between -1 and 1. In order to meet the two requirements stated above, eSQ_{SI} is calculated as:

$$eSQ_{SI} = \frac{C(i,j)+1}{2}$$

[1] Van Wanrooij, M.M., Van Opstal, A.J., 2005. Relearning sound localization with a new ear. J. Neurosci. 25, 5413–5424. https://doi.org/10.1523/jneurosci.0850-05.2005

From here, there are two potential methods of calculating a single metric from all angle and elevation pairs. In the paper, a method is used that calculates $C(i,j)$ for all angles and elevations over both cases; in the case that there are 168 (i,j) pairs, this leads to a 168x168 matrix of correlation coefficients. The single metric is then calculated as the standard deviation of the values in the matrix. If the standard deviation is 0, this means that all angles and elevations, compared between unoccluded and occluded, have comparable similarity, e.g., unoccluded at $(90^o,45^o)$ is as similar to occluded at $(90^o,45^o)$ as it is to $(0^o,0^o)$, so directionality is completely obscured. A larger standard deviation means that there is more similarity at certain (i,j) pairs than at others, presumably at the same angles and elevations at both occluded and unoccluded. This metric will be referred to as $eSL_{SI\sigma}$.

Further exploration of these alternative calculation methods will be performed in Year 3.

3.2.3.2. Level Dependency (eLD) and Self Noise (eSN)

Setup of tests related to eLD and eSN was completed in Year 1. In Year 2, the procedure was modified to include five test iterations per device to calculate the mean and standard deviation of the spectral insertion loss for the eLD tests.

Initial data analysis identified that level extrapolation would improve the eLD calculation for frequency-amplitude points not achievable due to speaker bandwidth limitations. Four fit equations were evaluated: linear, logarithmic, exponential and a modified exponential decay. Linear and logarithmic equations provided the best overall fit and a linear extrapolation was selected because it reduced uncontrolled growth for some data. Figure 34 shows before and after the linear extrapolation is applied to eLD collected for Combat Arms 4.1 in open mode.

Initial data analysis has been performed for six devices, some active devices at various levels, as shown in Figure 35. For these devices, active devices capable of active sound compression and/or microphone clipping were able to provide the best eLD scores.

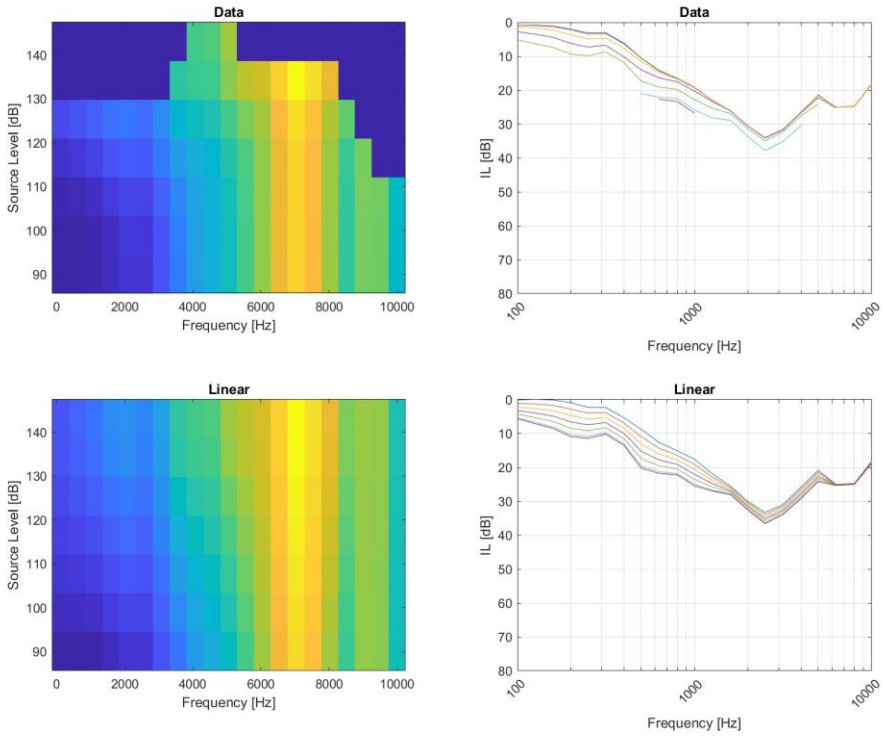

Figure 34 Linear extrapolation was performed on existing data so each level had an equal impact on the resultant eLD.

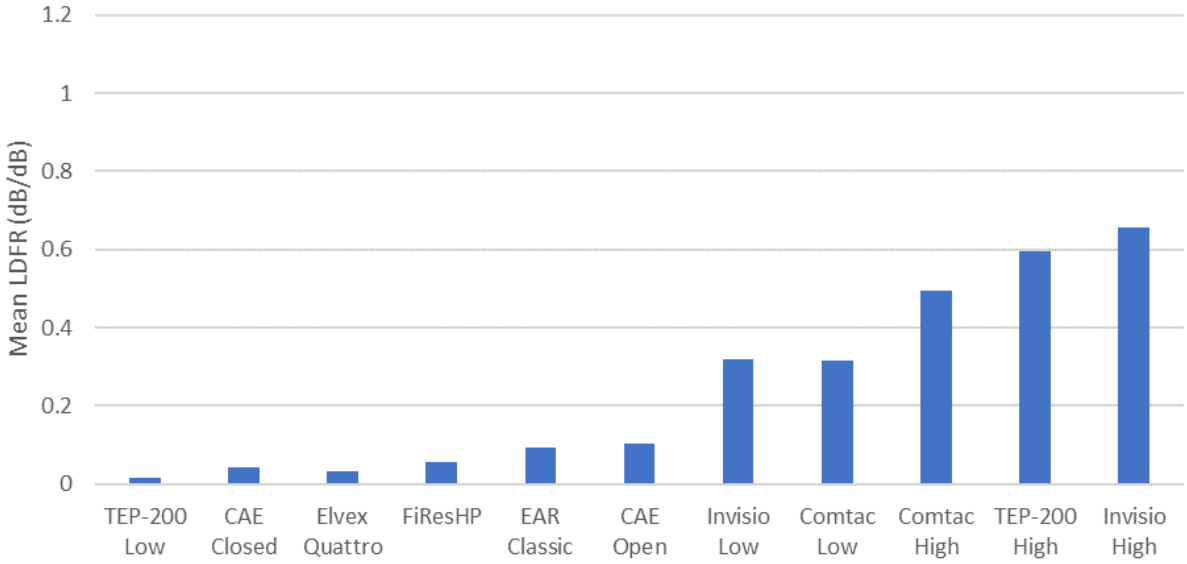

Figure 35 Initial mean LDFR results indicate higher eLD values for high level active devices compared to generally lower eLD for passive devices.

3.2.3.3. Impulse Noise (eIN)

For the eIN tests, two types of shock tubes were used: a custom short duration shock tube and a large ANSI shock tube. Setup of the two shock tubes to be used for eIN testing is complete and shown in Figure 36. The 4" ANSI shock tube shown on the left, manufactured by B/C Precision Tool, is used to create acoustic impulses that simulate blast waves with an A-duration of 0.5-2.0 ms at peak pressures between 132 and 183 dB. These exposures meet the requirements of ANSI S12.42 and extend the exposure range by 12 dB. The short duration shock tube, shown on the right, was developed under previous funding to produce peak pressures between 132 and 171 dB at a shorter A-duration of between 0.05-0.2 ms. Impulse pressures are measured using a pencil probe microphone and the GRAS 45CB. The user interface for the LabVIEW code used to control the shock tubes and record impulse pressure data is shown in Figure 37.

Figure 36. (Left) ARA ANSI-compliant shock tube and (Right) short duration shock tube for eIN testing.

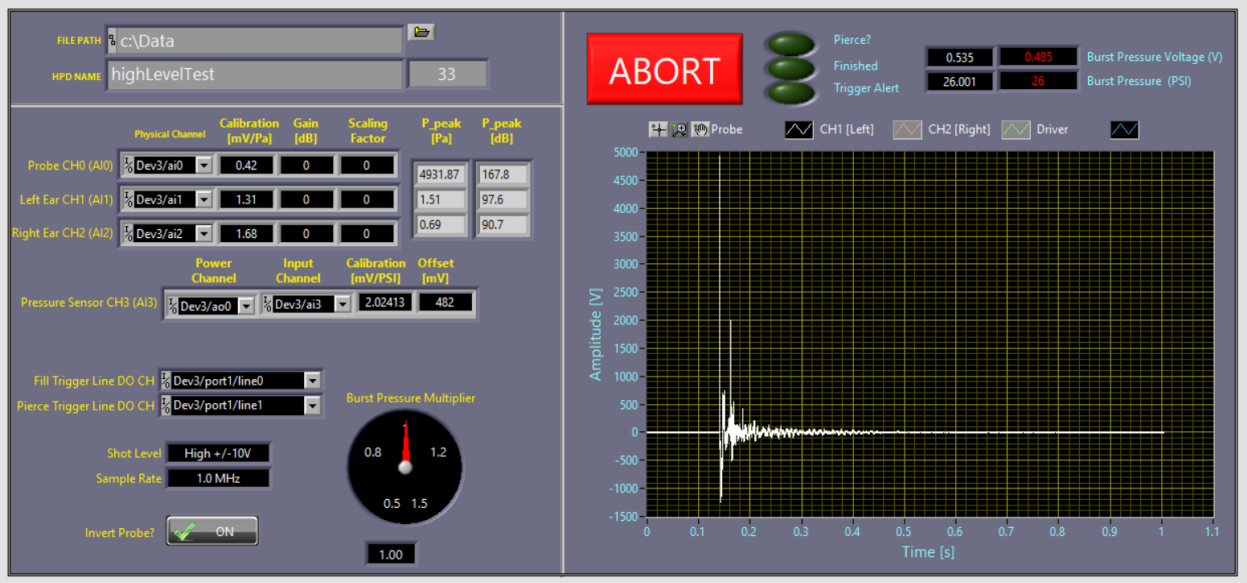

Figure 37. ARA Labview interface for controlling and collecting data from the ANSI-Compliant and Short-Duration Shock Tubes.

Setup of the ANSI shock tube data acquisition system is complete, verification of instrumentation was conducted at the low (130-134 dB), medium (148-152 dB), and high (166-170 dB) free field level. Membrane materials were purchased which corresponded with testing at each level. Usable data collection has been completed for most HPDs used in this study, as shown in Figure 38. For the open-ear case and for each device, ten test iterations have been conducted (device removal and re-insertion between tests) at each free field level. The results are reported as the mean and standard deviation of the insertion loss at each free field level for each HPD.

SD Shocktube				
Hearing Protection Device		**Low**	**Med**	**High**
Open Ear		X	X	X
EARClassic		X	X	X
Elvex Quattro		X	X	X
Combat Arms Open		X	X	X
Combat Arms Closed		X	X	X
Comtac	Silence	X	X	X
	Level 4	X	X	X
	Level 1	X	X	X
TEP-200	Level 4	X	X	X
Invisio	Level 1			
	Level			
FiResHP		X	X	X
WestoneTRU WR20		X	X	X
WestoneTRU WM16		X	X	X
WestoneTRU WM25		X	X	X
Alpine		X	X	X
HL Airsoft		X	X	X
Vibes		X	X	X
Shooters		X	X	X
Honeywell LaserLite		X	X	X
3M 1100		X	X	X
HL Honeywell (Fusion)		X	X	X
Westone Musicians (Etymotic)		X	X	X
Surefire EP7		X	X	X
IEEP		X	X	X

ANSI Shocktube				
Hearing Protection Device		**Low**	**Med**	**High**
Open Ear		X	X	X
EARClassic		X	X	X
Elvex Quattro		X	X	*
Combat Arms Open		X	X	X
Combat Arms Closed		X	X	*
Comtac	Silence	*	X	+
	Level 4	X	X	*
	Level 1	X	X	X
TEP-200	Level 4	X	X	X
	Level			
Invisio	Level			
FiResHP		X	X	X
WestoneTRU WR20			X	X
WestoneTRU WM16		X	X	X
WestoneTRU WM25		X	X	X
Alpine		X	X	X
HL Airsoft		X	X	X
Vibes		X	X	X
Shooters		X	X	X
Honeywell LaserLite		X	X	X
3M 1100		X	X	X
HL Honeywell (Fusion)		X	X	X
Westone Musicians (Etymotic)		X	X	X
Surefire EP7		X	X	X
IEEP		X	X	X

Figure 38 Short duration and ANSI shock tube testing matrix.

3.2.4. Specific Aim 2, Major Task 2: Develop Prototype Standards for Appropriate HPD Evaluation Methods

We examined key ANSI standards related to the evaluation of HPDs. These standards are being used as the baseline for developing prototype standards for the refined electromechanical test methods. The most relevant ANSI standards that were identified are listed in Table 4, along with a bullet point description of the standard and how it relates to specific electromechanical test methods.

Table 4. ANSI Standards Relevant to Electromechanical Test Methods

ANSI/ASA No.	Title/Description

S3.2 - 2020	Method for Measuring the Intelligibility of Speech Over Communications System
	• Covers Modified Rhyme Test (MRT) and other test methods for evaluating the speech intelligibility of communication systems (including HPDs) using human subjects
	  ○ Specifies validated English word lists, spoken to the human test subject (listener) from trained talkers. Listener tasked with selecting the correct spoken word from list of words displayed on a screen.
	  ○ For evaluation of HPDs, results are compared between tests where the listeners are wearing HPDs and have open ears
	• MRT type testing used in hSQ evaluations, relevant to verification of signal quality test (**eSQ**) in predicting human auditory performance

S3.35 - 2004	Method of Measurement of Performance Characteristics of Hearing Aids Under Simulated Real-Ear Working Conditions
	• Provides guidance on use of an ATF and ear simulator for testing
	  ○ Relevant to all electromechanical test methods under development
	• Covers techniques used to measure hearing aids under simulated conditions of real ear use
	  ○ Measurement of insertion gain provided by the hearing aid.
	  ○ Directional response of the manikin as a function of azimuth and elevation of the sound source, with and without the assistance of a hearing aid; calculation of the directivity index from the directional response. (Relevant specifically to **eSL**)

S3.42 - 1992 (R2002)	Testing Hearing Aids with a Broad-Band Noise Signal • Covers techniques for characterizing the steady-state performance of hearing aids with a broad-band noise signal • Provides guidance on measurement equipment requirements and further analysis of data ○ Relevant to all electromechanical test methods under development

S3.71 - 2019	Measuring the Effect of Head-Worn Devices on Directional Sound Localization in the Horizontal Plane
	• Covers assessment of sound localization performance using human subjects, both open ear and with head-worn devices.
	  ○ Human test subject sits at the center of a speaker array in the horizontal plane of the head, and is tasked with identifying the location of the speaker from which the test signal originated
	  ○ For evaluation of HPDs, results are compared between tests where test subjects are wearing HPDs and have open ears
	• Relevant to **eSL**, however eSL testing addresses sound localization at elevations above the horizontal plane

S12.6 - 2016 (R2020)	Methods for Measuring The Real-Ear Attenuation Of Hearing Protectors
	• Covers the Real-Ear Attenuation at Threshold (REAT) test method using human subjects for evaluating the passive noise-reducing capabilities of HPDs (does not evaluate active hearing protection with electronics turned on)
	  ○ Human test subject is tasked with indicating whether they can hear a tone as the level goes up and down around the hearing threshold. The test is performed at various discrete frequencies.
	  ○ For evaluation of HPDs, results are compared between tests where test subjects are wearing HPDs and have open ears
	• REAT type testing used in hSN evaluations, relevant to verification of self-noise test (**eSN**) in predicting human auditory performance

S12.42 - 2010 (R2020)	Methods for The Measurement Of Insertion Loss Of Hearing Protection Devices In Continuous Or Impulsive Noise Using Microphone-In-Real-Ear Or Acoustic Test Fixture Procedures
	• Covers methods for measuring the insertion loss of HPDs in specified continuous and impulsive noise environments
	  ○ Includes a microphone-in-real-ear (MIRE) and Acoustic Test Fixture (ATF) method
	  ○ For evaluation of HPDs, results are compared between open-ear tests and HPD occluded tests (levels above 155 dB require a transfer function rather than open ear test)
	• Relevant to **eIN**, specific test procedures using an ATF are followed for portions of eIN testing, however eIN tests expand upon the S12.42 scope
	• Relevant to **eLD**, S12.42 testing evaluates HPD performance at high SPL levels where level dependent HPD characteristics are observed

Prototype standards for each electromechanical test can either become new standards or modifications/additions to existing standards. Existing standards will be kept in mind during the project as electromechanical methods are refined to better reflect human performance. A key consideration is whether electromechanical test methods performed with acoustic test fixtures (ATFs) should be added to existing standards covering test methods performed with human subjects. ANSI S12.42 is one standard that covers test methods performed with ATFs and human subjects, however microphones are placed in the ears of the human subjects. Quantitative data is collected from the microphones and test results do not rely on the subjective responses of human subjects.

Table 5. Specifications included in ANSI/ASA S12.42 for electromechanical test methods

Topic	Specifications
Test Samples	• Number of test samples required for each product ○ Including HPDs with size options • Marking of test samples

Acoustic Test Fixture (ATF)	• Critical Head Dimensions
	• Self-Insertion Loss
	• Microphone & Preamplifier Requirements
	  ○ Sensitivity & Dynamic Range
	  ○ Distortion & Linearity
	• Earcanal Coupler & Extension Requirements
	  ○ Extension dimensions (length/diameter)
	  ○ Type/size of microphone incorporated
	• Flesh Simulation
	  ○ Locations (e.g., Earcanal lining, Pinnae)
	  ○ Dimensions (thickness/diameter)
	  ○ Durometer
	• Temperature

Test Signal Characteristics	• Type/Description • Bandwidth & Uniformity • Sound Pressure Level(s) to be tested
Sound Field Characteristics	• Uniformity & Directionality • Requirements for microphone used to verify sound field characteristics

Currently, the eIN test method is the only test method closely based on an existing standard (S12.42). As mentioned in the table above, portions of the eIN test method follow the procedures from S12.42. The expanded scope portions of eIN testing (beyond S12.42 specifications) could be relevant additions to the S12.42 standard, such as the small shock tube tests that evaluate HPD protection against simulated small arms fire (i.e., impulse noise with A-durations less than 0.5 ms).

The information we found most relevant to writing our draft test standards was pulled from ANSI S12.42. A summary of key content specified in S12.42 is given in Table 5.

Similar information will be specified in our draft test standards. As an example, sound field characteristics will be critical to specify in our draft test standards for eSQ and eSL. For continuous noise measurements using an ATF, S12.42 specifies the following for sound field uniformity (section 8.2.1):

> "Sound pressure levels in each one-third octave band centered from 100 Hz to 10,000 Hz measured using a Type 1 pressure/random incidence microphone (IEC 61094-4) at **six** positions relative to the reference point, **± 15 cm** in the front-back, up-down, and left-right axes, shall remain within a range of **5 dB**. The difference between the left-right positions shall not exceed **3 dB** in each band."

Measurements of the sound field will be verified in the vicinity of the ATF (w/o the ATF present) and variation limits will be specified in the draft standard for the eSQ and eSL test methods. This type of specification will enable consistency across test labs when the electromechanical test standards are adopted.

Using key ANSI standards as a guide, we began creating templates for writing our draft test standards. Since the electromechanical Signal Quality (eSQ) and Sound Localization (eSL) standards use the same test set-up and test equipment, a template for this draft standard was created first and we began writing sections of content. The high-level outline for this draft test standard is as follows:

1. Scope
2. Normative References
3. Terms & Definitions
4. Applicability of Test Methods
5. Product Sample Requirements
6. Acoustic Test Fixture Requirements
7. Facilities & Instrumentation
8. Test Procedures & Data Reduction

In addition, we reviewed ANSI/ASA S1.1-2013 Acoustical Terminology and S3.20-2015 Bioacoustical Terminology to determine the terms relevant to eSQ/eSL that are already defined within these standards and established a list of new terms that will need to be defined in the draft standard. Table 6 lists several relevant terms that are already defined within ANSI/ASA S1.1-2013/S3.20-2015 and a preliminary list of terms that will be defined and included in the Terms and Definitions section of the eSQ/eSL draft standard.

We are currently working on refining the data reduction and analysis procedures for the Signal Quality metric. This section of the draft standard will be updated once the eSQ and eSL data is correlated with human subject test data.

Table 6. Preliminary List of Terms to be Referenced and Defined in the eSQ/eSL Draft Standard

Relevant Terms Defined in S1.1/S3.20	Terms to be Defined in eSQ/eSL Draft Standard
• Acoustic Coupler • Auditory Localization (same definition as Localization, Sound Localization) • Auditory Perception • Dynamic Range • Ear Simulator • Frequency Response • Gaussian Noise • Head-Related Transfer Function (HRTF) • Insertion Loss • Peak Sound Level (same definition as Peak Sound Pressure Level) • Reference Point • Signal-to-Noise Ratio • Sound Field • Sound Pressure Level • Total Harmonic Distortion Level	• Acoustic Test Fixture • Aliasing • Anechoic Chamber • Attenuation • Autocorrelation • Broadband • Clipping • Cross-Correlation • Directional Transfer Function • Interaural Level Difference (ILD) • Interaural Time Delay (ITD) • Open-Ear Transfer Function • Signal Quality Metric • Sound Isolation • Sound-Isolating Room • Sound Localization Metric • Sound Source • Spectral Similarity Index

3.2.5. Specific Aim 3, Major Task 1: Hearing Protection Device Evaluations

Electromechanical testing began during the second quarter of Year 2. Summary results are presented below by test. Table 7 lists the status of data collection with all HPDs and all tests. In this table, green indicates that usable data has been collected (though this data is still subject to updates), yellow indicates that initial data has been collected but further refinements are being made to the system to collect better data, and red indicates that the system is still undergoing setup/calibration and that no useable data has been collected. Gray indicates that the test is not applicable to the HPD. Data collection for the electromechanical tests is essentially complete, though new datasets may still be collected moving forward as test methods are modified or devices are re-tested. The number of trials for each device and test is now indicated in the table.

Table 7. HPD electromechanical test status matrix. Green indicates that usable data has been collected on the device and test. The number in the respective box indicates the number of trials that are being averaged to analyze the data.

HPD name	eSQ/eSL	eLD	eSN	eIN
EAR Classic	5	10		10
Elvex Quattro	5	10		9
Combat Arms 4.1 (Open Mode)	5	10		10
Combat Arms 4.1 (Closed Mode)	5	10		9
3M PELTOR TEP-200 (Low Volume)	5	10	1	10
3M PELTOR TEP-200 (High Volume)	5	10	1	10
3M PELTOR ComTac V (Low Volume)	5	10	1	9
3M PELTOR ComTac V (High Volume)	5	10	1	9
Invisio V50/X5 (Low Volume)	5	10	1	0
Invisio V50/X5 (High Volume)	5	10	1	0

3.2.5.1. Signal Quality (eSQ) and Localization (eSL)

The results in the following figures illustrate eSQ/eSL results for the tests described in Section 3.2.3.1. The localization ability for the manikin with open ears (no earplugs being used) is shown in Figure 39. In these figures, color represents SQ score value (shown in the color-bar legend) and the radius of each circle is proportional to the standard deviation of the data at that point (also denoted in the legend). Elevation is denoted by the radial position; azimuth is angular position.

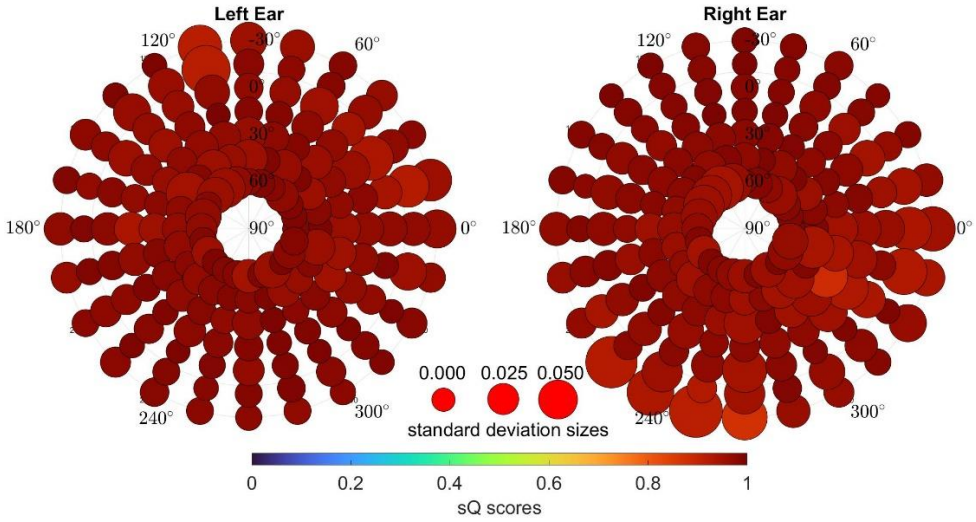

Figure 39. Localization (eSQ/eSL) graphs for unoccluded ears.

Figure 40, Figure 41, and Figure 42 illustrate various methods of calculating eSQ metrics from the same dataset: 5 trials of chirp responses for the Combat Arms 4.1 in open mode from 0^o to 360^o angle and -30^o to 60^o elevation in 15^o increments.

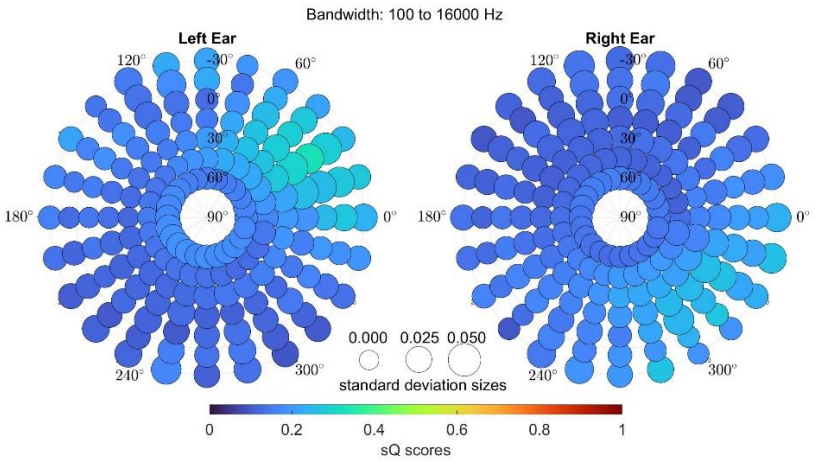

Figure 40. Spatial distribution of eSQ_{org} values for the Combat Arms 4.1 in Open Mode. Color represents score and circle size represents standard deviation over 5 trials.

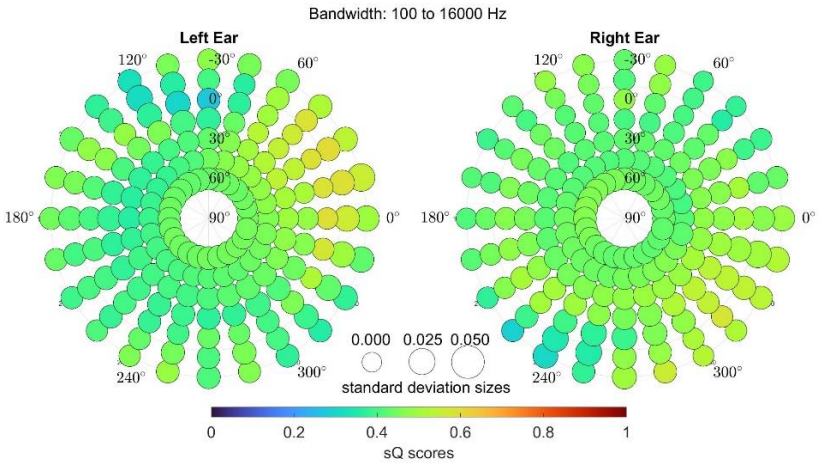

Figure 41. Spatial distribution of eSQ_{SIF} values for the Combat Arms 4.1 in Open Mode. Color represents score and circle size represents standard deviation over 5 trials.

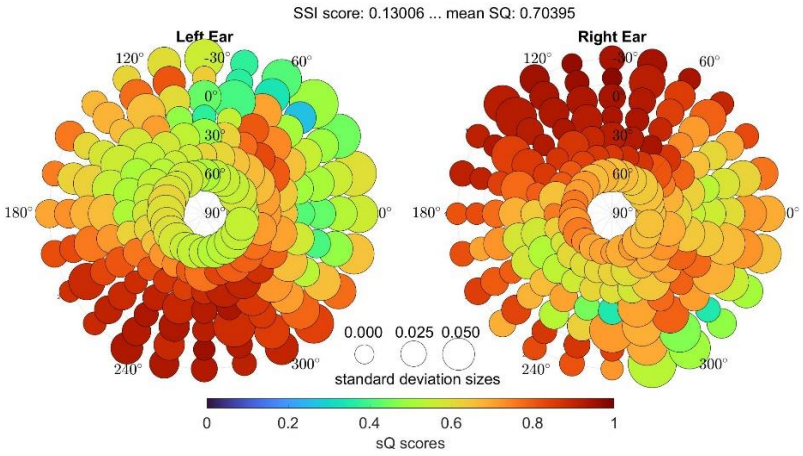

Figure 42. Spatial distribution of eSQ_{SI} values for the Combat Arms 4.1 in Open Mode. Color represents score and circle size represents standard deviation over 5 trials.

The eSQ_{org} and eSQ_{SIF} spatial distributions display similar characteristics – there appears to be an area of higher fidelity at roughly 60^o angle in the left ear and 300^o angle in the right ear for both methods. The eSQ_{SI} spatial distribution shows a very different response, with highest localization at 240^o in the left ear and 120^o in the right ear. This difference is likely due to the use of the DTF, which averages out the spectral features over all angles and elevations for unoccluded and occluded tests, but this will be the focus of future investigations.

From these measurements and the resultant eSQ metric at each point, the response for the open ear and the Combat arms is distinctly different. First, the signal quality for the open ear is near the expected value of 1.0 across all azimuths and elevations. The standard deviation is also small with the exception of a few points near 120 and 240 degrees azimuth and -30 degrees elevation. The Combat Arms shows much lower eSQ throughout the virtual hemisphere due to the changes in the spectral content of the sound reaching the ear. Areas of highest eSQ are those where the

ear is pointed directly toward the speaker. These areas also show more variability due to differences in device insertion from test to test.

3.2.5.2. Level Dependency (eLD) and Self Noise (eSN)

New eLD data was collected on all devices used in this study, using five test iterations per device (device removal and re-insertion between each iteration) and reporting the results as the mean insertion loss at each frequency of interest. Error bars, representing one standard deviation above and below the mean insertion loss, are also included for each level tested on each device. Results for all devices used with the human subjects are shown in Figure 43.

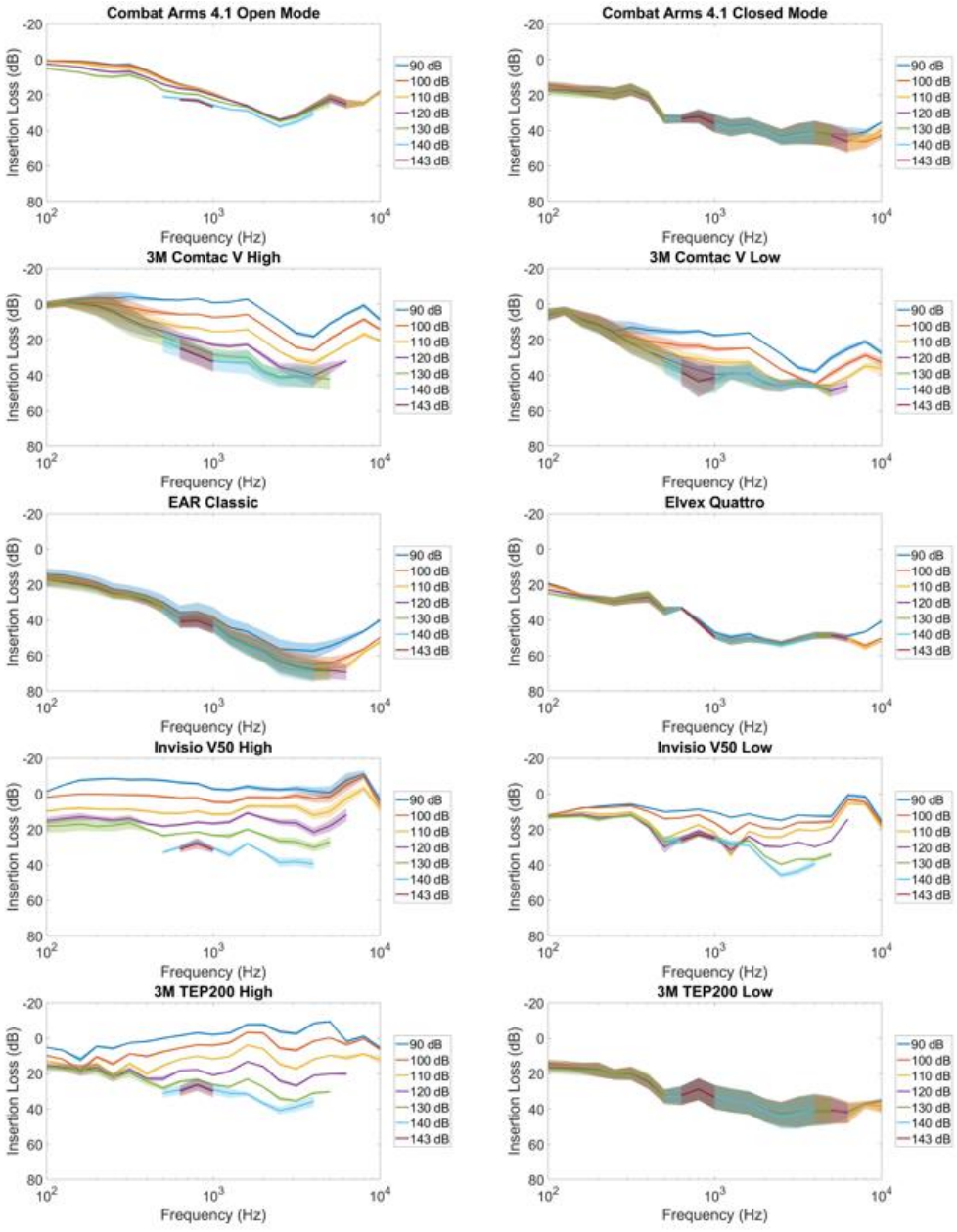

Figure 43. eLD testing results (mean and standard deviation error bars) for all devices.

In Year 3, the results from eLD testing will be refined into a single value for each device that is reflective of the level-dependence of the insertion loss. Currently, calculation of this single value metric (SVM) for each device involves the following steps:

1. Calculate the mean insertion loss $\overline{IL}$ at each exposure level over all tested frequencies.
2. For each exposure level above 90 dB, calculate the change in $\overline{IL}$ from the previous exposure level. For example, if $\overline{IL}$ was 23 dB at a 90 dB exposure level and was 26 dB at a 100 dB exposure level, the rate of change for 100 dB will be 3 dB.
3. For each rate of change, divide by the increase in exposure level. This will give the change in insertion loss per change in exposure in dB/dB, or a unitless ratio. From the previous example, the 3dB change over the increase from 90 to 100 dB gives 0.3 as the ratio.
4. Calculate the mean of all exposure level ratios. This is the single value matric for that device.

One issue calculating the SVM with our collected data is that, due to power and frequency limits of the loudspeakers, high exposure levels have a very limited frequency range. This can often skew the value of $\overline{IL}$ at high exposure levels. For that reason, we've chosen to extrapolate data from low exposure levels into high exposure levels to fill in the missing frequency points. See Section 3.2.3.2 for details.

3.2.5.3. Impulse Noise (eIN)

Two shock tubes are a part of this project: an ANSI S12.42 compliant shock tube for generating pressure waves with a long A-duration, and a "short-duration" shock tube for shorter A-duration pressure waves. Ten test iterations were performed for each device or mode (with removal and insertion between each repetition). The mean insertion loss was calculated and error bars representing one standard deviation above and below the mean are also included for each level on a device. The status of the two tests in terms of the number of trials collected for each device is shown in Figure 44. We anticipate completing data collection in the next quarter.

SD Shocktube

Hearing Protection Device		Low	Med	High
EARClassic		X	X	
Elvex Quattro		X	X	
Combat Arms Open		X	X	
Combat Arms Closed		X	X	
	Silence	X	X	
	Level 1	N/A	N/A	N/A
	Level 2	N/A	N/A	N/A
	Level 3	N/A	N/A	N/A
Comtac	Level 4	X	X	
	Level 1	X		
TEP-200	Level 4	X		
	Level			
Invisio	Level			

ANSI Shocktube

Hearing Protection Device		Low	Med	High	
EARClassic		X	X	X	
Elvex Quattro		X	X	*	*only 9 iterations
Combat Arms Open		X	X	X	
Combat Arms Closed		X	X	*	*only 9 iterations
	Silence	*	X	+	+only 5 iterations
	Level 1	N/A	N/A	N/A	
	Level 2	N/A	N/A	N/A	
	Level 3	N/A	N/A	N/A	
Comtac	Level 4	X	X	*	
	Level 1	X	X	X	
TEP-200	Level 4	X	X	X	
	Level				
Invisio	Level				

X = 10 "good" iterations
* = only 9 "good" iterations
+ = only 5 "good" iterations
N/A = have some amount of data collected, but it's not being used currently
N/A = Data not necessary for current scope but could be examined in the future

Figure 44. Current status of shock tube testing for SD shocktube (left) and ANSI shocktube (right).

Interim results for a selection of the devices tested are shown in Figure 45. The passive, level-dependent Combat Arms clearly shows the nonlinear behavior when in open mode and much less nonlinear behavior in closed mode. In contrast, the EAR Classic and Elvex Quattro show little nonlinear behavior. The Comtac and TEP200, both electronic devices, also show nonlinear behavior. The highest variability is shown for passive devices with high attenuation due to magnification of changes in insertion loss due to small changes in the insertion of the devices.

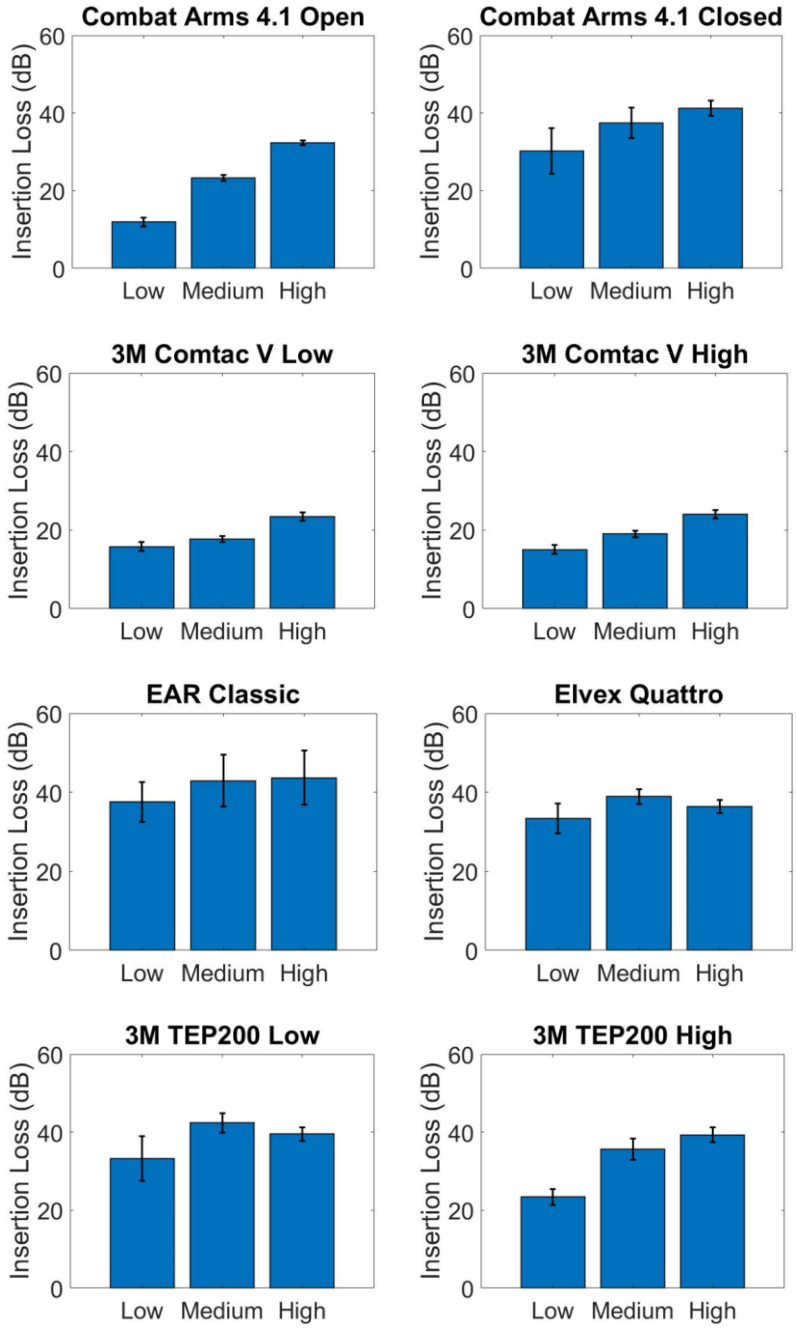

Figure 45. eIN testing results (mean and standard deviation error bars) for five devices (some devices are tested at different levels or settings).

3.2.5.4. Subtask 1: Refinement of Electromechanical Metrics: Interim Comparison of Electromechanical Data with Human Performance

As human testing has progressed, the research team as recently acquired enough data to being making comparisons between electromechanical test methods and human subject data. Examples of the types of preliminary comparisons being performed are shown in the following sections.

3.2.5.4.1. eSQ and hSQ Comparison

The hSQ measures, QuickSIN and Modified Rhyme Test, are compared with the eSQ calculation at 0° Azimuth, 0° Elevation in Figure 46 for four hearing protection devices. Both MRT and QuickSIN are shown for the 0 dB SNR condition for the purposes of comparison. In the next program year, the comparison will focus on the most appropriate signal to noise ratio for human subjects and the most appropriate source level for the electromechanical measurements to achieve the greatest correlation between human performance and electromechanical measurement.

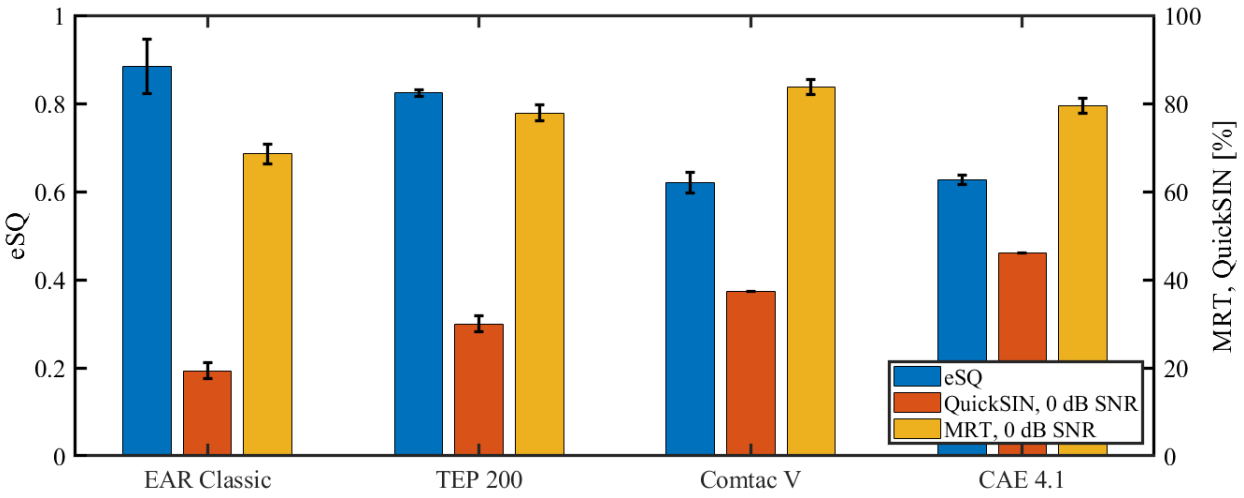

Figure 46. hSQ results for QuickSIN and MRT at 0 dB SNR contrasted with eSQ at 0° Azimuth, 0° Elevation.

3.2.5.4.2. eSL and hSL Comparison

The divergence from open ear performance of human subject localization responses (left) is compared with the monaural electromechanical localization metric (center/right) for four of the HPDs undergoing human subject testing in Figure 47 through Figure 50. For the plots of human subject error divergence, 0 (red) is a perfect score identical to the open ear and 2 (blue) is a poor score, whereas for the electromechanical data, 1 (red) is a perfect score and 0 (blue) is a poor score.

Note that the eSQ monaural measurement points are asymmetric about the centerline of the head, whereas the hSQ binaural measurements are symmetric. In the next program year, a method to combine the monaural measurements into a binaural metric will be explored.

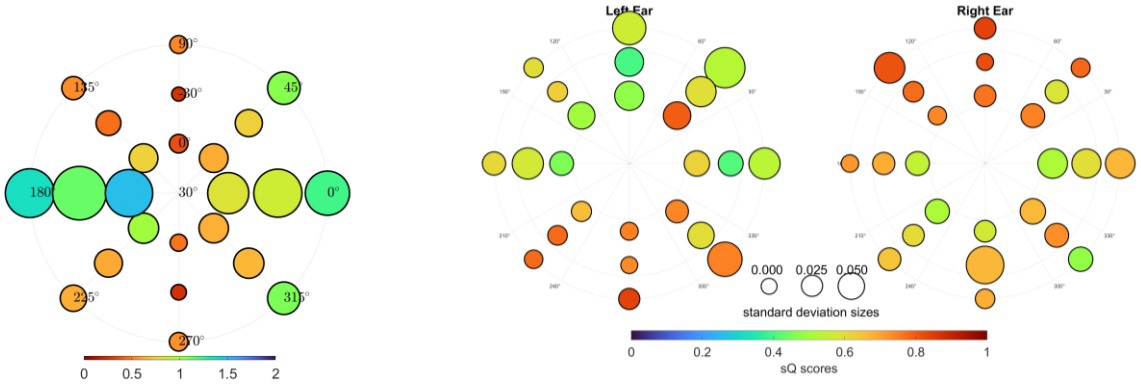

Figure 47 Combat Arms 4.1 open mode hSL visualization showing divergence of the localization responses (left) compared with eSQ measured across the same elevations and azimuths (center, right).

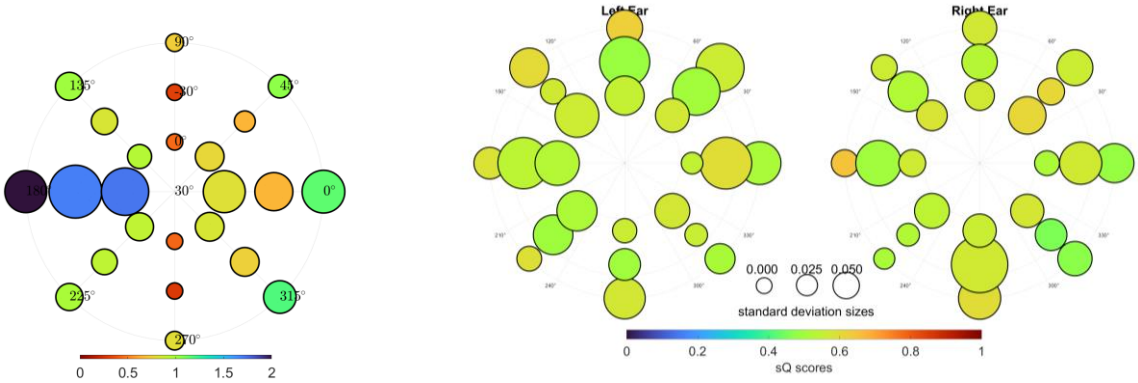

Figure 48 Comtac V hSL visualization showing divergence of the localization responses (left) compared with eSQ measured across the same elevations and azimuths (center, right).

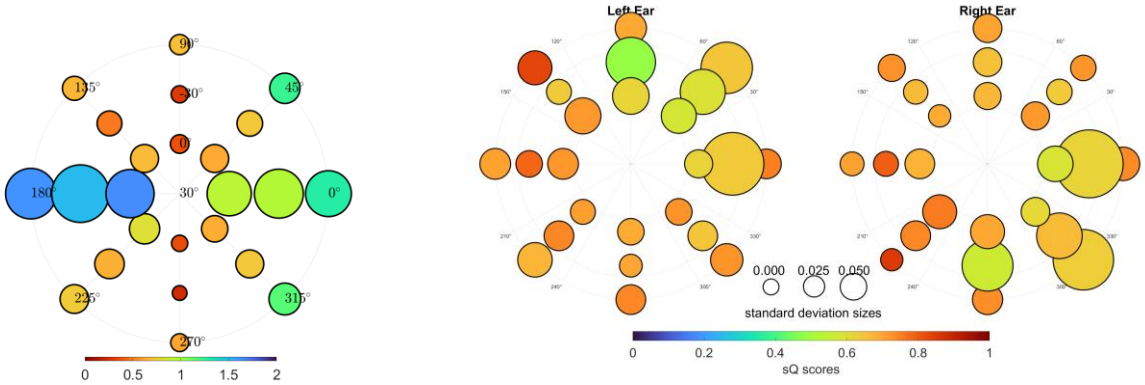

Figure 49 TEP-200 hSL visualization showing divergence of the localization responses (left) compared with eSQ measured across the same elevations and azimuths (center, right).

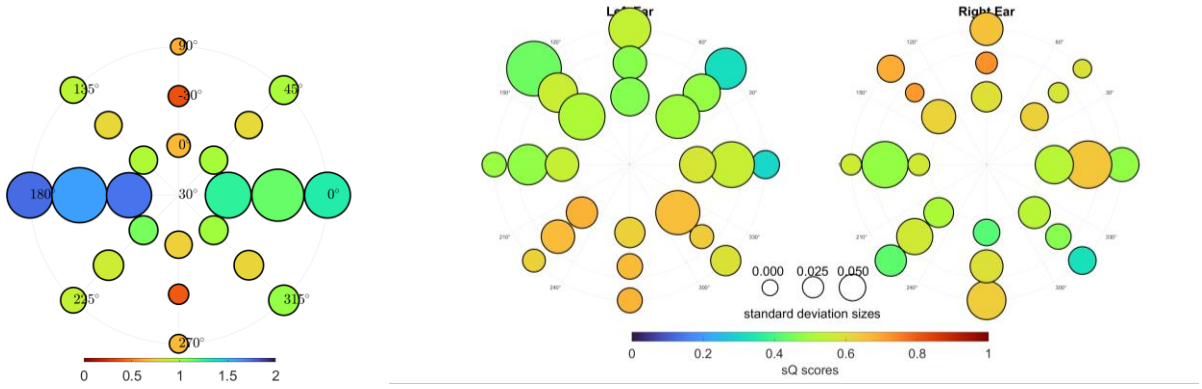

Figure 50 EAR Classic hSL visualization showing divergence of the localization responses (left) compared with eSQ measured across the same elevations and azimuths (center, right).

3.2.5.4.3. eSN and hSN Comparison

Results of human subjects undergoing REAT testing (hSN) are compared with the electromechanical measurements of self noise (eSN) in Figure 49 for two active devices. Error bars are representative only of experimental variability and not measures of systematic error. Both the Invisio and TEP-200 have threshold levels broadly similar between measures. There is some variation in the spectral shape of the levels, however, with the Invisio demonstrating a larger deviation between eSN and hSN measurements. Alternative calculation methods for determining the noise level and addition of systematic measurement error will be incorporated in Year 3.

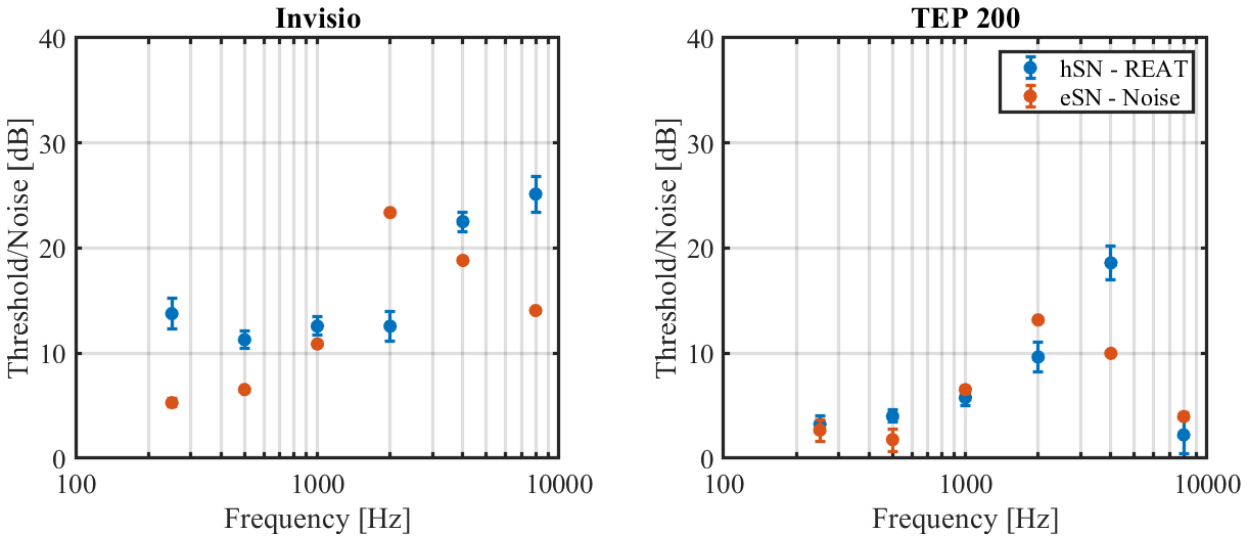

Figure 51. Comparison of electromechanical self-noise (eSN) and REAT under headphones with active devices (hSN) versus frequency.

3.2.6. Specific Aim 3, Major Task 2: Hearing Protection Selection Tool

3.2.6.1. Transition

The project team continued to coordinate with William Martinous from the Defense Logistics Agency (DLA) for the transition plan for the Hearing Protection Device Optimization Selection Tool. The DLA designated the Defense Medical Logistics Standard Support (DMLSS) Business Process Support Office to support the tool. Details on the specific requirements are to be coordinated with Nora Steigerwalt and DLA J6 (Communications) to host the application on the DLA Medical Web Portal.

We completed a Problem Statement form for DLA that was submitted to DLA J6 Chief Information Officer team for processing. This form is currently under review, and once accepted, will result in an approved new requirement for the tool. We received a set of technical questions about the software and provided answers along with a teleconference to review and discuss the requirements from J6. Once the J6 approves the new requirement, it will be sent to the Defense Medical Logistics Standard Support (DMLSS) Business Process Support Office to support the tool. Upon approval of the requirement, we will adapt the current tool to conform to necessary DLA computing requirements.

We also provided slides and a write up to Dr. Theresa Schulz for her to brief the Defense Health Agency Chief Information Officer (DHA-CIO) to provide command emphasis on moving the transition planning process forward.

3.2.6.2. Front-end Development

In Year 2 the front-end development of the Hearing Protection Optimization Tool (HPOT) was implemented using React with Typescript integration. We also updated the graphics to include new general HPD type icons provided by the Hearing Center of Excellence to represent HPDs for which there is no custom graphic or photo. Additional changes were recommended during a feedback call organized by Kristy Hentchel, Auditory Neuroscience Program Manager, Office of Naval Research, and attended by researchers and audiologists from the Navy and Air Force. The call was also supported by the DOD Hearing Center of Excellence. The following figures show the implemented mocked-up designs for the Hearing Protection Selection Tool:

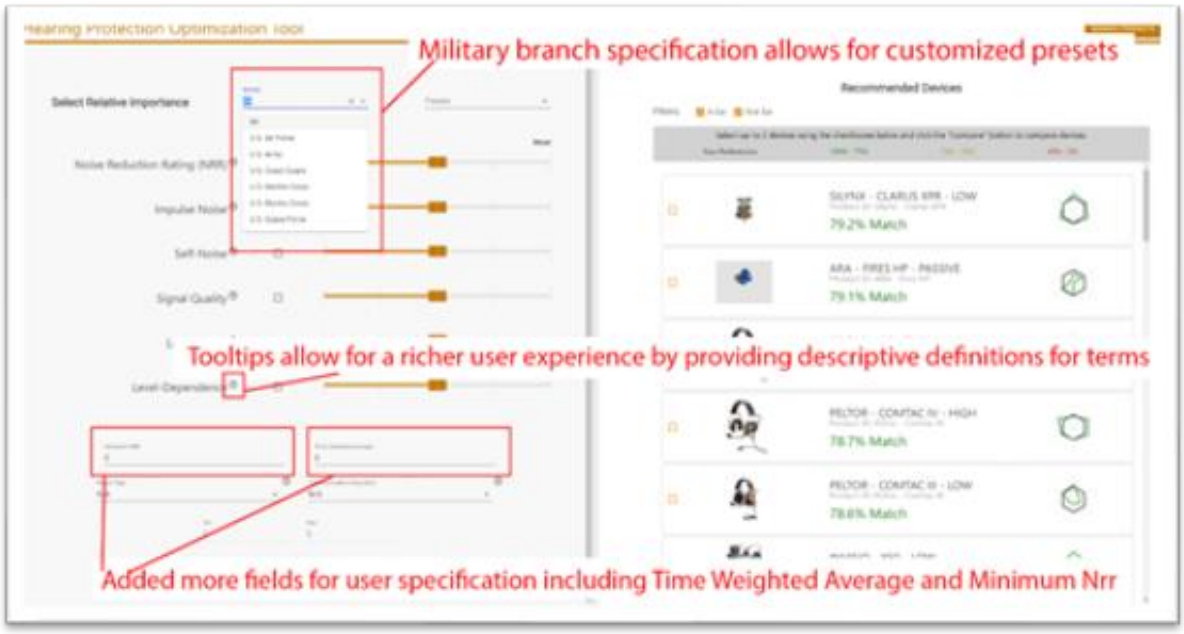

Figure 52. Hearing Protection Optimization Tool Landing Page.

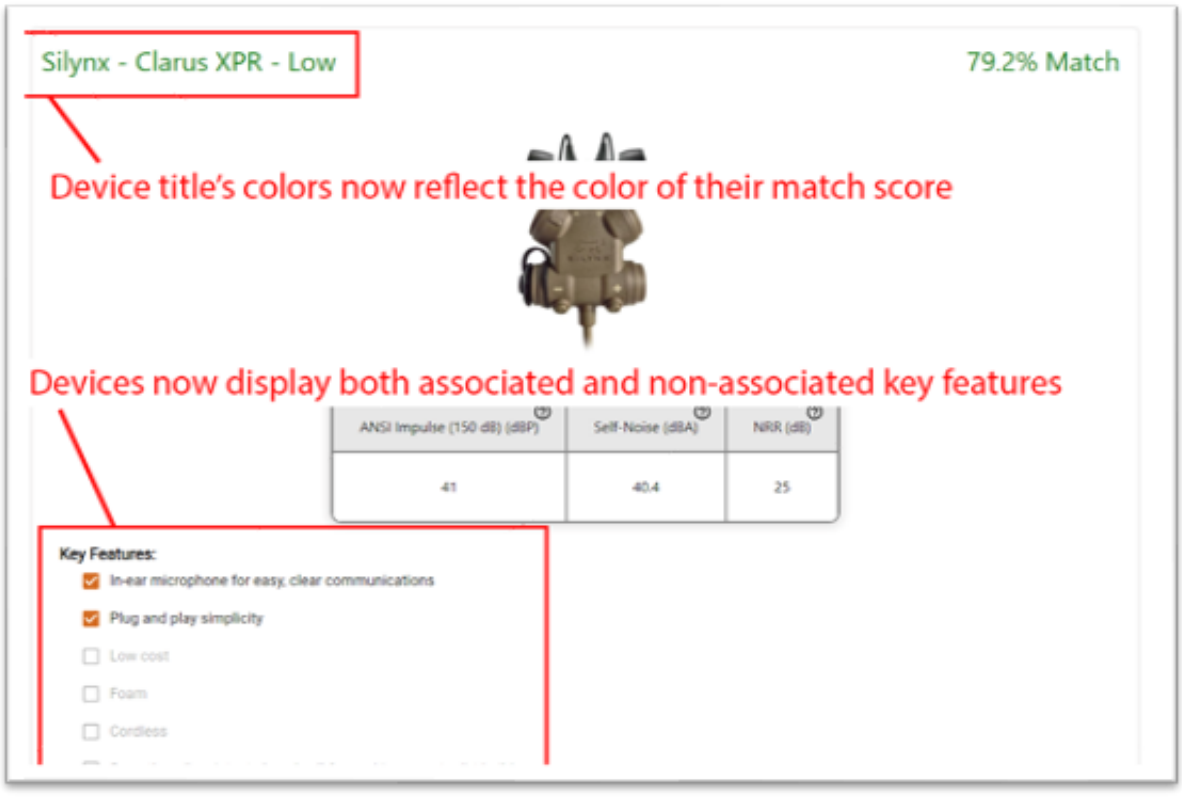

Figure 53. Device Details Page.

Figure 54. Hearing Protection Device Compare Page.

Figure 55. Hearing Protection Device Add Page.

3.2.6.3. Back-end Development

We are currently developing the back-end interface to ensure updated HPD data can be imported to the software tool. Tooltips are also being integrated into the user interface to aid users of all technical levels in understanding the meaning of each category and what device capabilities are impacted by changing the category values. The back-end API has been built using C# Entity Framework, .NET 5.0, and a PostgreSQL database.

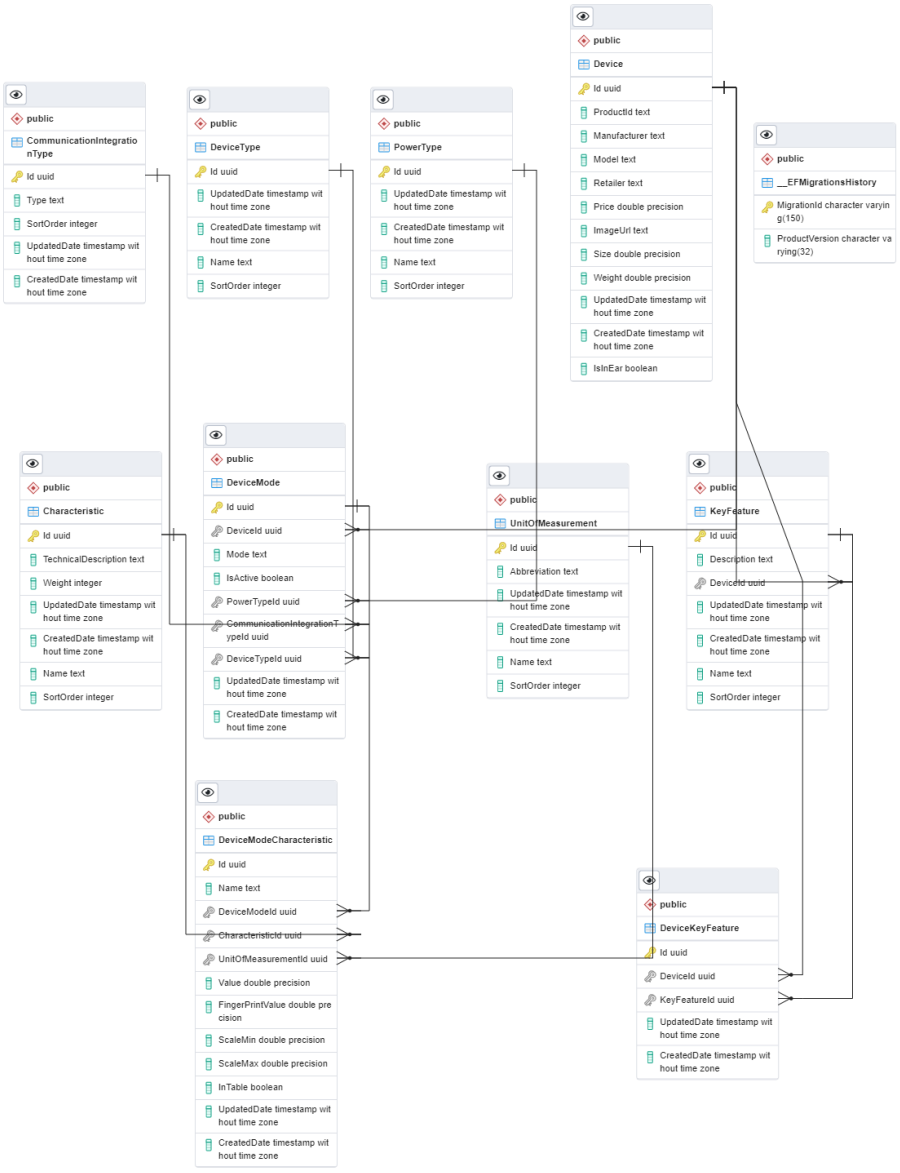

Figure 56. PostgreSQL database structure for the HPOT.

3.2.6.4. AWS Setup

An AWS pipeline was used to deploy and host the Hearing Protection Optimization Tool. The pipeline implementation includes Route 53, Certificate Manager, CloudFront, Elastic Computing with load balancers, Simple Storage Service, and Relational Database Service.

This allows a user to input our domain and Amazon Route 53 is used to direct the user to a CloudFront distribution that is pointing to an S3 bucket, which holds our production version of the HPOT application. As the user interacts with the application, API calls are dispatched to the Elastic Load Balancer, which directs the call to our EC2 instance with the API running on it. The EC2 instance interfaces with the Relational Database Service to grab the data requested by the API call and sends the data back to the application as requested.

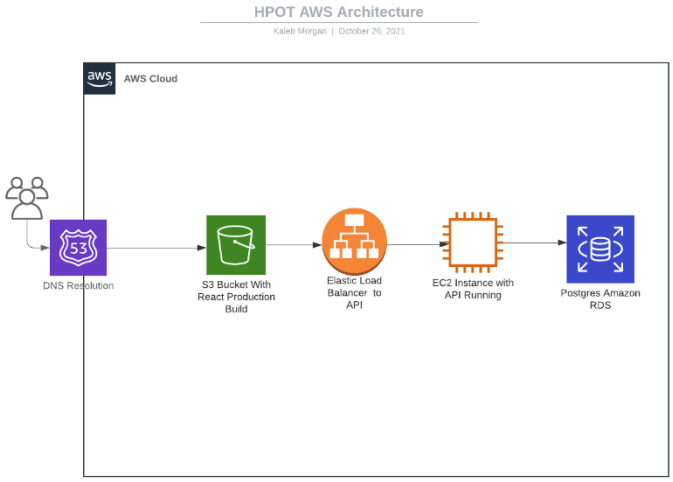

Figure 57. HPOT AWS Architecture.

3.3. What opportunities for training and professional development did the project provide?

Nothing to report.

3.4. How were the results disseminated to communities of interest?

Program progress was consistently presented to communities of interest through video and audio teleconferencing and participation in several conferences. Specific briefings include:

- An update brief was presented to the Hearing Protection Working Group on November 19, 2021.
- Ted Argo presented "Validation of Electromechanical Hearing Protection Evaluation Methods" to the National Hearing Conservation Association Conference on February 2022.
- Ted Argo presented "Validation of Electromechanical Hearing Protection Evaluation Methods" to the 182nd meeting of the Acoustical Society of America on May 24, 2022.
- An update brief was presented to the Navy on February 17, 2022.
- An abstract was submitted for the Military Health System Research Symposium (MHSRS). A podium presentation is scheduled for September 15, 2022.

3.5. What do you plan to do during the next reporting period to accomplish the goals and objectives?

In the final program year we will complete the following activities:

- Specific Aim 1
  - Continue recruiting, consenting, and testing human subjects for hSQ, hSL, hLD, and hSN tests at UW and CU.
  - Complete hIN testing at CU.
- Specific Aim 2
  - Perform comparisons between human subject performance and electromechanical metrics to determine areas where the electromechanical metrics should be recalculated, rescaled, or restructured.
- Specific Aim 3
  - Continue discussions regarding standards and optimization tool transition path through the Defense Logistics Agency.
  - Transition the optimization tool to the DLA.

4. Impact

This research will produce the knowledge products of data and prototype standards suitable for direct incorporation into relevant military and civilian hearing protection standards. These standards will guide the testing of HPDs in a manner that augments current human subject evaluations by providing an electromechanical approximation of human subject performance. By transitioning these methods into standards, time-consuming, repetitive, and expensive human subject testing may be minimized, thereby bringing new technology to the Warfighter much faster than is presently possible. By providing simple, electromechanical testing methods to potential vendors to validate their products, the risk of future product failures and subsequent loss of hearing by warfighters will be significantly reduced.

It is noted, however, that changing existing standards or creating new standards is a time-intensive process. Therefore, the results of this research can be readily transferred directly to the Warfighter through a hearing protection device selection and optimization software program. By allowing the Warfighter to directly access the information from this program, as it relates to the HPDs they have already been issued, the time to develop standards and observe their use is lessened. By enabling mission planners to identify the optimal hearing protection equipment based on their mission requirements, they will reduce risk to Soldiers and increase their lethality on the battlefield through improved situational awareness and communications ability.

Fewer personnel experiencing hearing injury will also reduce the burden on the entire military health care system, from recruitment through Veterans Affairs medical support. The reduction in cost of billions of dollars (Saunders 2009) will ensure more funding is available for critical care situations, further research and development, and/or simple reduction in overall budget. Due to the nature of hearing loss caused by repetitive noise exposure, observing optimal protective strategies will make certain that overall healthcare costs decrease, and quality of life for veterans will increase.

5. Changes/Problems

Nothing to report.

6. Products

6.1. Abstracts/Presentations

Year 2:

1. Argo, T. F., Anderson, D. A., Brown, A. D., Greene, N. T., McCallick, C., Rule, G., & Sammeth, C. (2022) Validation of Electromechanical Hearing Protection Evaluation Methods. Accepted for presentation at the 2022 National Hearing Conservation Association Conference.

2. Anderson, D. A., & Argo, T. F. (2021, October). Evaluating the Relationship Between Kurtosis Loss and Spectral Insertion Loss for Musicians' Hearing Protection Devices. In Audio Engineering Society Convention 151. Audio Engineering Society.

3. Argo, T. F., Greene, N. T., Brown, A. D., McCallick, C., Sammeth, C. A., Anderson, D. A., Rule, G. T. (Abstract – Accepted for podium presentation) Validation of Electromechanical Hearing Protection Evaluation Methods. For submission to the Military Health System Research Symposium.

4. Andrew Brown*[1], Nathaniel Greene[2], David Audet[1], Caylin McCallick[2], Carol Sammeth[3], David Anderson[4], Gregory Rule[4], Theodore Argo[4]. Quantifying impacts of hearing protection devices on sound localization in azimuth and elevation: Toward predictors of performance, MHSRS, September 12-15, 2022

5. Theodore Argo*[1], Andrew Brown[2], David Audet[2], Nathaniel Greene[3], Caylin McCallick[3], Carol Sammeth[4], David Anderson[1], Gregory Rule[1] Methods for Validation of Electromechanical Evaluation of Hearing Protection.

6. Brown, A. D., Greene, N. T., Audet, D. J., McCallick, C., Sammeth, C. A., Anderson, D. A., Rule, G. T., Argo, T. F. (Abstract Submitted) Quantifying impacts of hearing protection devices on sound localization towards identifying predictive patterns. Submitted to the Acoustical Society of America Conference.

7. Nathaniel Greene*[1], David Anderson[2], Theodore Argo[3]. Occluded insertion loss from intracochlear pressure measurements during acoustic shock wave exposure.

8. Theodore F. Argo[1], David A. Anderson[1], Andrew D. Brown[2], Nathaniel Greene[3], Jennifer Jerding, Development of an electromechanical test system and acoustical metrics to predict impacts of hearing protection devices on sound localization, to be presented at ASA Spring 2022.

9. David A. Anderson[1], Andrew D. Brown[2], Nathaniel Greene[3], Theodore F. Argo[1], Bruno Mary[1], Development of an in-ear microphone for individualized measurement of hearing protection device output, to be presented at ASA Spring 2022.

Year 1:

1. Argo, T., Greene, N.T., Brown, A., McCallick, C., Sammeth, C., Anderson, D., and Rule, G. (2021) “Validation of Electromechanical Hearing Protection Evaluation Methods”. Military

Health Science Research Symposium, Orlando, FL. **CANCELLED, abstract accessible through MHSRS Website.*

2. Anderson, D., and Argo, T. (2021) “Evaluating the Relationship Between Kurtosis Loss and Spectral Insertion Loss for Musicians' Hearing Protection Devices”. 151st International Audio Engineering Society Convention, Las Vegas, NV. October 11-13, 2021.

6.2. Manuscripts/Papers

Year 2:

1. Anderson, D. A., Greene, N. T., and Argo IV, T. A. (Submitted) Occluded insertion loss from intracochlear pressure measurements during acoustic shock wave exposure. Submitted to *Hearing Research*.

2. David A. Anderson and Theodore F. Argo , "Kurtosis loss as a metric for hearing protection evaluation in impulsive noise environments", JASA Express Letters 2, 033603 (2022) https://doi.org/10.1121/10.0009659.

6.3. Other Products

None to report.

7. Participants and Other Collaborating Organizations

7.1. Participants

Name: **Ted Argo, Ph.D.**
Project Role: Principal Investigator
Researcher Identifier *NA*
Nearest person month worked: 7
Contribution to Project: Wrote reports, conducted planning meetings with subcontractors, development/review of test plans and apparatus. Conducted stakeholder meetings, reviewed and submitted protocols.

Name: **Gregory Rule**
Project Role: Program Manager
Researcher Identifier *NA*
Nearest person month worked: 3
Contribution to Project: Contributed to and reviewed quarterly report, coordinated and supported planning meetings with subcontractors, development/review of test plans. Conducted stakeholder meetings.

Name: **David Anderson, Ph.D.**
Project Role: Acoustic Engineer
Researcher Identifier *NA*
Nearest person month worked: 12
Contribution to Project: Test plan review and development support. Electromechanical test equipment development. Analysis of PMHS acoustic overpressure data.

Name: **Kaleb Morgan**
Project Role: Software Developer
Researcher Identifier *NA*
Nearest person month worked: 2
Contribution to Project: Development of HPD optimization software tool.

Name: **Bruno Mary**
Project Role: Staff Scientist
Researcher Identifier *NA*
Nearest person month worked: 3
Contribution to Project: Electronics development and testing operations support for EM testing.

Name: **Jennifer Jerding**
Project Role: Senior Engineer
Researcher Identifier *NA*
Nearest person month worked: 2
Contribution to Project: Review and analysis of existing test standards.

Name: **Alexandria Podolski**
Project Role: Laboratory Assistant
Researcher Identifier *NA*
Nearest person month worked: 6
Contribution to Project: Testing operations support for EM testing.

Name: **Luke Runyon**
Project Role: Software Developer
Researcher Identifier *NA*
Nearest person month worked: *1*
Contribution to Project: *Development of the HPD selection tool user interface.*

Name: **Frederick Stolzle**
Project Role: Software Developer
Researcher Identifier *NA*
Nearest person month worked: *1*
Contribution to Project: *Development of the HPD selection tool back end.*

Name: **Summer Graham**
Project Role: Intern
Researcher Identifier *NA*
Nearest person month worked: *1*
Contribution to Project: *Laboratory preparation.*

Name: **Nick Brunstad**
Project Role: Staff Scientist
Researcher Identifier *NA*
Nearest person month worked: *1*
Contribution to Project: *Testing operations support for EM testing.*

Name: **Amy Carter**
Project Role: Accounting Support
Researcher Identifier *NA*
Nearest person month worked: *1*
Contribution to Project: *Subcontractor management and billing.*

7.2. Collaborating Organizations

Organization: The University Colorado Anschutz Medical Campus
Principal Investigator: Prof. Nate Greene, Ph.D.

Organization: The University of Washington
Principal Investigator: Prof. Andrew Brown, Ph.D.

8. Special Reporting Requirements

Quad Chart. See Section Appendix B.

9. Appendices

Appendix A. Summary of Activities Accomplished

Description	Timeline (Months)	Complete (Percent)	Start (Date)	Completed (Date)
Specific Aim 1: Human Subject Evaluations.				
Major Task 1: Submission of Human Use Protocols and Preparation of Facilities				
Subtask 1: Develop and submit human use protocols	1–3	100%	28 Jul 20	13 Jan 21
Subtask 2: Develop and submit human cadaver use protocols	1	100%	28 Jul 20	30 Sep 20
Subtask 3: Prepare human test facilities	2–4	100%	28 Jul 20	30 Apr 21
Milestone #1: Local IRB Approval	4			*COMPLETE*
Subtask 4: Submit protocols for Army HRPO approval	5	100%	28 Jul 20	13 Jan 21
Milestone #2: HRPO Approval	*6*			*COMPLETE*
Major Task 2: Test Method Verification				
Subtask 1: Obtain pilot psychoacoustic measures of hearing protective device (HPD) effects	6-12	100%	28 Jan 21	31 Jan 22
Subtask 2: Analyze pilot psychoacoustic measures of hearing protection device effects	10-12	100%	28 Apr 21	31 Jan 22
Subtask 3: Obtain psychoacoustic measures of hearing protective device (HPD) effects • Testing is ongoing	12-30	40%	28 Jul 21	
Subtask 4: Analyze pilot human cadaver measures of HPD attenuation to impulse noise exposures	1-5	100%	15 Jan 21	31 Jan 22
Subtask 5: Obtain human cadaver measures of HPD attenuation to impulse noise exposures • Three PMHS subjects obtained and prepared	6-24	15%	01 Apr 21	
Subtask 6: Conduct ongoing quality assurance review of psychoacoustic, cadaver, and associated data	6-36	40%	28 Jul 21	
Milestone #3: Manuscript on impulsive noise measurements on cadaveric subjects with HPDs	*24*	100%	28 Jul 21	*COMPLETE*
Milestone #4: Manuscript on HPD effects on perception	*30*			
Specific Aim 2: Refinement of HPD Evaluation Methods.				
Major Task 1: Verification of Electromechanical Test Methods				
Subtask 1: Refine the electromechanical metrics • Comparison of human subject and electromechanical data underway • Preliminary testing of some devices completed to refine metrics	1-24	75%	21 Dec 20	
Major Task 2: Develop prototype standards for appropriate HPD evaluation methods				
Subtask 1: Develop data and prototype standards	25-33	10%	1 Nov 21	
Milestone #5: Deliver standards input to appropriate standards committees	*36*			
Specific Aim 3: Application of HPD Evaluation Methods.				
Major Task 1: Hearing Protection Device Evaluations				
Subtask 1: Evaluate a broad array of HPDs using the refined electromechanical test methods	18-30	75%	1 Nov 21	
Milestone #6: Conference presentation on comparative HPD performance	*30*			
Major Task 2: Develop Hearing Protection Optimization Tool				
Subtask 1: Incorporate HPD test results	24-36			
Subtask 2: Compile HPD optimization tool on multiple platforms • Software tool is operational pending further input from end users and transition partners	30-36	75%	1 Aug 21	
Milestone #7: Deliver HPD optimization tool to sponsor	*36*			

Appendix B. Quad Chart